Experimental Study on Physio-Mechanical Properties of Hybrid Teff-Straw and Polyethylene Terephthalate Fibers Reinforced Concrete

Neway Yeshitla Aklilu

A Thesis Submitted to the Department of Civil Engineering

School Of Civil Engineering and Architecture

Presented in Partial Fulfillment of the Requirement of Masters of Science in Civil Engineering (Specialization in Construction Engineering and Management)

Office of Graduate Studies

Adama Science and Technology University

June, 2023

Adama, Ethiopia

Experimental Study on Physio-Mechanical Properties of Hybrid Teff-Straw and Polyethylene Terephthalate Fibers Reinforced Concrete

Neway Yeshitla Aklilu

Advisor: Meseret Getnet (Ph.D.)

A Thesis Submitted to the Department of Civil Engineering
School of Civil Engineering and Architecture
Presented in Partial Fulfillment of the Requirement of Masters of Science in Civil Engineering (Specialization in Construction Engineering and Management)
Office of Graduate Studies
Adama Science and Technology University

June, 2023
Adama, Ethiopia

DECLARATION

I declare that this thesis proposal entitled "**Experimental Study on Physio-Mechanical Properties of Hybrid Teff-Straw and Polyethylene Terephthalate Fibers Reinforced Concrete** " is my work and has not been submitted to any university for a similar purpose. The references used in this proposal are duly recognized by proper citations.

Neway Yeshitla Aklilu	____________________	________________
Name of student	Signature	Date

RECOMMENDATION OF ADVISOR

I, the major advisor of this thesis, hereby certify that I have closely advised the student while developing this thesis and read the draft thesis entitled "**Experimental Study on Physio-Mechanical Properties of Hybrid Teff-Straw and Polyethylene Terephthalate Fibers Reinforced Concrete**" prepared under my guidance by Neway Yeshitla Aklilu.

Therefore, I recommend the submission of the thesis to the department for further review and evaluation.

Meseret Getnet (Ph.D.)	____________________	________________
Advisor Name	Signature	Date

APPROVAL PAGE

I hereby certify that the recommendation and suggestion given by the thesis review committee are appropriately incorporated into the final thesis entitled "**Experimental Study on Physio-Mechanical Properties of Hybrid Teff-Straw and Polyethylene Terephthalate Fibers Reinforced Concrete**" by Neway Yeshitla Aklilu.

Meseret Getnet (Ph.D.)	______________________	_______________
Major Advisor	Signature	Date

APPROVAL OF BOARD OF REVIEWERS

We, the undersigned, members of the board of reviewers of the thesis open defense by Neway Yeshitla Aklilu have read and evaluated the thesis entitled "**Experimental study on Physio-Mechanical Properties of Hybrid Teff-Straw and Polyethylene Terephthalate Fibers Reinforced Concrete** " and assessed the understanding of the candidate about the research. This is, therefore, to certify that the thesis is accepted and we recommend its implementation.

______________________	______________________	______________________
Chairperson	Signature	Date
Tesfaye Alemu, PhD.	______________________	20/07/2023
External Examiner	Signature	Date
______________________	______________________	______________________
Internal Examiner	Signature	Date
______________________	______________________	______________________
Department Head	Signature	Date
______________________	______________________	______________________
School Dean	Signature	Date
______________________	______________________	______________________
Office of Postgraduate Studies, Dean	Signature	Date

ACKNOWLEDGMENT

First, I would like to thank almighty GOD for helping me throughout this research and I would like to thank Oda Bultum University for giving me the MSc opportunity and research fund to accomplish this thesis. Furthermore, I would like to acknowledge the Civil Engineering Department of ASTU for allowing me to use laboratory facilities. I would like to express my deepest gratitude to my advisor, Meseret Getnet (Ph.D.), for his continual support and guidance throughout the preparation of this thesis. I am greatly indebted to my friends, Mr. Kumera Daka and Mr. Zewdu Sileshi, for their many-sided support. My thanks also extend to Mr. Mesele Yoma, Mr. Abiyot, Mr. Mulat, Mr. Debele Beri, and Mis. Martha who helped me to accomplish this thesis. I would like to express my special thanks to my family. I am also greatly indebted to the different researchers and authors whose work I have quoted in my work. Finally, I am grateful to all the people who contributed to the successful completion of this work.

TABLE OF CONTENTS

LIST OF TABLES

LIST OF FIGURES

LIST OF ACRONYMS

TSF	Teff straw fiber
TFRC	Teff fiber reinforced concrete
FRC	Fiber reinforced concrete
PET	Polyethylene terephthalate
PETF	Polyethylene terephthalate fiber
HFRC	Hybrid fiber reinforced concrete
HTPF	Hybrid teff straw and polyethylene fibers
HTPFRC	Hybrid teff straw and polyethylene fibers reinforced concrete
GGBS	Ground granulated blast furnace slag
ACI	American Concrete Institute
Asg	Apparent specific gravity
ASTM	American Society for Testing Materials
Bsg	Bulk specific gravity
CA	Coarse Aggregate
FA	Fine Aggregate
FM	Fineness Modulus
VPV	Volume of permeable voids
SSD	Saturated Surface Dry

ABSTRACT

Concrete is one of the world's most versatile and widely used construction materials. It is subject to many limitations in engineering applications because of poor ductility, high brittleness, low tensile strength, low tensile strain, and poor resistance to crack opening and propagation. Fiber hybridization with different types of fibers helps in resisting these cracks in concrete structures. Earlier studies have investigated the use of fibers in concrete structures to mitigate these weaknesses of plain concrete. However, the use of hybrid teff straw and polyethylene terephthalate fibers as hybrid reinforcing fibers in concrete has not been studied yet. In the current study, teff straw fiber was taken from harvested teff grain, and the polyethylene terephthalate fibers were extracted from plastic bottles to make hybrid fiber-reinforced concrete. To make hybrid teff straw and polyethylene terephthalate fiber reinforced concrete samples, ordinary Portland cement, fine aggregate, coarse aggregate, water, teff straw fiber, and polyethylene terephthalate fibers were directly mixed. The results of the slump and compaction factor values showed a reduction as the percentage of hybrid fibers increased compared to the control mix due to the interlocking of fibers and the incorporation of fibers absorbed more water from the concrete mix. At 28 days of cure, concrete mix with 0.2%, 0.4%, and 0.6% fibers concentration showed a compressive strength of 30.33Mpa, 21.72 MPa, and 19.21 MPa which is approximately 15.08%, 39.19%, and 46.21% lower than the control mix, respectively. This could be due to fiber balling effects and concrete becoming too hard to compact which in turn leads to more air voids thereby a decline in compressive strength. The investigation of splitting tensile and flexural strengths also revealed that the addition of 0.2% hybrid fiber concentration resulted in a 23.66% enhancement in splitting tensile strength and 7.84% enhancement in flexural strength, with the highest strengths of about 2.77 MPa and 5.09 MPa at 28-days, respectively. Failure mode during the test showed higher fiber concentration leads to a more ductile failure mode with fewer cracks than the brittle failure of control concrete, providing a sufficient warning before final failure. Furthermore, the current study revealed the enhanced tensile properties of concrete by incorporating teff straw and polyethylene terephthalate fibers.

***Keywords/Terms**: Hybrid fiber reinforced concrete; Teff straw fiber; Polyethylene terephthalate fiber; Crack; Fresh properties; Hardened properties*

CHAPTER 1
INTRODUCTION

1.1 Background of the study

Concrete is one of the world's most versatile and widely used construction materials, which plays an important role in constructing dams, buildings, roads, storage tanks, tunnels, seaports, bridges, subways, and other infrastructures (El-Din et al., 2017). Concrete is mainly composed of cement, coarse aggregate, and fine aggregate mixed with water (Das et al., 2020; Tarekegn et al., 2022). The paste, composed of cement and water, binds and fills the voids between the aggregates into a rock-like mass as the paste hardens due to the hydration reaction of water and cement (Tarekegn et al., 2022). The properties of concrete, including high compressive strength, versatility, availability, affordability, simple preparation, fire resistance, excellent thermal resistance, compatibility with steel reinforcement bar, and the possibility of casting in desired shapes, make concrete the most used construction material in the world than other conventional construction materials (Najaf et al., 2022; Yuan et al., 2021).

Concrete is subject to many limitations in engineering applications because of poor ductility, high brittleness, low tensile strength, low tensile strain, and poor resistance to crack opening and propagation (Nilforoush et al., 2017; Yuan & Jia, 2021). Mechanical loading as well as drying shrinkage can cause conventional concrete to crack with subsequent reduction in the overall strength and stiffness of the concrete structure (M. Cao et al., 2014). Once a crack has formed, water and destructive agents like chlorides and sulfates can penetrate quickly into the concrete, and they subsequently accelerate the corrosion process and seriously degrade the serviceability of the structures (Passuello et al., 2009).

The term fiber reinforced concrete is defined by ACI committee 544 as "a concrete consisting of hydraulic cement comprising fine or fine and coarse aggregate and discontinuous discrete fibers". Based on the material used for manufacturing, fibers are classified as metallic fibers, mineral fibers, synthetic fibers, and natural fibers. (Z.-X. Li et al., 2017). Hybrid fiber reinforced concrete (HFRC) is the combination of one metallic and non-metallic fiber or simply the combination of two different types of fibers (Yao et al., 2003). It is one of the most promising construction techniques and repairing materials in recent times for the construction industry. Fiber hybridization with different types of fibers helps in resisting these cracks in concrete structures (Das et al., 2020). HFRC is being considered nowadays due to its several structural benefits as compared to that plain concrete

(Khan et al., 2018). It is being used in a big number of applications such as bridges, hydraulic structures, tunnels, pipes, canal linings, and safety vaults, in addition to explosion-resistant structures, cladding, and roller-compacted concrete. The main purpose of the combination of different types of fibers is to control cracks at different zones of the cementitious material, at different size levels, and during different loading stages (Afroughsabet et al., 2015). The fiber properties considered are fiber type, length, diameter, strength, elastic modulus, and so on (B. Li et al., 2018).

The incorporation of various discontinuous chopped fibers in a matrix greatly influences the properties of concrete and various studies have shown that the fibers can significantly improve the engineering properties of the concrete such as the tensile strength, flexural strength, impact, fatigue, and abrasion resistance, deformation capability, toughness, and load bearing capacity after cracking (Grzymski et al., 2019; Teng et al., 2018). Reinforced concrete with short fibers distributed randomly improves the strength of cementitious matrices by controlling the initiation, propagation, and/or merging of cracks. The efficiency of the fiber is dependent upon factors such as the properties of the fiber matrix, volume of fiber inclusion, fiber geometry, type of fiber, and orientation of fiber in the concrete mixture (El-Din et al., 2017; Grzymski et al., 2019).

Natural fibers like teff straw, are environmentally friendly and economical construction materials with efficient cost and enormous abundances (Tesfaye, 2021). Teff straw is a by-product of teff grain harvesting, a crop with significant cultural and nutritional importance in Ethiopia and other regions of Africa (Amentae et al., 2016). Teff straw is a low-value material that is usually discarded, but recent studies have shown it to have excellent mechanical properties, making it suitable for use in concrete (Biratu et al., 2022). Polyethylene terephthalate fibers, on the other hand, are waste material from plastic bottles and containers (Manatura et al., 2021). They have been found to improve the tensile strength of concrete and reduce shrinkage and cracking (Nkomo et al., 2022). Studies have investigated the use of PET fibers separately in concrete production. However, there are limited researches on teff straw fiber and the effect of combining teff straw and polyethylene terephthalate fibers in concrete production. In the current study, the properties of Hybrid teff straw and polyethylene terephthalate fibers concrete such as workability, compressive strength, flexural strength, splitting tensile strength, water absorption and permeable void space were investigated experimentally.

1.2 Statement of the Problem

Now a day, civil engineering constructions have their own structural and durability requirements. Every structure has its intended purpose and hence to meet this purpose, modification in traditional cement concrete has become mandatory (Patil, 2015). It is well known that concrete is an extensively used construction material for its various advantages such as low cost, availability, fire resistance and the ability to be molded to any shape based on the requirement (Najaf & Abbasi, 2022; Yuan & Jia, 2021). However, due to its weakness in tension and issues with cracking, it is has problem to use alone everywhere. Once a crack has formed, water and destructive agents like chlorides and sulfates can penetrate quickly into the concrete, and they subsequently accelerate the corrosion process and seriously degrade the serviceability of the structures (Passuello et al., 2009). Therefore, it is necessary to enhance its strength and resistance to cracking.

The addition of fibers into concrete is most commonly used in construction industries as the resistance to cracking and strengthening of concrete. The inclusion of a single type of fiber into concrete has been proven by different researchers at different times showing an enhancement in concrete strength to a limited extent (Afroughsabet et al., 2016). Recently it was found that the performance of concrete reinforced with hybrid fibers of different sizes and types is superior to other fibers of monotype and size (Raj et al., 2020).

Previous studies have been reported on the development of a suitable hybrid fiber combination and most of these studies have mainly focused on using hybrid fibers like steel and Polypropylene, steel and glass, steel and carbon, and steel and palm fibers (Caggiano et al., 2017; Das et al., 2020; Martinelli et al., 2015). However, the use of hybrid teff straw and polyethylene terephthalate fibers as hybrid reinforcing fibers in concrete has not been studied yet. Therefore, the current study aimed to investigate the performance of concrete made with a combination of teff straw and polyethylene terephthalate fibers and determine their effects on properties such as workability, compressive strength, flexural strength, tensile strength, water absorption, and permeable void space.

1.3 Objectives of the Study

1.3.1 General Objective

The main objective of this research was to study the physio-mechanical properties of hybrid teff-straw and polyethylene terephthalate fiber reinforced concrete.

1.3.2 Specific Objectives

- ❖ To study the workability of control and hybrid teff straw and polyethylene terephthalate fibers concrete

- To determine the mechanical properties of hybrid teff straw and polyethylene terephthalate fiber reinforced concrete and conventional concrete
- To determine the effect of hybrid teff straw and polyethylene terephthalate fibers concrete on the water absorption and permeable void properties of concrete

1.4 Research Questions

- What is the workability of control and hybrid teff straw and polyethylene terephthalate fibers concrete?
- What are the mechanical properties of hybrid teff straw and polyethylene terephthalate fiber reinforced concrete compared to conventional concrete?
- What is the effect of hybrid teff straw and polyethylene terephthalate fibers concrete on the water absorption and permeable void properties of concrete?

1.5 Significance of the Study

The current study aims to use hybrid teff straw and polyethylene terephthalate fibers in concrete. Teff straw is agricultural waste material, which creates environmental problems (Biratu et al., 2022). Incorporating locally available agricultural byproduct teff straw and recycled materials PET fibers into construction materials promotes sustainability and reduces the accumulation of waste. The use of these agricultural waste and recycled materials in construction can reduce the cost of fiber-reinforced concrete. In addition, concrete arresting cracks and strength can be enhanced. Furthermore, this research plays a great role as a benchmark for further investigation.

1.6 Scope of the Study

The goal of the study was to look into the effect of the addition of hybrid Teff straw and polyethylene terephthalate fibers on C-30 concrete properties. The research focused on determining the physical properties of concrete ingredients properties. Slump and compaction factor tests of Workability, compressive strength, flexural strength, and splitting tensile strength of control concrete and hybrid teff straw and polyethylene terephthalate fibers reinforced concrete on the 7th and 28th days were conducted. Water absorption and permeable voids of hardened concrete on the 28th day were also determined. Finally, this study did not take into account the potential additional volume that could have resulted from the addition of concrete fibers without proportionally decreasing the amount of each ingredient.

1.7 Organization of the Study

The study was organized mainly into five chapters. The first chapter introduces the background, the statement of the problem, the objectives, the significance of the study, and the scope of the study. The second chapter was mainly a literature review that stated the study's matter. This section covers reviews on concrete ingredients; the meaning of fiber-reinforced concrete; factors affecting fibers reinforced concrete; the effect of fibers on the properties of concrete; and research gaps were covered. Third chapter presented the materials utilized and the experimental methodologies used to conduct various experiments. The fourth chapter relied on the presentation, analysis, and interpretation of the results of various tests. The fifth chapter was concerned with the conclusion and recommendations.

1.8 Summary

In this chapter, the background of the study and statement of the problem have been presented. Further, the general objective, specific objectives, scope of the study, significance of the study, and the organization of the study to achieve these objectives have briefly been presented. In the next chapter, the literature review and the gaps in the previous research have been presented.

CHAPTER 2
LITERATURE REVIEW

2.1 Introduction

To develop a better understanding of the research objective related to the use of hybrid teff straw and polyethylene terephthalate fibers on concrete properties, a comprehensive literature review has been conducted. As part of the study process, chapter two provides a literature review on the aspects of teff straw and polyethylene terephthalate fibers that have been previously researched and their effectiveness in enhancing the properties of concrete. Hence, the literature review structure consists of a detailed review of previous studies on the physical, mechanical, and durability properties of concrete reinforced with hybrid teff straw and polyethylene terephthalate fibers. The findings of the literature review would be reviewed and presented in subsequent sections.

2.2 General Concepts of Concrete and its Ingredients

Concrete is a mixture of aggregates and binders (Demissew et al., 2019). Concrete is one of the most widely implemented materials in the construction area worldwide, which is mainly composed of cement, coarse aggregate, and fine aggregate mixed with water (Das et al., 2020; Tarekegn et al., 2022).

2.2.1 Cement

Cement is a generic term that can be applied to all binder materials. From earliest times, builders have used binders in conjunction with stone to form more stable structures. Simple mud was employed as a binder and is still in use in parts of the world today (Gagg, 2014). Cement is a fine-gray powder that is used to form mortar or concrete when combined with water and other ingredients. When mixed with water, it forms a paste that hardens and sets due to hydration reactions and processes, allowing it to gain strength after hardening (Gashaahun, 2020). Almost all types of cement produced globally are used in combination with sand, gravel, and water to make concrete and mortar (Gagg, 2014). It is a necessary substance for today's civilization because it is an important part of concrete, and a necessary ingredient for the construction of homes and infrastructure (Z. Cao et al., 2020).

Construction cement has either hydraulic or non-hydraulic properties. While non-hydraulic cement won't set in damp or submerged conditions, hydraulic cement, like Portland cement, hardens as a result of hydration. Instead, when it is dry, it freezes and interacts with atmospheric carbon dioxide (Khatib et al., 1999). Hydration is the cement's reaction with water, according to cement chemistry. Even in humid air, cement can partially hydrate;

nevertheless, total hydration requires mixing cement with enough water (Beaudoin et al., 2019)

2.2.1.1 Normal Consistency of Cement

A conventional plunger with a diameter of 10 mm can be inserted up to a depth of 5 to 7 mm above the bottom of Vicat's mold when the cement paste is of a normal consistency, which is defined as a percentage of water by weight of cement. When cement is old and too fine with a high specific surface area, the normal consistency of cement paste is observed at higher levels (Dinku, 2002). According to (ASTM C187, 2016), normal consistency is measured as a percentage of dry cement weight and ranges from 22 to 30 %.

2.2.1.2 Setting Time of Cement

The amount of time it takes for the cement paste to stop being plastic after being mixed with water is known as the cement paste setting time. Initial and final setting times are the two categories under which cement setting time is divided. The time elapsed between adding water to the cement and the paste losing its flexibility and hardening is referred to as the initial setting time. While, the final setting time is the time interval between when water is added to the cement and when the paste has completely lost its plasticity (Zhang et al., 2010). According to (ASTM C150/C150M, 2012), the initial setting time should be no less than 45 minutes, and the final setting time should be no more than 375 minutes.

2.2.2 Fine and Coarse Aggregates

The most essential elements of concrete are the aggregates, which make up around 75% of the total volume. The massive amount of aggregates in concrete highlights their significance. In order to produce concrete, fine aggregates (less than 4.75 mm) and coarse aggregates (greater than 4.75 mm) must be graded (Ukala, 2019).

2.2.2.1 Grading and Fineness Modulus of Fine and Coarse Aggregates

Aggregate grading is the term used to describe the particle size distribution of an aggregate. Grading is the process of filling in the spaces left by bigger particles. A composite aggregate mix that is correctly graded may be created by using the appropriate ratios of different-sized aggregates. Since dense concrete is made with appropriately graded aggregate, it uses less fine aggregate than cement. Aggregate is graded using the percentage of weight retained on a set of specified sieves. Mesh sizes for sieves of (25 mm, 19 mm, 12.5 mm, 9.5 mm, 4.75 mm, and pan) are used grade coarse aggregate is given in Table 2.1 (Das et al., 2020).

Table 2. 1 Coarse Aggregate Grading Requirements

Sieve opening(mm)	Cumulative passing (%) ASTM C33
25	100
19	90-100
12.5	-
9.5	20-55
4.75	0-10
Pan	--

In addition, sieves with (9.5,4.75 mm, 2.36 mm, 1.18 mm, 0.60 mm, 0.30 mm, 0.15 mm, and pan) are used for grading fine aggregate (Table 2.2).

Table 2.2 Fine Aggregate Grading Requirements

Sieve opening(mm)	Cumulative passing (%) ASTM C33
9.5	100
4.75	95-100
2.36	80-100
1.18	50-85
0.6	25-60
0.3	5-30
0.15	0-10
Pan	--

The results of the sieve analysis are usually used to calculate a numerical index termed the fineness modulus (FM). According to ASTM C 136, the fineness modulus (FM) of fine or coarse aggregate is computed by combining the cumulative percentages by mass retained on each of a set of sieves and dividing the total by 100. The higher the value of FM the coarser the aggregate (Rahman et al., 2020). According to ASTM C 33, the FM for fine aggregate used in concrete is typically between 2.3 and 3.1

2.2.2.2 Specific Gravity and Water Absorption of Fine and Coarse Aggregates

Specific gravity is defined as the mass of a unit volume of aggregate divided by the mass of the same volume of water at a certain temperature. It's a non-dimensional value that's used to assess material strength and quality. Specific gravity is used to differentiate between unwanted particles that are lighter than other particles and good aggregates (Dinku, 2002).

The weight of the material in relation to the weight of the same amount of water is known as its specific gravity. This term assumes that the substance or material is solid.

Table 2.3 Specific Gravity and Water Absorption Formula for FA

Descriptions	Formula (ASTM C 128)
Weight of oven-dry specimen in the air(A)	$Bsg = \frac{C}{(B+C-D)}$
Weight of pycnometer filled with water (B)	$Asg = \frac{A}{(B+A-D)}$
Weight of the saturated surface dry specimen (C)	
Weight of pycnometer with specimen and water to calibration mark (D)	$WA(\%)=\frac{(C-A)}{A}*100$

Table 2.4 Specific Gravity and Water Absorption Formula for CA

Descriptions	Formula (ASTM C 128)
Weight of oven-dry specimen in the air(A)	$Bsg = \frac{C}{C-(D-B)}$
Weight of wire basket in water (B)	$Asg = \frac{A}{A-(D-B)}$
Weight of the saturated surface dry specimen (C)	
Weight of Saturated Specimen in water with wire basket (D)	$WA(\%)=\frac{(C-A)}{A}*100$

The apparent specific gravity of an aggregate refers to the solid components of the aggregate that do not include the pores, whereas the bulk specific gravity refers to the aggregate's entire volume that does include the pores (Warati et al., 2019). The quantity of water that a solid aggregate material can absorb is referred to as its water absorption capacity. The maximum water absorption capacity of fine aggregate is limited to only 3% as per the (ASTM C128, 2015) specification. The Pycnometer technique allows for the determination of both the specific capacity and water absorption capacity (Warati et al., 2019).

2.2.2.3 Silt Content of Fine Aggregate

The material in the fine aggregates that has a smaller size than 75µm is generally regarded as silt. Silt in the fine aggregate can have a severe effect on the quality of the concrete. It mainly affects the workability of the concrete, and also results in a reduction in strength. The silt content of the sample was determined in the laboratory using the ASTM C117 standard specification. According to the standard, the maximum silt content is limited to 3%.

2.2.3 Water

One of the most important components of cement concrete is water, which is also necessary for curing, washing, and cleaning concrete equipment as well as for washing aggregates. Concrete is affected by water in both positive and negative ways (Neville, 2000). Water contaminants might alter its physical properties, which would negatively affect the concrete's strength and cause the steel reinforcing to corrode. Acid, oil, salt, alkali, silt, sugar, organic loads, and other poisonous components that might harm the concrete should be absent from it. In order to produce special concrete, potable water is, therefore, necessary to ensure the proper curing time, strength, and chemical reaction of the cement (Biratu et al., 2022).

2.3 Teff Plant

Teff grain production accounts for 25% of total cereal production in Ethiopia, and was reported to be about 4.3 million ton in 2015 (Lyddon, 2015). Tef straw yield is about 3 times that of the grain, at about 5-7 ton DM/ha (Keftasa, 1988). It can thus be estimated that there was about 13 million ton of teff straw available in Ethiopia in 2015 (Lyddon, 2015).Teff is the most important cereal crop farmed in Ethiopia's high-rainfall and drought-prone regions, where it takes up over 30% of the land designated for cereal (Bayable et al., 2021). Teff comes in three primary varieties: red (brown), white, and mixed (white, red, and brown), each of which is unique to certain growth circumstances. Only a few places in Ethiopia cultivate white teff, which is quite popular. It is the most costly, contains surplus straw, and calls for the most exact growth conditions (Hagos et al., 2012).

2.4 Teff straw

One of the best and most abundant sustainable construction materials in the world is straw. Teff straw, a byproduct of agriculture, is a useful source of animal feed during the rainy season and is widely accessible in Ethiopia (Wassie et al., 2017). Since ancient times, Ethiopia has utilized teff straw, one of the oldest natural fibers, as a reinforcement fiber for mud brick baking and mud plastering (A. Tadesse, 2019). During house construction (mainly in rural areas), use teff straw to reinforce the mud used to cover the wooden material. Although it is used for plastering, its usage is very rare and undergoes unnecessary burning which, in turn, results in an emission problem (Biratu et al., 2022). Every year, more than 2 million tons of teff straw are discarded like garbage in Ethiopia (Bachewe et al., 2019). Numerous unprocessed natural fibers are available in many of the developing countries, and some are potentially attractive as reinforcement for cement-based composites simply because of ready availability in large quantities at low cost as a continuously renewable resource. Natural fibers appear as a low cost and eco-friendly alternative than synthetic fibers (Vajje et al., 2013). Natural fibers appear as a low-cost alternative, due to their natural and large-scale occurrence, mainly in developing countries and with high housing deficit (de Souza Castoldi et al., 2022).

2.5 Polyethylene Terephthalate (PET) fibers

The most widely used thermoplastic polyester is polyethylene terephthalate (PET). For storing carbonated and non-carbonated drinks, PET is mostly utilized in the form of bottles (Manatura & Samaksaman, 2021). The majority of PET bottles are single-use, and they are disposed of after use by either being buried or burned. PET trash may be used in a variety of applications, including the building of bases, subbases, walls, load-bearing bricks, and components of asphalt (Awoyera et al., 2021). Recycling plastic material is an environmentally friendly method to reduce plastic pollution and also conserve precious raw petrochemical resources (Ghalampour et al., 2019).

Utilizing plastic waste as fibers in concrete could become very common, mitigate environmental risks, and improve concrete properties. Plastic fibers are a viable substitute for steel fibers in concrete because they are inexpensive, low-energy-consuming, and exhibit good corrosion resistance (Pereira et al., 2017). For instance, polyethylene terephthalate (PET), one of the most popular plastics recovered from used bottles, has achieved many major environmental advantages by discovering a possible sustainable use by turning this sort of trash into useful material (Al-Hadithi et al., 2019). Additionally, the addition of PET fibers to concrete improved its desirable characteristics.

In their research, (Kassa et al., 2019b) investigated the cost implications of incorporating polyethylene terephthalate (PET) fiber reinforced concrete with fly ash as a partial replacement for cement. The cost analysis of PET fibers took into account the expenses associated with labor for collection, cleaning, and cutting. The unit price per kilogram for the collection, cleaning, and cutting of PET fibers was equivalent to 100 Kenyan shillings, which was roughly equal to 1 USD.

2.6 Properties of teff straw and polyethylene terephthalate fibers

Different properties of teff straw and polyethylene terephthalate fibers from the reviewed literatures were summarized in the Table 2.5 below.

Table 2.5 Summary of properties of teff straw and polyethylene terephthalate fibers (Aziz, 2017; Biratu et al., 2022; Devnani et al., 2020; Hidaya et al., 2017; Kassa et al., 2019a; Tesfaye, 2021; Teshome, 2022; Zhou et al., 2018)

Properties	Teff straw fiber	PET fiber
Length	40mm-60mm	12mm-100mm
Diameter/width	0.4mm-1.2mm	0.038mm- 5mm
Aspect ratio	30-100	8- 50
Water Absorption (%)	60.7	0
Shape	Cylindrical	Rectangular
Color	Brown-reddish and white	Colorless
Tensile strength	280 MPa –326 MPa	290 MPa –800 MPa
Modulus elasticity	9.2GPa–10.7 GPa	1160MPa-11500 MPa
Density	0.998 g/cm^3-1.2 g/cm^3	0.97g/cm^3-1.37g/cm^3

2.7 Hybrid fiber reinforced Concrete

2.7.1 Meaning of Hybrid fiber reinforced Concrete

One of the construction industry's most promising current construction techniques and repair materials is hybrid fiber-reinforced concrete (HFRC). By combining different types of fibers, fiber hybridization helps concrete constructions resist cracking (Das et al., 2020). One metallic and one non-metallic fiber are combined to create HFRC or simply two distinct types of fibers (Yao et al., 2003). Hybrid fiber reinforced concrete is being considered nowadays due to its several structural benefits as compared to that plain concrete (Khan et al., 2018). In HFRC, hybridization refers to the appropriate combination of two or more fibers with various characteristics to maximize the benefits of each product. Fiber type, length, diameter, strength, elastic modulus, and other characteristics are taken into account (B. Li et al., 2018).

2.8 Concrete Batching

The act of weighing or volumetrically distributing several concrete ingredients (cement, sand, coarse aggregate, and water) before mixing is known as “concrete batching” (Joshua et al., 2018). In a study on concrete, Hedidor et al. (2017) concluded that using the volumetric batching method in concrete production is bad construction practice.

2.9 Concrete Mix Design

For concrete to have the necessary strength, the proper ratios of cement, fine aggregate, and coarse aggregate must be established. In order to maximize strength and durability, depending on the construction site, concrete components are cost-effectively proportioned in a mix design. The two forms of concrete mix design are nominal concrete mix and designed concrete mix. The nominal concrete mix may contain more cement, while the amount of cement required for the same grade of concrete for a specific site may be less in a designed mix (Chabi et al., 2018).

2.10 Concrete mixing

According to the findings of He et al. (2020), the initial step involved dry mixing all the solid components, such as cement, river sand, and recycled coarse aggregates, using a rotary mixer for approximately 30 to 60 seconds. Subsequently, fibers were manually introduced into the mixture in a flowing state and mixed for approximately 60 seconds to guarantee even dispersion as observed visually. Finally, pre-prepared mixtures of water and superplasticizer were incorporated, and the mixing process continued for another 90 to 120 seconds.

2.11 Effect of fibers on properties of fresh concrete

2.11.1 Workability

The workability of fresh concrete gives an idea of the frictional behavior of the concrete from the time it is mixed to the time it is compacted. It has four major components: the ability of the concrete to be mixed, transported, molded, and compacted (Biratu et al., 2022). Rahmani et al. (2013) the slump test is performed for mixes before pouring into molds following ASTM C143/143M-15a for the workability of Plain Concrete. The same procedure was used to determine the workability of all concrete mixes.

Belhadj et al. (2014) investigated that straw fiber will reduce workability. The slump value of concrete decreases as the amount of straw fiber increases. Due to the presence of thin straw fibers in the concrete, the slump value of the concrete is low, and the water absorption coefficient is increased. When straw fiber is added to concrete, it will absorb the moisture present in the concrete and a smaller amount of free water in the concrete. Tadesse (2019) studied the fresh characteristics of concrete containing 0%, 0.10%, 0.20%, and 0.30% teff straw fibers and found that the fibers decrease the workability of the concrete. As the amount of straw fiber is increased, the slump value of concrete drops. The workability of fresh concrete decrease with increased content of PET fibers for all mixtures (Adnan et al., 2020).

According to Das et al. (2020), increasing the amount of hybrid fibers reduced the slump value of all HFRC mixtures. The drop for the control mix was 98 mm, whereas it was 76 mm, 64 mm, and 42 mm for the Mix 1, Mix 2, and Mix 3 mixes, respectively. This drop in slump value was linked to the hybrid fiber inclusion, which can cause fiber balling and lower the slump value, in the concrete mix. A similar consistent finding was also observed in the reduction trend of the slump by the addition of hybrid fiber in the concrete mixes (Rudraswamy et al., 2018)

Das et al., 2020 observed that HFRC exhibited a gradual reduction of a compacting factor with increasing the concentration of hybrid fiber in the concrete mix, suggesting that the mechanical interlocking of hybrid fiber leads to the significant controlling mechanism of a compacting factor of the concrete. The compaction factor value was obtained around 0.93 for the control mix, while it was about 0.81, 0.70, and 0.62 for the hybrid fiber mixes 2%, 4%, and 6% respectively.

2.12 Concrete Casting and Curing

Curing concrete needs to provide adequate moisture, temperature, and time for the cement to continue to hydrate until the concrete reaches the desired properties. Curing enhances the toughness, water tightness, abrasion resistance, volume stability, and resistance to freezing and thawing of hardened concrete (Dnyanoba et al., 2020).

2.13 Effect of Fibers on Properties of Hardened Concrete

2.13.1 Compressive Strength

In their study of the compressive behavior of concrete reinforced with natural wheat straw and treated wheat straw, Farooqila et al. (2016) found that natural wheat straw reinforced concrete had a 10% reduction in compressive strength while treated wheat straw reinforced concrete had a 26% reduction. Wang et al. (2018) identified the performance of Rice straw fibers on concrete with the addition of straw fibers at 1%, 2%, and 3%. Increasing the fiber content will affect the strength of the concrete, with the increase in fiber dosage will decrease the compressive strength of fiber-reinforced concrete for 7, 14, and 28 days. results show that the compressive strength decreases with the increase in straw fiber content. According to the study by Biratu et al. (2022) investigated the potential use of nano silica-based teff straw as an eco-friendly replacement for special concrete, there was an enhancement in compressive strength of the special concrete when compared to the conventional concrete.

Based on tests by Nibudey et al. (2013) compressive strength enhancements of 5.26% and 7.35% were obtained as the concrete is reinforced with 1% PET fiber of aspect ratios of 35 and 50, respectively. In another study by Aziz (2017), there is a 5.1% compressive strength increase when 0.75% PET fiber is used. Compressive strength loss was also observed by Kim et al. (2010) on using PET fiber of 50 mm length in concrete, being increased with increasing fiber volume up to 1%. One can find that PET fiber addition has a limited beneficial action to enhance the compressive strength of some normal concrete mixes, but for high-strength concrete, there is a relatively large strength loss (Mohammed et al., 2020). Ataei et al. (2017), studied the compressive strength effect of recycled PET particles in concrete. The research reported a decrease in compressive strength after adding PET particles. This occurrence was attributed to the weak cohesion between the particles and the cement resin. A similar conclusion of a general decrease in compressive strength with PET particles to concrete. Due to poor bonding caused by the fibers' smooth texture, which made it difficult to compact the mixture to attain the appropriate strength, the compressive strength and density of concrete declined as the amount of PET fibers increased. PET fibers thus cannot be utilized to increase concrete's compressive strength (Hidaya et al., 2017).

Concrete's engineering properties, such as its tensile strength, flexural strength, impact, fatigue, abrasion resistance, deformation capability, toughness, and load-bearing capacity after cracking, can be significantly improved by the inclusion of fibers in the matrix, according to numerous studies (Awang et al., 2013; Jiang et al., 2014; Monteiro, 2006). There is no consensus on the effect of fibers of different types on the compressive strength of concrete. According to some reports, the presence of fibers in concrete can result in a reduction in its compressive strength, due to matrix disturbances increasing the porosity of the material (Neves et al., 2005). However, some reported an increase in compressive strength (Atiş et al., 2009; Bei-Xing et al., 2004).

2.13.2 Split Tensile Strength

Abayomi (2018) has observed a percentage increment of sisal fiber reinforced concrete for both at 7 and 28 days of curing. The percentage increment was 19.07% and 29.14% at 7 days and 29.68% and 47.17% at 28 days and the results were obtained at 0.5 and 1% fiber additions. Further addition of sisal fiber of more than 1% results in a percentage reduction of split tensile strength at 7 and 28 days. Biratu et al. (2022) have indicated that the inclusion of 0.15% nanofiber-based teff straw was the optimal proportion leading to a noteworthy enhancement in splitting tensile strength. Tests on normal concrete by Nibudey et al. (2013) showed maximum splitting tensile enhancements of 15.47% and 24.91% related to using 1% PET fiber of aspect ratio equal to 35 and 50, respectively. In other tests, showed a maximum tensile strength enhancement of 12.5% related to using 1% PET fiber volume. One can observe a different action of PET fiber in normal strength and high strength concretes on the splitting tensile strength, and there is a chance for this kind of plastic fiber to enhance the tensile behavior of concrete of low strength performance (Mohammed & Rahim, 2020).

According to research conducted by Hidaya et al. (2017), concrete's splitting tensile strength can be increased by up to 1% by adding pet fibers. Beyond 1%, however, the strength may be reduced by the addition of more fibers. Therefore, 1% PET fiber addition can also promote ductility and crack control by serving as bridges across cracks. This improved strength is due to the fibers bridging across cracks and adding more ductility, as the concrete requires more time to break down than normal concrete specimens do. The bridging effect of fibers defers the appearance of cracks, and lowers the concrete stress concentration at the cracks, so it can increase the splitting tensile strength of concrete (Jiang et al., 2014; jun Li et al., 2016). However, high content of fibers may lead to an increase in porosity, which will adversely affect concrete and reduce the tensile strength of concrete (Yehia et al., 2016). Dawood et al. (2012),investigated the mechanical properties of hybrid fiber as a 2 vol.% fraction. The researchers tested hybridizations of steel fibers, palm fibers, and synthetic fibers (barchip) by incorporating them with high strength flowing concrete (HSFC) in terms of splitting tensile strength. The results demonstrated that the hybridizations of these fibers enhanced the tensile strength of the HSFC.

2.13.3 Flexural Strength

Wang and Han (2018) observed the compressive and flexural strength of rice straw-reinforced concrete and obtained a result of less improvement in flexural strength. As the percentage addition of fiber increases the strength of concrete decreases compared to the control mix. Sabarish et al. (2017) investigated the strength and durability of sisal fiber reinforced concrete and observed that for all curing ages of concrete produced with sisal fiber as reinforcement, the flexural strength has been improved to the maximum. For each, all percentage addition of sisal fiber the flexural strength was increased. Bederina et al. (2016) found that with the addition of treated barley straw fiber by any type of treatment, there was an improvement in flexural strength. With Hot water treatment, maximum flexural strength was recorded to be 5.21N/mm2 compared to normal concrete.

In their recent, Biratu et al. (2022) investigated the potential use of nano silica-based teff straw as an eco-friendly replacement for special concrete. The authors produced C-25 grade concrete cubes, cylinders, and prisms with teff straw fibers added in proportions of 0%, 0.15%, 0.25%, and 0.35% by weight of concrete, and evaluated the 7-day and 28-day strength of the specimens. The results indicated that the inclusion of 0.15% nanofiber-based teff straw was the optimal proportion leading to a noteworthy enhancement in the flexural strength of the special concrete when compared to the conventional concrete.

In a study conducted by Najaf and Abbasi (2022), the use of macro-synthetic polypropylene fibers (Forta and Barchip) in concrete was investigated. The fibers were added at varying percentages (0.5% to 2% of cement weight) and different combinations were tested using various concrete specimens. The study found that incorporating certain fiber percentages led to significant improvements in concrete strength and ductility. Hybrid samples combining both Forta and Barchip fibers had increased flexural strength by 58%. In the research conducted by Bankir et al. (2020), the interactional effects of four different fiber types (steel, glass, synthetic, and polypropylene) were investigated. The total fiber volume used in the high fiber content (HFC) was determined by four groups of fiber combinations, ranging from 0% to 2% of the total blend volume. The hybridization of fibers in concrete was found to enhance the flexural strength by combining the unique properties of the fibers.

2.14 Effect of Fibers on Density, water absorption, and permeable void pores

The ability of concrete to endure weathering, chemical attacks, abrasions, and other degrading processes is referred to as its durability. The ability of concrete to move fluids through it as a result of a pressure head differential is referred to as permeability. This property of concrete contributes to the concrete's durability by preventing the entry of moisture, which may contain harsh chemicals, as well as the flow of water during heating and freezing (Swaroop et al., 2013). In a study conducted by Abayomi (2018), it was observed that the density of concrete was generally found to be less than 2400 kg/m^3**.** The density of sisal fiber reinforced concrete were decreased with an increase in sisal fiber content. The water absorption test is a vital durability test. Quality concrete is expected to exhibit low permeability of water. According to (ASTM C642, 2006), water absorption indicates the ingress of water into the pores of the concrete.

Abayomi (2018) examined the sisal fiber-reinforced concrete's water absorption characteristics, and the results showed that sisal fiber increases concrete's water absorption significantly. It was observed that there was a sudden rise in water absorption with the addition of 0.5% fiber and the absorption increases while the fiber content rises. Because there were more pores in the mix when PET fibers were added, the concrete absorbed more water. Because this will reduce the concrete's durability, PET fiber concrete should not be utilized in corrosive environments (Hidaya et al., 2017).

The volume of permeable voids (VPV) is an important property of concrete as it affects the transport mechanisms through the concrete such as ingress of aggressive liquids and gases

(Teo et al., 2010). The ASTM C642 method measures the volume of permeable voids as a percentage of the volume of the solid. Porosity is one of the major parameters, which influence the strength, and durability of concrete. The porosity of a porous material, such as cement paste, mortar, concrete and other porous material can be determined by measuring any of two quantities; bulk volume, pore volume or solid volume. The porosity is the fraction of the bulk volume of the material occupied by voids (Kreem, 2012).

2.15 Factors affecting hybrid fiber reinforced concrete

Because fiber-reinforced concrete is a composite material made of cement matrix and fiber-reinforced material that can be dispersed either randomly or in an organized fashion, the performance of the material depends on the stress transfer between the fiber and cement matrix. The workability of the concrete, the size, shape, and distribution of the aggregates, as well as the number, kind, and distribution of the fibers, all affect the performance of the material.

2.15.1 Quantity of fibers

The amount of fibers employed greatly affects the strength and toughness of fiber and cement composites (Z. Li et al., 2006). This relationship is usually linear, meaning that the form of fibers increases the strength and toughness of the composite. The disadvantage of high fiber value leads to the segregation of concrete and mortar (Matar et al., 2019). Between 0.5 % and 2.5 % of the total volume of concrete in concrete mixes are the most useful volume fractions of fiber (Yazıcı et al., 2007).

2.15.2 Fiber Aspect Ratio

The aspect ratio of the fiber (the ratio of length to diameter) is one of the important characteristics. The fiber aspect ratio plays a key role in effectively improving the mechanical properties of concrete (Mostofinejad et al., 2015). When the aspect ratio is high, the relative strength and toughness will decrease. The lower fiber aspect ratio can produce higher compressive strength, while higher energy-absorbing materials can lead to higher flexural strength, toughness index, and impact strength (Sudhikumar et al., 2014).

2.15.3 Orientation and Distribution of Fibers

The orientation and distribution of the fibers will affect the final hardened properties and the flow of fresh concrete properties (Zhao et al., 2021). Unlike standard steel bars, which have the steel bars orientated in the desired direction, the orientation of the fibers is random. To enhance the properties of concrete, fiber orientation, and distribution should be uniformly dispersed and randomly orientated (F.-Y. Li et al., 2018).

2.15.4 Workability of Concrete

By making aggregate movement more difficult by lowering the lubricating effect of cement paste, the use of fibers in concrete will make it less workable and have a significant impact on concrete compaction (Figueiredo et al., 2015).

2.16 life cycle cost analysis

Life Cycle Cost Analysis (LCCA) is a method used to assess the total cost of owning a facility or running a project . It is an analytical technique that uses economic principles to evaluate long-term alternative investment options. LCCA can be applied to any capital investment decision in which relatively higher initial costs are traded for reduced future cost obligations. It is particularly suitable for the evaluation of building design alternatives that satisfy a required level of building performance but may have different initial investment costs, different operating and maintenance and repair costs, and possibly different lives (França et al., 2021).

LCCA should be performed early in the design process while there is still a chance to refine the design to ensure a reduction in life-cycle costs. The analysis enables total cost comparison of competing design alternatives with equivalent benefits. LCCA accounts for relevant costs to the sponsoring agency, owner, operator of the facility, and the roadway user that will occur throughout the life of an alternative. The scope of LCCA might vary from a "back-of-the-envelope" study to a detailed analysis with thoroughly researched input data, supplementary measures (Durairaj et al., 2002).The first step when performing an LCCA is determining the economic impact of the alternatives available. The effects are then quantified and expressed in monetary terms. Probably another important element of LCCA is disposal cost. When the disposal cost is incorporated, it is possible to offset any additional cost incurred during a particular year .

Comparative Life Cycle Cost (LCC) Analysis is necessary for several reasons. Firstly, it helps in selecting the most cost-effective approach among various alternatives by comparing the total cost of ownership. This allows decision-makers to choose the option that provides the lowest long-term cost of ownership while meeting the desired performance objectives. Secondly, comparative LCC analysis serves to demonstrate the most cost-effective solution within the limits of the analysis (Fuller, 2010). By comparing the total cost of ownership of different alternatives, it helps identify the option that offers the best value. Furthermore, it is commonly used to evaluate different pavement design strategies and determine their relative value. Comparative LCC analysis enables a comparison of the total cost of ownership of various pavement design strategies, aiding in the selection of the most cost-effective approach. Lastly, comparative LCC analysis is essential for estimating the overall cost of project alternatives. By comparing the total cost of ownership of different alternatives, it provides an estimation of the overall cost of each option, aiding in decision-making.

2.17 Summary of literature review

Table 2. 6 Summary of literature review on fiber-reinforced concrete test results

S.No	References	Types of fiber	Concentration of fibers	Main Findings
1	Farooqila et al. (2016)	Wheat straw	3% by mass of cement	Reduction in compressive strength by 10%
2	Biratu et al. (2022)	Teff straw	0.15% - 0.35% by weight of concrete	Reduction of slump value
				Reduction of fresh concrete density Improvement of compressive strength by 17.08%
				Improvement of tensile strength by 5.21%
				Improvement of flexural strength by 19.38%
3	Nibudey et al. (2013)	PET	0% - 3% by volume of concrete	Reduction of slump and compaction factor values
				Enhancement in compressive strength by 5.26%
				Enhancement in split tensile strength by 15.47%
				Enhancement in flexural strength by 17.32%
4	Aziz (2017)	PET	0.5% - 2% by volume fraction	Showed reduction in a slump
				Increment in compressive strength by 5.1%
				Enhancement in flexural strength by 12.5%

				Enhancement in split tensile strength by 12.5%
5	Das et al. (2020)	Steel and Coconut	2%, 4%, and 6% by weight of cement	A drop of the slump by 38%
				Reduction in compaction factor by 12.9%
				5% to 16% reduction in fresh concrete density
				18.36% improvement in tensile strength
				24.87% strength improvement in flexural
6	Raj et al. (2020)	Polyvinyl alcohol and coir	volume fraction 0.3%, 0.4%, and 0.5%	34% improvement in compressive strength Increment in tensile strength by 27%
7	Hidaya et al. (2017)	PET	1%, 2%, and 3% of the weight of cement	Reduction in the slump values
				Increment in water absorption
				Reduction in compressive strength
				Improvement in the splitting tensile strength
8	Awang et al. (2013)	Polypropylene and kenaf fiber	0.25% and 0.4% by volume fraction	Not much contribution in compressive strength
				Improvement in the flexural and tensile splitting
9	Jiang et al. (2014)	basalt	0.05%, 0.1%, and 0.3% by volume fraction	Slump dropped to a certain extent
				The compressive strength showed no increment

				Improvement in the tensile strength and flexural strength
10	Abayomi (2018)	sisal	0.5%, 1.0%, 1.5% and 2.0% by weight of cement	The workability reduced Couldn't improve the compressive strength Improvement in in the split tensile strength Decrement in density as fiber increase Increment water absorption and void space
11	Najaf et al. (2022)	Forta and Barchip	0.5%, 1%, 1.5%, and 2% by weight of cement	The hybrid usage of fibers Improved flexural strength
12	Dawood et al. (2012)	steel, palm, and synthetic	2 % by volume fraction	Enhancement the flexural toughness Enhancement the tensile strength of the HSF

2.18 Research Gap

The literature review in the previous sections on the effect of fibers on the properties of concrete reveals that several researchers have carried out studies on the subject. However, there is a gap in the use of hybrid teff straw and polyethylene terephthalate fibers (HTPF) as an addition to concrete to minimize the consumption of non-renewable materials, and environmental pollution is crucial. When it comes to the use of inferential statistics, there is a gap. These statistical techniques have not been sufficiently applied by earlier researchers to analyses their data. In addition, a noticeable gap emerges when previous researchers fail to reach a consensus on the impact of fibers on the compressive strength of concrete. This inconsistency calls for further investigation and presents an opportunity for the current study to contribute valuable insights. Due to this, the current study focused on the experimental investigation of hybrid teff straw and polyethylene fibers reinforced concrete properties such as effect on the workability, compressive strength, flexural strength, split tensile strength, and density, water absorption and permeable void space of concrete. Furthermore, the application of the Two-Way ANOVA method, however, used in the current study to show statistical significance.

In this chapter, various research works carried out across the world in the area of hybrid teff straw and polyethylene terephthalate fibers on the properties of concrete were reviewed to identify the research gaps that enabled setting the objective for this research. The next chapter discusses the materials and methods adopted to achieve the objectives of the study.

CHAPTER 3

MATERIALS AND METHODS

3.1 Materials

The literature review in the previous chapter has discussed various past studies and research gaps about hybrid fibers reinforced concrete. Based on the identified research gaps, chapter one outlines the research objectives set for this study. This chapter explains the materials and methods adopted to accomplish the study's objectives.

3.1.1 Cement

Cement consists of a fine, powdery mix of argillaceous, siliceous, and calcareous components, combined with iron oxide, gypsum, and a few other chemicals to create a durable and strong bonding material when combined with water. Ordinary Portland Cement (OPC) is a popular construction material known for its mechanical properties, ability to enable early stripping, and overall high quality. In this experiment, locally available National OPC 42.5 N grade cement was used obtained from shops within Adama, Ethiopia. During the experiment, the selected OPC was carefully stored in an airtight container to prevent exposure to moisture, atmospheric elements, and humidity. This cautious storage method ensured that the cement maintained its quality and conformed to the (ASTM C150/C150M, 2012) standard throughout the experimental period.

3.1.2 Fine Aggregate

Fine aggregate is a granular substance composed of tiny rock grains that is finer than gravel but coarser than silt. Fine aggregate is sand that passes through a sieve size of 4.75 mm and is retained at 150 mm. It should be free from lumps, organic material, silt, etc. Additionally, it should be robust and durable (Dinku, 2002). According to ASTM specifications, fine aggregate should not absorb more than 5% of water. Fine aggregate for the current study was obtained based on the (ASTM C33/C33M, 2018) standards requirements.

3.1.3 Coarse Aggregate

The aggregates retained on the 4.75 mm sieve are classified as coarse aggregates. It is an irregular and granular material made of crushed stone, obtained from quarries by crushing by hand or using a crusher. Clay, silt, dirt, and organic materials must be removed from the coarse aggregate. Soft, porous rock can limit the strength and wear resistance; it may also disintegrate during concrete mixing, which affects the workability of fresh concrete by increasing the number of fines adversely. The coarse aggregate used to make up the concrete samples in this work consists of crushed gravel, which was collected from a local quarry that confirms the requirements of ASTM C33. Crushed natural stone chips with a nominal maximum size of 19 mm were used in this study. According to ASTM C33, the coarse aggregate utilized for the experiment should be strong, durable, free of vegetable matter, with less than 5% water absorption, and not sharp and angular.

3.1.4 Water

Water is an essential component of concrete because it participates in the chemical reaction between cement and water. Water was also utilized to mix the concrete, cure it, and wash the aggregate. As a result, water must be free of pollutants that cause quality degradation, such as alkalis, suspended particles, acids, silt, clay, and dissolved salt. The water utilized in this study was tap water from Adama Science and technology university construction material laboratory water supply pipe, which meets the ASTM C1602 standard.

3.1.5 Fibers

Fibers are one of the most important materials used in the current study. Teff straw and Polyethylene Terephthalate Fibers were employed in this investigation as natural and synthetic fibers, respectively. The fibers in this paper are utilized in various dosages and combinations.

3.1.5.1 Teff straw fiber and Preparations

Natural teff straw fibers used in this study were collected from the local farmers around Adama City.

Then the teff straw fibers were kept in water for 24 h to extract harmful components. After that, the fibers were collected from water and sundried for 6 h. Teff Straw of length in the range of 45-60 mm and 0.8 to 1.2 mm diameter, to have the aspect ratio of 30- 100 mm taken

(a) (b)

Figure 3.1 a) Cutting teff straw using a pair of scissors, b) Teff straw washed and air-dried and used as an additive material in this study. Teff straw fiber was cut to get appropriate aspect ratio sizes manually as shown in Figure 3.1(a).

3.1.5.2 Polyethylene terephthalate fiber and Preparations

The PET fibers were obtained by collecting discarded PET drinking water bottles of 10 L storage capacity from the surrounding environment, labels removed, cleaned, dried, and then

Figure 3.2 Preparation of PET fibers

shredded into rectangular strips manually using a pair of scissors and a knife. The fibers were prepared with a constant width of 3 mm and lengths of 60 mm hence the Aspect ratio-20.

3.2 Methods

The current study employed an experimental method to achieve the aim of the research. The main purpose of the test method was to investigate the effect of HTPFs on concrete properties. To achieve the aim of the current study, different laboratory tests were conducted according to different standard procedures. The outcomes of the tests were quantitatively and qualitatively analyzed based on the standard requirements or specifications. Origin Pro 2022 software and Excel software were used to analyze the results. Furthermore, analyzed data was presented through the table, figures, and chart. Figure 3.3 illustrated the research methodology flow chart of the current study.

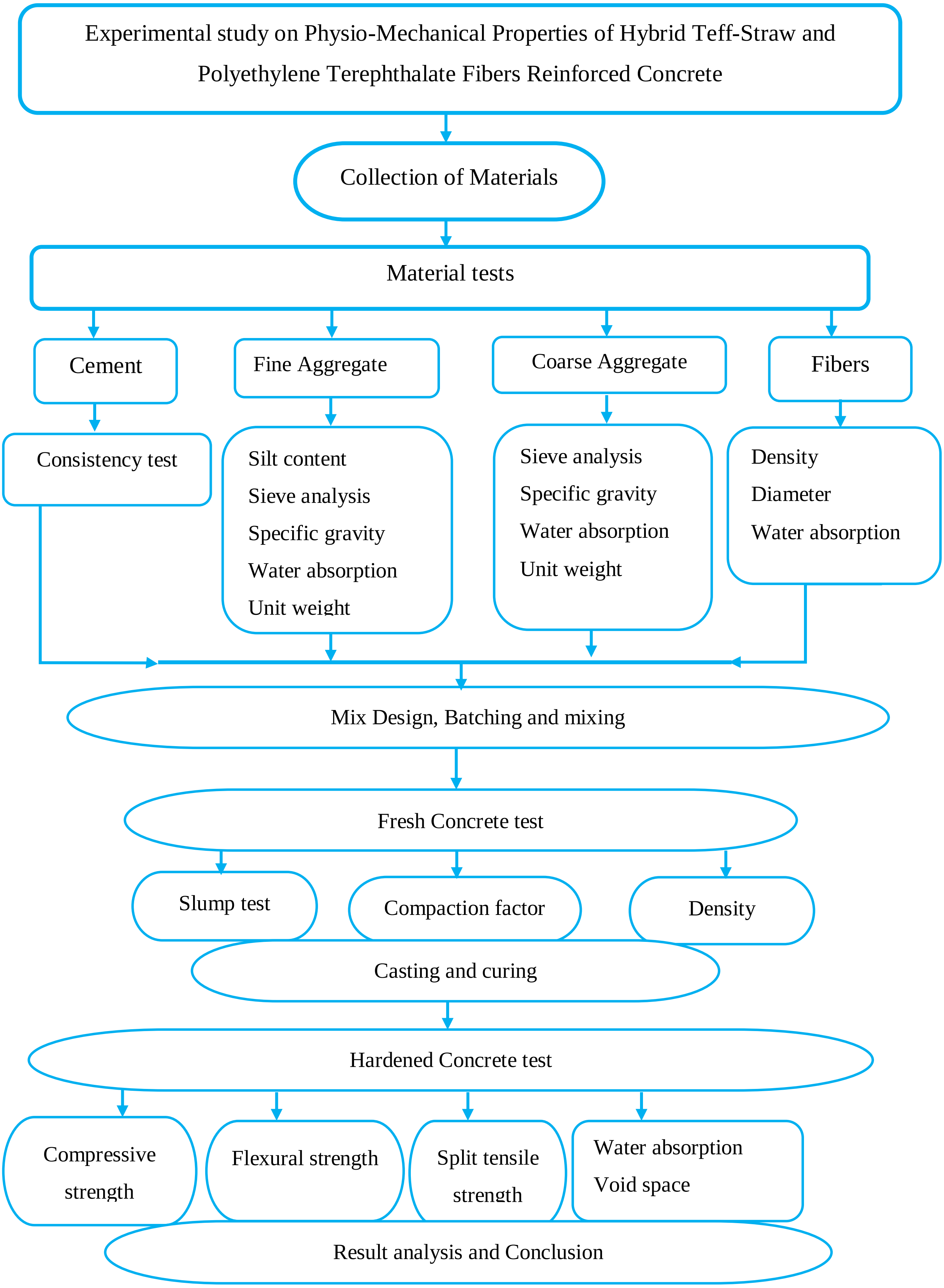

Figure 3.3 Research methodology flow chart of the current study.

3.2.1 Tests on Cement

3.2.1.1 Normal Consistency Test for Cement

The consistency of cement test is used to evaluate how much water should be added to cement to achieve standard consistency. The normal consistency test of cement is recommended to be measured using the (ASTM C187, 2016) method. As a result, a Vicat apparatus was used to determine the typical consistency. This test was performed according to the instructions in (ASTM C 187, 2016) shown in the Appendix A.

Figure 3.4 Normal consistency of cement test

3.2.2 Tests for Fine Aggregate

3.2.2.1 Silt Content of Fine Aggregate

Silt content is a fine material, which is less than 150 μm. It is unstable in the presence of water, which will reduce its strength and cause rework (Dinku, 2002). This test was carried out according to (ASTM C117, 2017) standards. As a result, testing the silt content of sand and comparing it to acceptable limits is critical. The major goal of this test was to figure out how much silt was in the sand. For this experiment, sample sand, clean water, a graduated jar, a spoon, a dish for taking a sand sample, and a funnel were used. The detailed procedures were followed based on ASTM C 117 as shown in the Appendix B1. The silt content was calculated based on Equation 3.1.

$$\text{Silt content (\%)} = \frac{\text{The volume of silt deposited above the FA(A)}}{\text{Volume of FA(B)}} * 100 \qquad \text{Equation 3. 1}$$

3.2.2.2 Sieve Analysis of Fine Aggregate

Sieve analysis is a procedure used to assess the particle size distribution of granular material by allowing the material to pass through a series of sieves of progressively smaller mesh sizes and weighting the amount of material that is retained in each sieve as a fraction of the whole mass. Hence, this test aimed to determine the fineness modulus of fine aggregate with the help of a series of sieves having (9.5 mm, 4.75 mm, 2.36 mm, 1.18 mm, 0.6 mm, 0.3 mm, 0.15, and pan) sizes from top to bottom, respectively, 500 g of fine aggregate, a balance, sieve shaker, shovel, and sieve brush. The test procedure was as per (ASTM C136, 2006). According to ASTM C 33, the FM for fine aggregate used in concrete is typically between 2.3 and 3.1. The gradation chart was filled in and the fineness modulus (FM) was computed.

$$FM = \frac{\sum(\text{Cumulative \% retained sieve of } 150\mu m \text{ or above})}{100} \qquad \text{Equation 3. 2}$$

3.2.2.3 Specific Gravity, and Water Absorption of Fine Aggregate

Specified gravity is defined as the mass of a specific volume of a substance divided by the mass of an identical amount of water, and it indicates how much heavier the material is than water. The difference in weight between the surface-dried saturated aggregate and the oven-dried aggregate is used to calculate an aggregate's water absorption. The specific gravity and water absorption capacity of fine aggregate were calculated using the ASTM C128 standard in this experiment. The range of specific gravity is 2.5–3 (ASTM C128, 2015).

Preparation of the Test Specimen:

1. Approximately 1 kg of the fine aggregate was prepared and at 110°C, the sample was dried to a constant weight in a suitable pan. Allow it to cool for 24 hours and then make it saturated.
2. The excess water was decanted with care to avoid loss of fines, spreading the sample on a flat, non-absorbent surface exposed to a gently moving current of warm air.
3. The sample was stirred frequently to get homogeneous drying until achieving the saturated surface dry condition by using the cone test for surface moisture.
4. Hold the mold firmly on a smooth, non-absorbent surface with a large diameter. Placed a portion of partially dried fine aggregate loosely in the mold by filling it to the brim and heaping additional materials above the top of the mold.
5. Lightly tamp the sand into the mold with 25 light drops of the tamper about 5 mm above the top surface of the sand.
6. The surface was adjusted by removing loose sand from the base and lifting the mold vertically. If surface moisture was still present, the sand would retain the molded shape. When the sand slumped slightly, it indicated that it had reached S.S.D. condition.

Bulk specific gravity, apparent specific gravity, and absorption capacity of fine aggregate were computed through 3.3 to 3.5 equations.

$$\text{Bulk specific gravity} = \frac{C}{B+C-D} \qquad \text{Equation 3. 3}$$

$$\text{Apparent specific gravity} = \frac{C}{B+C-D} \qquad \text{Equation 3. 4}$$

$$\text{Water Absorption (\%)} = \frac{C-A}{A} * 100 \qquad \text{Equation 3. 5}$$

Where; A: Weight of oven-dry specimen in the air (g)

B: Weight of water-filled pycnometer (g)

C: Weight of the saturated surface-dry specimen (g)

D: Pycnometer weight with specimen and water to calibration mark (g)

3.2.2.4 Unit Weight of Fine Aggregate

The unit weight of fine aggregate is the weight of sand required to fill a container of a specific unit volume. It is affected by many variables, including wet, dry, and loose circumstances.

The unit weight of fine aggregate was calculated through equation 3.6.

$$\text{Unit weight} = \frac{A-B}{C} \qquad \text{Equation 3. 6}$$

Where; A: Fine aggregate plus cylinder weight (kg)

B: Weight of empty cylinder (kg)

C: Cylinder volume (m^3)

3.2.3 Tests on Coarse Aggregate

3.2.3.1 Sieve Analysis of Coarse Aggregate

The particle size distribution of the coarse aggregate obtained from the local quarry should be checked against grading. Hence, this test aimed to determine the fineness modulus of coarse aggregate with the help of apparatus like a series of sieves of sizes (25 mm, 19 mm, 12.5 mm, 9.5 mm, 4.75 mm, and pan) from the top to bottom, respectively, 2kg of coarse aggregate, a balance, sieve shaker, shovel, and sieve brush. The test procedure followed was (ASTM C136, 2006) as shown in the Appendix C1.

The gradation chart was filled in and the fineness modulus (FM) was computed. The range of fineness modulus of coarse aggregate according to ASTM C33 is 5.5-8.

$$FM = \frac{\sum(\text{Commulative \% retained})}{100} \qquad \text{Equation 3. 7}$$

3.2.3.2 Specific Gravity and Water Absorption of Coarse Aggregate

Specific gravity is the ratio of the weight of a certain amount of coarse aggregate to the weight of the same amount of water. This is a measure of the strength or quality of a particular material. Water absorption capacity represents the maximum amount of water that the aggregate can absorb. It gives an idea of the internal structure of the aggregate and the strength of the aggregate. The specific gravity and water absorption capacity were determined based on the (ASTM C127, 2015) standard. The test procedure was shown in the Appendix C2.

Bulk specific gravity, apparent specific gravity, and absorption capacity of coarse aggregate was computed through 3.8 to 3.10 equations.

$$\text{Bulk specific gravity} = \frac{C}{C-(D-B)} \qquad \text{Equation 3. 8}$$

$$\text{Apparent specific gravity} = \frac{A}{A-(D-B)} \qquad \text{Equation 3. 9}$$

$$\text{Water Absorption (\%)} = \frac{(C-A)}{A} * 100 \qquad \text{Equation 3. 10}$$

Where; A = Weight of oven-dry specimen in the air (g)

B = Weight of wire basket in water (g)

C = Weight of the saturated surface dry specimen (g)

D = Weight of Saturated Specimen in water with wire basket (g)

3.2.3.3 Unit Weight of Coarse Aggregate

The unit weight of coarse aggregate is the weight of the coarse aggregate required to fill a container of a specified unit volume. This test was carried out in the same way that the procedure for determining the unit weight of fine aggregate was carried out in the previous section.

3.2.3.4 Moisture content of aggregates

One of the properties of the aggregates, which should be known to design a concrete mix, is their moisture content. It is necessary to determine the net water-cement ratio in a batch of concrete made with job aggregate. The apparatus used was; a balance sensitive to 0.5gm, an Electrical oven at a temperature of 105 °C, a Container with a cover, and a Sample splitter. The moisture content of aggregates was determined based on the (ASTM C566, 2019) standard shown in the Appendix C3. The moisture content of coarse and fine aggregates was calculated through equation 3.11.

$$\text{Moisture content}(\%)=\frac{B-C}{C-A}*100 \qquad \text{Equation 3. 11}$$

3.2.4 Properties of teff straw and Polyethylene terephthalate fibers

The properties of the Teff straw and PET Polyethylene terephthalate fibers are summarized in Table 3.1

Table 3.1 Properties of Teff straw and Polyethylene terephthalate fibers

Properties	**Teff straw fiber**	**PET fiber**
Average Length(mm)	50	60
Average Diameter(mm)	1	3
Aspect ratio	50	20
Water Absorption (%)	40.23	0
Shape	cylindrical	Rectangular
Color	Brownish	Colorless
Density (g/cm^3)	0.97	1.34

3.2.5 Mix Design

Concrete mix design is the process of choosing appropriate concrete ingredients and figuring out their relative proportions in order to produce concrete with a minimal level of strength and durability as affordably as feasible. The C-30 concrete grade was designed since the construction of bridges and asphalt concrete is the primary application for fiber-reinforced concrete because these structures frequently develop cracks from severe loads and require ongoing repair. For bridge and road construction, C-30 concrete grade is used.

The amount of cement, fine aggregate, coarse aggregate, and water was determined by the properties of the concrete ingredients and the test results obtained from the ingredients. Teff straw and polyethylene terephthalate fibers were added to the concrete mix directly in three percentages 0.2%, 0.4%, and 0.6% by weight of concrete to prepare the HFRC mixes in this study. The concentration of polyethylene terephthalate fibers was maintained at a constant rate of 0.1% for the HFRC mixes. A total of four concrete mix batches were prepared for this current investigation. The first mix was prepared with a conventional mix design, which is called a control mix and identified as M_0. The other three mixes (M_1, M_2, and M_3) were prepared with 0.2%, 0.4%, and 0.6% inclusion of fibers concentration by weight of concrete respectively. The proportioning of concrete ingredients was done by ACI Committee 211 (2002) methods of mixing by the following procedures. From the Appendix E the quantity of materials for 1m^3 was summarized in the Table 3.2.

Table 3.2 Quantities of materials for each mix in Kg for 1m^3 concrete

Mix code	Hybrid fiber (%)	Cement (kg)	Fine aggregate (kg)	Coarse Aggregate (kg)	Water (kg)	Hybrid Fiber(kg)	W/C
M_0	0	413.79	785.31	993.94	191.22	0	0.44
M_1	0.20	413.79	785.31	993.94	191.22	7.76	0.44
M_2	0.40	413.79	785.31	993.94	191.22	9.53	0.44
M_3	0.60	413.79	785.31	993.94	191.22	14.30	0.44

The ratio of concrete mix design was computed by dividing the quantity of fine and coarse aggregate by the quantity of cement. From Table 3.3, the mix ratio of concrete ingredients is 1: 1.9: 2.4.

Table 3.3 Mix Ratio for C-30 Concrete Grade

Ingredients	Cement	Fine Aggregate	Coarse Aggregate
Amount/m^3	413.79/413.79	785.31/413.79	993.94/413.79
Ratio	1	1.90	2.40

3.2.6 Batching and Mixing

3.2.6.1 Batching

Measuring the ingredients of concrete to create mixes is the procedure known as batching. For this specific experiment, batching by weight was preferred over volume batching to get a proper mix of concrete ingredients since it is difficult to find the exact volume of granular materials because of their voids.

3.2.6.2 Concrete Mixing

Concrete mixing is the process of combining concrete components like cement, fine aggregate, coarse aggregate, water, and other ingredients to get effective and good-quality concrete. Mixing of fiber-reinforced concrete needs careful conditions to avoid balling of fibers, segregation, and in general the difficulty of mixing the materials uniformly. An increase in the aspect ratio, volume percentage, and size and quantity of coarse aggregate intensifies the difficulties and balling tendency (Vyom et al., 2013). In the production of HFRC, the coarse aggregate was first placed in the electrical tilting drum of 0.16 m^3 capacity was used, which is then followed, by sand and cement. The materials were then dry mixed for 1 min until uniform mixing.

(a) (b)

Figure 3.5 Sprayed fibers on concrete mix: (a) PET fiber, (b) Teff straw fiber

The water was then added to the mix and continued for further mixing till visibly flowable. Afterward, fibers were sprayed continuously in small amounts on concrete inside the tilting drum while rotating, and this process was finished in about three minutes to avoid fiber balling and to produce a homogeneous concrete mixture. The possibility of such mixing was taken by the researcher (Das et al., 2020). The overall mixing was performed according to guidelines (ASTM C192, 2000).

3.3 Fresh Concrete Test

3.3.1 Slump Test for Workability of Concrete

The slump test is the most common method for measuring the workability of freshly mixed concrete. The uniformity of the concrete regarding workability and quality aspects can be assessed from batch to batch by observing the nature in which the concrete slumps. Slump tests were conducted for both control and HFRC mixes to understand the effect of hybrid fibers on concrete workability. The test was carried out by using a steel mold called Slump cone as per (ASTM C143, 2012) specification. A standard slump cone 300mm high with a bottom diameter of 200mm and 100mm upper diameter was used.

(a) (b)

Figure 3.6 Slump test a) Control mix, b) HFRC mix

3.3.2 Compaction Factor Test for Workability of Concrete

The compaction factor test is an alternative way of measuring the workability of concrete. It is more accurate than the slump test and it is better for low workability below 25mm slump. The following Figure 3.7 shows the apparatus used for the compaction factor test for the workability of concrete found in the laboratory. The compaction factor was determined according to the terms of (BS 1881, 1983).The values of the compaction factor were calculated using equation 3.17 below.

$$\text{Compaction Factor} = \frac{\text{Weight of partially compacted concrete}}{\text{Weight of fully compacted concrete}} \qquad \text{Equation 3. 12}$$

Figure 3.7 Compaction factor test

3.4 Casting of Concrete Specimens and Curing

3.4.1 Concrete Casting

Cube samples of size 150mm, cylindrical samples of size 150mm diameter and 300mm height, and prismatic beam samples of size 100mm x 100mm x 500mm for testing compressive strength, tensile strength, and flexural strength; respectively, were cast.

Table 3.4 Number of specimens

Mix code	Weight of HFRC (%)	Types and number of tests on 7 and 28 days				Total
		Compressive strength	Flexural strength	Splitting tensile strength	Water absorption And void space	
M_0	0.00	6	6	6	6	24
M_1	0.20	6	6	6	6	24
M_2	0.40	6	6	6	6	24
M_3	0.60	6	6	6	6	24
Total						96

Note: All percentages are in weight fractions of concrete.

3.4.2 Curing of Concrete Specimens

Figure 3.8 Concrete Casting and marking

Curing of concrete is a process of providing sufficient moisture, temperature, and time so that the hydration of cement continues till the concrete achieves its desired properties for the intended use based on (ASTM C192, 2000). After demolding the concrete specimens, the concrete specimens were cured at room temperature for 7 and 28 days in a water-curing tank. The minimum number of samples specified by ASTM C39 is three. The concrete specimens were prepared by incorporating major concrete ingredients (cement, sand, coarse aggregate, and water) with different percentages of hybrid teff straw and polyethylene terephthalate fibers.

3.5 Hardened Concrete Test

Hardened concrete is one of the most durable and robust building materials available, capable of supporting structural and service loads. One of the goals of hardened concrete testing is to guarantee that the concrete used has the strength and durability required.

3.5.1 Compressive Strength Test

Compressive strength is the ability of hardened concrete to withstand axial loads without any cracks or deflection. Therefore, this test aimed to determine the compressive strength of conventional concrete and Hybrid Teff straw and polyethylene terephthalate Fiber reinforced concrete (HTPFRC). A concrete cube of sample size 150 x 150 x 150 mm were cast to investigate the compressive strength of control concrete and HTPFRC. The compressive strength after 7 and 28 days of curing was determined by using an automatic compressive strength test machine at Adama Science and Technology University, Construction Material Laboratory, in accordance with (ASTM C39, 2018). To undergo the compressive strength test, the casted cubes were taken out of the curing water after 7 and 28 curing periods and wiped out excess water from the surface. The test machine was then cleaned, placed the sample was in the test machine, and applied the load was at a rate of 14 N/mm^2/minute, having a load capacity of 3000 KN. When the specimens failed, the maximum load was recorded, and finally, the compressive strength was calculated.

$$CS = \frac{F}{A} \qquad \text{Equation 3. 13}$$

Where, CS- Compressive strength in N/mm^2

F- Force or load at the point of failure in N

A- Cross sectional surface area in mm^2

Figure 3.9 Compressive strength test setup

3.5.2 Flexural Strength Test

Flexural strength, also known as modulus of rupture, bend strength, or transverse rupture strength is a material property, defined as the stress in a material just before it yields in a flexure test. The test was carried out as per (ASTM C78, 2002) standard specification requirements. 100x100x500mm molds made from steel and wood were used. Three samples for 7 and three samples for 28-day test from each mix were cast. After 24 hours the molds are removed and the specimens are cured in a curing tank using potable water up to the date of the test. A two-point loaded flexural strength testing machine having 100KN was used at Adama Science and Technology University, Construction Material Laboratory. For two-point loading, the flexural stress at the mid-span of the beam is calculated as using the Equation 3.19.

$$\text{Flexural stress} = \frac{PL}{bd^2} \qquad \text{Equation 3. 14}$$

Where; P-rupture load in N

L- Length of the beam between the two supports

b- Width of the beam cross-section

d- Depth of the beam

Figure 3.10 Flexural strength test setup

3.5.3 Splitting Tensile Strength Test

One of the common methods used to measure the tensile strength of concrete is the split tensile strength test. The test was conducted as per (ASTM C496, 2004) specification for split tensile strength. The samples were cast by using steel cylinder molds having 150mm diameter and 300mm length. After 24 hours the samples were removed from the molds and placed in a curing tank for 7 days of curing and 28 days of curing period. The cylinders were tested using a compression-testing machine having 1000 KN capacity by using a manual compressive strength test machine at Adama Science and Technology University, Construction Material Laboratory.

Figure 3.11 Splitting tensile strength test setup

The test was conducted by placing the cylinder sample in the opposite direction to its longitudinal axis and the load is gradually applied and peak load was recorded. The stress was determined by using equation 3.20.

$$\text{Split tensile stress} = \frac{2P}{\pi dl} \qquad \text{Equation 3. 15}$$

Where P-Peak load (N)

d- Diameter of cylinder (mm)

l- Length of the cylinder (mm)

3.5.4 Density, water absorption, and Voids

The density, water absorption, and volume of voids are performed as per the guidelines of the American Society for Testing and Materials (ASTM C642, 2006) on 150 mm cubes. In this research, the cubes used were carefully inspected for any visible gaps, cracks, or broken edges to ensure their good condition. Once confirmed, they were moved to a water tank for curing, which lasted for 28 days. A minimum of three cubes from each mix was prepared for testing at the end of the 28-day curing period. The test procedures was shown in the Appendix D. Density, water absorption, and voids were calculated through equations 3.21 to equation 3.27.

$$\text{Absorption after immersion, \%} = \frac{B\text{-}A}{A} * 100 \qquad \text{Equation 3. 16}$$

$$\text{Absorption after immersion and boiling, \%} = \frac{C\text{-}A}{A} * 100 \qquad \text{Equation 3. 17}$$

$$\text{Bulk density, dry} = \frac{A}{C\text{-}D} \cdot \rho = g_1 \qquad \text{Equation 3. 18}$$

$$\text{Bulk density after immersion} = \frac{B}{C\text{-}D} \cdot \rho \qquad \text{Equation 3. 19}$$

Bulk density after immersion = $\frac{C}{C-D} \cdot \rho = g_2$ Equation 3. 20

Apparent density = $\frac{A}{A-D} \cdot \rho$ Equation 3. 21

The volume of permeable pore space (voids), % = $\frac{g_2 - g_1}{g_2}$ Equation 3. 22

Where: A = mass of oven-dried sample in air, g

B = mass of surface-dry sample in the air after immersion, g

C = mass of surface-dry sample in the air after immersion and boiling, g

D = apparent mass of sample in water after immersion and boiling, g

g_1 = bulk density, dry, Mg/m3 and

g_2 = apparent density, Mg/m3

ρ = density of water = 1 Mg/m3 = 1 g/cm3

3.6 Statistical tools

Statistical tools play a crucial role in analyzing data, drawing conclusions, and making informed decisions. Descriptive statistical analysis and two-way ANOVA were the two statistical tools used. Origin Pro 2022 software was used to perform these analyses. To conduct statistical data analysis using Origin Pro 2022 the following steps were taken. First, the compressive strength, flexural strength, and splitting tensile strength data were loaded into the Origin Pro 2022 software. Then, the descriptive statistics menu within the software was accessed. Within this menu, the statistics such as mean, standard deviation, standard error, 95% confidence interval, and coefficient of variation were chosen. Following the selection of statistics, Origin Pro generated a comprehensive report comprising all the descriptive statistics for the selected variables. This report provided valuable insights and information about the dataset, thereby facilitating further analysis and interpretation.

For conducting a two-way ANOVA in Origin Pro 2022, the steps followed were as follows. Firstly, the independent variables (hybrid percentages, curing period) and dependent variables (compressive strength, flexural strength, and tensile strength) were loaded into the software. The data was then arranged, with columns designated for the dependent variable and two columns allocated to the independent variables. Next, the analysis menu was accessed, and the ANOVA option was selected. In the ANOVA dialog box, the specific two-way ANOVA option was chosen. Then, the dependent variable, the two independent variables, as well as interaction terms, were specified within the software. Finally, Origin Pro conducted the analysis and provided an ANOVA table, an interaction plot, and other relevant outputs related to the two-way ANOVA.

3.7 Summary

In this chapter, the materials and methods for studying the effect of hybrid teff straw and PET fibers in concrete were discussed. After presenting the overall materials of the study, the methods adopted for individual objectives were also discussed. Furthermore, the methods for the concrete ingredient tests, mix design, fresh concrete test, hardened concrete test, and statistical tools such as descriptive statistical analysis and two-way ANOVA were discussed. The results of various analyses and discussions using the materials and methods for different research objectives are described in the next chapter.

CHAPTER 4
RESULTS AND DISCUSSION

4.1 Introduction

The previous chapter discussed the materials and methods adopted in this study. The current chapter presented the results of various experimental tests. The physical tests of fibers were mentioned, including the properties of the materials used in this study. Workability, compressive strength, flexural strength, tensile splitting strength, water absorption, and void space of the concrete were also discussed. Finally, the cost implication of using HTPF as an addition to concrete production were presented.

4.2 Material properties

The test results of cement, fine aggregate, coarse aggregate, and water were covered in this section.

4.2.1 Tests on Cement

4.2.1.1 Normal Consistency of Cement

Normal consistency is defined as the consistency that allows the Vicat plunger of 10 mm in diameter to penetrate to a point of 5 mm to 7 mm from the bottom of the Vicat mold (ASTM C187, 2016). From the test result, the normal consistency of cement paste was 28% as the Vicat plunger penetrated about 7 mm, which was in the range of 22-30 %. This indicates that the amount of water to make a cement paste is 28% of the weight of cement.

4.2.2 Fine Aggregate Test Result Analysis

In this section, the results obtained from the physical tests of fine aggregate were discussed. Silt content, sieve analysis, unit weight, specific gravity, and water absorption of fine aggregate were determined and discussed.

4.2.2.1 Silt Content of Sand

The silt content was calculated using Equation 3.1. From Table 4.1, the amount of silt that the fine aggregate had was 2.89%, which is in the range to be used for concrete production as per ASTM C 33.

Table 4.1 Silt content test result of fine aggregate

Trial	The volume of separated layer (A)	Amount of fine aggregate (B)	Silt content (%) = (A/B)*100
1	9	300	3.00
2	7	300	2.33
3	10	300	3.33
Average	8.67	300	2.89

4.2.2.2 Sieve Analysis of Fine Aggregate

Sieve analysis is used to measure the particle size distribution of material. For this work, sieve sizes of (9.5, 4.75 mm, 2.36 mm, 1.18 mm, 0.6 mm, 0.3 mm, 0.15 mm, and pan) were used. Table 4.2 and Figure 4.1 illustrate the fineness modulus of fine aggregate. The fineness modulus of fine aggregate was computed by using Equation 3.2. The result indicated that the fineness modulus of the fine aggregate was 2.82.

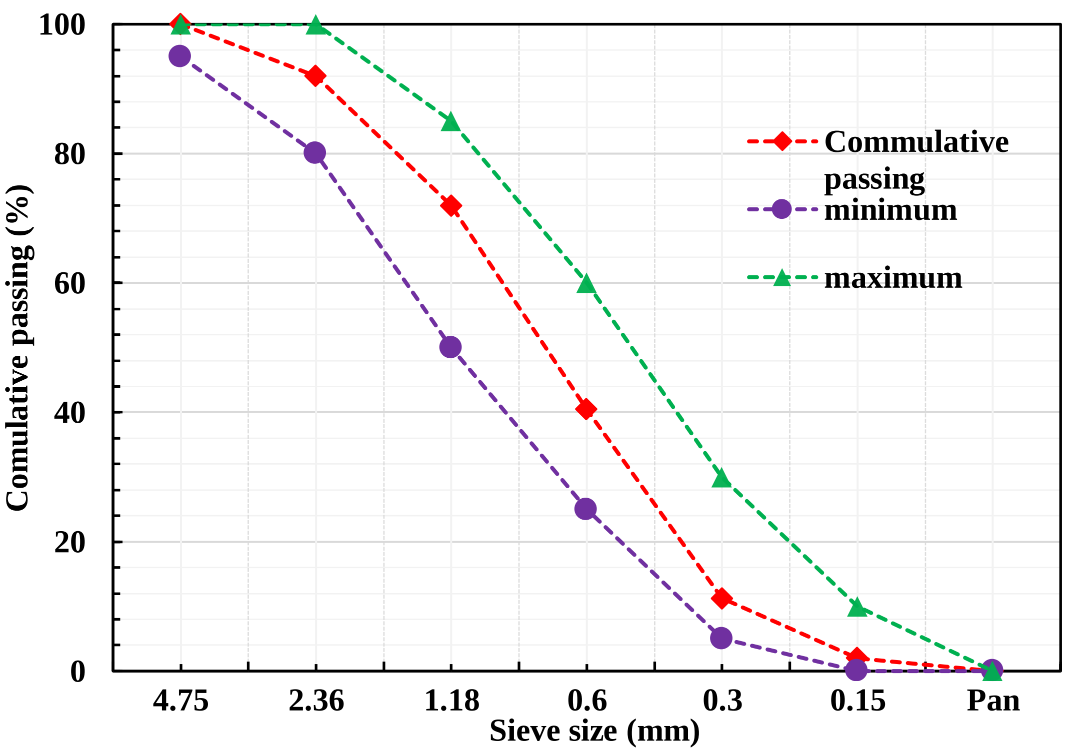

Figure 4.1 Gradation Curve of Fine Aggregate

Fineness modulus value was in the range specified by ASTM C33 (2003) which is from 2.3 to 3.1. The gradation curve of the used fine aggregate was laid between ASTM lower and upper limits as seen in Figure 4.1. So the used fine aggregate met the ASTM C136 requirement.

Table 4.2 Sieve Analysis of Fine Aggregate

Sieve opening (mm)	Weight of Sieve +FA (gm)	Weight of Sieve(gm)	Weight of FA retained (gm)	Percent of FA retained (gm)	Cumulative retained (%)	Cumulative Passing (%)	Range (ASTM C-33)
9.5	432	432	0	0	0	100	100
4.75	440	440	0	0	0	100	95-100
2.36	445	405	40	8.02	8.02	91.98	80-100

1.18	580	480	100	20.04	28.06	71.94	50-85
0.6	620	463	157	31.46	59.52	40.48	25-60
0.3	445	299	146	29.26	88.78	11.22	5-30
0.15	325	279	46	9.22	98.00	2.00	0-10
Pan	265	255	10	2.00	100	0	0
Summation of Commutative weight retained on 0.15mm					282.36		

4.2.2.3 Specific Gravity and Water Absorption of Fine Aggregate

Specific gravity is the ratio of the mass of a given volume of material to the mass of an equal volume of water. The water absorption of an aggregate is calculated as the ratio of the difference between the weight of the aggregate in the surface-dried saturated state and the weight of the oven-dried aggregate. In this study, the bulk specific gravity (Bsg), apparent specific gravity (Asg), and water absorption of fine aggregate were determined using Equations 3.3, 3.4, and 3.5, respectively. The Bsg, Asg, and water absorption were 2.63, 2.77, and 3.09% (Table 4.3), and the obtained result, for specific gravity of fine aggregate, was between the limit (2.5 to 3.0) specified by ASTM C127.

Table 4.3 Result of specific gravity and absorption capacity of fine aggregate

Descriptions	Quantity	Formula	Calculations	Result
Weight of oven-dry specimen in the air(A)	485 gm	$Bsg = \frac{C}{(B+C-D)}$	$\frac{500}{(1495+500-1805)}$	2.63
Weight of pycnometer filled with water (B)	1495 gm	$Asg = \frac{A}{(B+A-D)}$	$\frac{485}{(1495+485-1805)}$	2.77
Weight of the saturated surface dry specimen (C)	500 gm			
Weight of pycnometer with specimen and water to calibration mark (D)	1805 gm	$WA(\%) = \frac{(C-A)}{A} * 100$	$\frac{500-485}{485} * 100$	3.09%

4.2.2.4 Unit Weight of Fine Aggregate (UW)

The unit weight of fine aggregate measures the volume that the aggregate will occupy in the concrete.

Table 4.4 Result for Unit Weight of Fine Aggregate

Descriptions	Quantity	Formula	Calculation	Result
Weight of fine aggregate plus the cylinder (A)	10.340 kg	$UW = \frac{A-B}{C}$	$UW = \frac{10.34-3.44}{0.005}$	1380 kg/m^3
Weight of the empty cylinder (B)	3.440 kg			
The volume of the cylinder (C)	0.005m^3			

The UWFA was computed by using Equation 3.6 and the result shows that the unit weight of fine aggregate was 1380 kg/m3 (Table 4.4). Therefore, the computed unit weight of fine aggregate was within the range (1200 to 1750) kg/m3 that specified by ASTM C29.

4.2.3 Tests on Coarse Aggregate

To keep the gradation within the range required by the ASTM standard, basaltic crushed rock aggregates with a nominal maximum size of 19 mm were employed in this study. The aggregates were tested for physical properties such as Sieve analysis, specific gravity, water absorption, moisture content, and unit weight.

4.2.3.1 Sieve Analysis for Coarse Aggregate

The coarse aggregate obtained from the local quarry was tested against gradation to determine its particle size distribution. The fineness modulus of coarse aggregate was computed based on Equation 3.7, which gave a value of 7.18. The value of the fineness modulus of coarse aggregate was found within the range of the (ASTM C33) standard.

Table 4.5 Result of sieve analysis of coarse aggregate

Sieve opening(mm)	Weight of Sieve(gm)	Weight of Sieve + Coarse Aggregate (gm)	Weight of Coarse Aggregate retained (gm)	Percent of CA retained(gm)	Cumulative retained (%)	Cumulative Passing (%)	Range (ASTM C-33)
25	1256	1256	0	0.00	0.00	100.00	100
19	435	562	127	6.35	6.35	93.65	95-100
12.5	440	1120	680	34.00	40.35	59.65	40-80
9.5	446	1083	637	31.85	72.20	27.80	20-55
4.75	444	1000	556	27.80	100	0	0-10
Pan	265	265	0	0	100	0	0

The gradation curve of the employed coarse aggregate was within the ASTM C33 lower and higher limits, as shown in Figure 4.2. As a result, the fine aggregate used met the requirements.

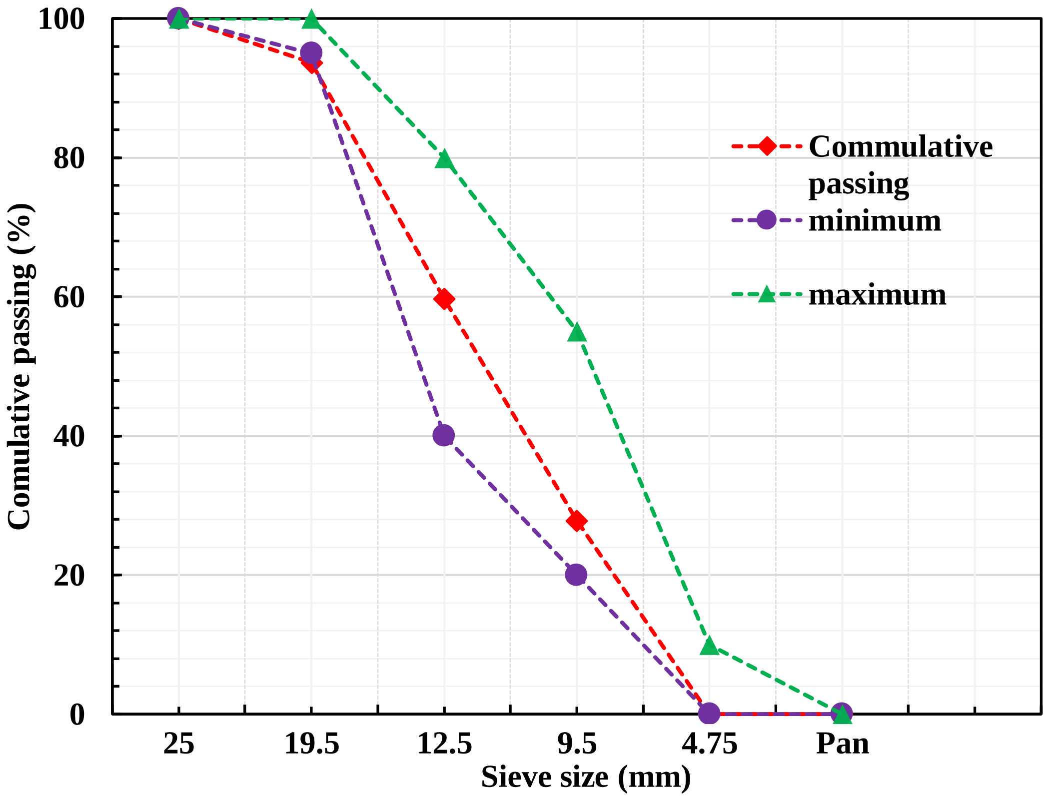

Figure 4.2 Gradation Curve of Coarse Aggregate

4.2.3.2 Specific Gravity and Water Absorption Capacity of Coarse Aggregate

In this thesis work, bulk specific gravity (Bsg), apparent specific gravity (Asg), and water absorption capacity of coarse aggregate were determined and discussed based on the test results obtained in the laboratory. Table 4.6 illustrates the Bsg, Asg, and water absorption of coarse aggregate, which were computed using Equations 3.8, 3.9, and 3.10, respectively. The test result showed that the Bsg, Asg, and water absorption capacities of coarse aggregate were 2.65, 2.72, and 1.70%, respectively. The test result obtained here satisfies the standard set by (ASTM C127).

Table 4.6 Result of specific gravity and absorption capacity of coarse aggregate

Descriptions	Quantity	Formula	Calculations	Result
Weight of oven-dry specimen in the air(A)	3000gm	$Bsg = \frac{C}{C-(D-B)}$	$\frac{3051}{3051-(2200-300)}$	2.65
Weight of basket in water (B)	300gm	$Asg = \frac{A}{A-(D-B)}$	$\frac{3000}{3000-(2200-300)}$	2.72
Weight of the saturated surface dry specimen (C)	3051gm			
Weight of Saturated Specimen in water with basket (D)	2200gm	$WA\ (\%) = \frac{C-A}{A} * 100$	$\frac{3051-3000}{3000} * 100$	1.70%

4.2.3.3 Unit Weight of Coarse Aggregate (UW)

The unit weight of coarse aggregate measures the volume that the aggregate will occupy in the concrete. The UWCA was computed using Equation 3.6 and the result is given in Table 4.7. The result shows that the unit weight of coarse aggregate is 1,631.64 kg/m3. The test result obtained in this section satisfies the (ASTM C29) standard.

Table 4.7 Unit Weight of Coarse Aggregate

Descriptions	Quantity	Formula	Calculation	Result
Weight of Coarse aggregate plus the cylinder (A)	11.580 kg			
Weight of the empty cylinder (B)	3.440 kg	$UW = \frac{A-B}{C}$	$UW = \frac{11.58-3.440}{0.005}$	1627.6 kg/m^3
The volume of the cylinder (C)	0.005m^3			

4.2.3.4 Moisture content of fine and coarse aggregates test

In the design mix workability and water-cement ratio are affected by the moisture content of the coarse aggregate sample.

Table 4.8 Moisture content for fine aggregate

Trial	Mass of Aggregate in the air(gm)	Oven-dried mass (gm)	Mass of water (gm)	Moisture content %
1	500	485	15.00	3.09
2	500	482	18.00	3.73
3	500	486	14.00	2.88
Average				3.24

Water-cement ratio in a mix design is based on the assumption that aggregates are inert (neither absorb nor give water to the mixture) and hence aggregates from different sources do not comply with this assumption of the Water-cement ratio. The moisture content of the fine aggregate in this specific research was calculated to be 3.24% as shown in Table 4.8. The moisture content of the coarse aggregate in this study was calculated to be 0.79%.

Table 4.9 Moisture content of coarse aggregate

Trial	Mass of Aggregate in the air(gm)	Oven-dried mass (gm)	Mass of water (gm)	Moisture content %
1	2000	1987	13.00	0.65
2	2000	1982	18.00	0.91
3	2000	1984	16.00	0.81
Average				0.79

The material test results of cement, fine aggregate, and coarse aggregate in the current study can be summarized in Table 4.10 below.

Table 4.10 Summary of material test results

Item		Cement	FA	CA
Silt content			2.89	
Fineness modulus			2.82	7.18
Unit weight			1380 kg/m^3	1627.6 kg/m^3
Specific gravity	Bsg		2.63	2.65
	Asg		2.77	2.72
Water Absorption			3.09%	1.70%
Moisture content			3.24%	0.79%
Normal consistency		28%		

4.2 Workability of fresh concrete

4.2.1 Slump test

The ability of fresh concrete to be mixed, transported, easily flowed, and placed is referred to as workability (ASTM C143). In this experimental investigation, the workability of HFRC and conventional concrete was investigated. The result of the slump value of HFRC and control concrete can be illustrated in Table 4.11 and Figure 4.3 below.

Table 4.11 Slump value of HFRC and Control Concrete

Mix code	HFRC (%)	Average Slump value (mm)
M_0	0	55.00
M_1	0.2	41.00
M_2	0.4	21.00
M_3	0.6	10.67

According to the results of the current experiment, the slump test shows a decreasing tendency as the proportion of hybrid fibers in the concrete mix increases. For the M_0 mix, the slump was found around 55 mm, while for M_1, $M_{2,}$ and M_3 mixes the slump values were recorded at about 41 mm, 21 mm, and 10.67 mm respectively. In addition, an average of 55.96% slump dropped for HFRC mixes as compared to the control mix. The lowest workability recorded falls in the very low range (0–25 mm) and the highest workability observed (55 mm) is classified as medium workability (50–100 mm). A similar consistent finding was also observed in the reduction trend of the slump by the addition of hybrid fiber in the concrete mixes (Das et al., 2020).

The addition of the hybrid fiber to the concrete mixture is responsible for the slump value's decline. In other words, hybrid fibers absorb more water from the concrete mix and interlock, which might affect the slump value, making them stiffer than the control mix. In other words, the increased fiber content in freshly mixed concrete causes a tendency for fiber balling, which significantly lowers the slump value. However, the formation of the slump was accomplished true slump for all types of mixes.

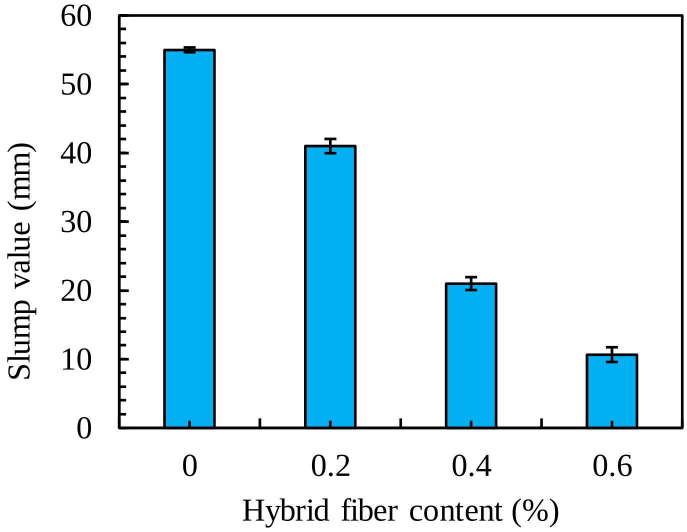

Figure 4.3 Slump values for HFRC and Control Concrete

4.2.2 Compaction factor

Similar to the slump test, the compaction factor test of fresh concrete shows a decreasing fashion when the percentage of hybrid fibers increased in the concrete mix as shown in Figure 4.4 and Table 4.12. As can be seen, the control mix M_0 had a compaction factor value of roughly 0.94, but the hybrid fiber mixes M_1, M_2, and M_3 had values of about 0.886, 0.880, and 0.664, respectively. The mixes containing 0.2%, 0.4%, and 0.6% fibers had compaction factor reductions of 5.74%, 6.38%, and 29.36% compared to the control concrete respectively.

Table 4.12 Compaction factor value of HFRC and Control Concrete

Mix code	HFRC (%)	Average Compaction factor value
M_0	0	0.940
M_1	0.2	0.886
M_2	0.4	0.880
M_3	0.6	0.664

All values obtained except M_3 falls within the range of 0.70- 0.98 based on BS 1881- 103. The test results observed by Das et al. (2020) that with an increase in the amount of hybrid fiber in the concrete mix, HFRC showed a gradually declining compaction factor. This consistent decline in HFRC indicates, as would be predicted, that a key governing mechanism for the concrete compacting factor results from the dominance of mechanical interlocking of hybrid fiber.

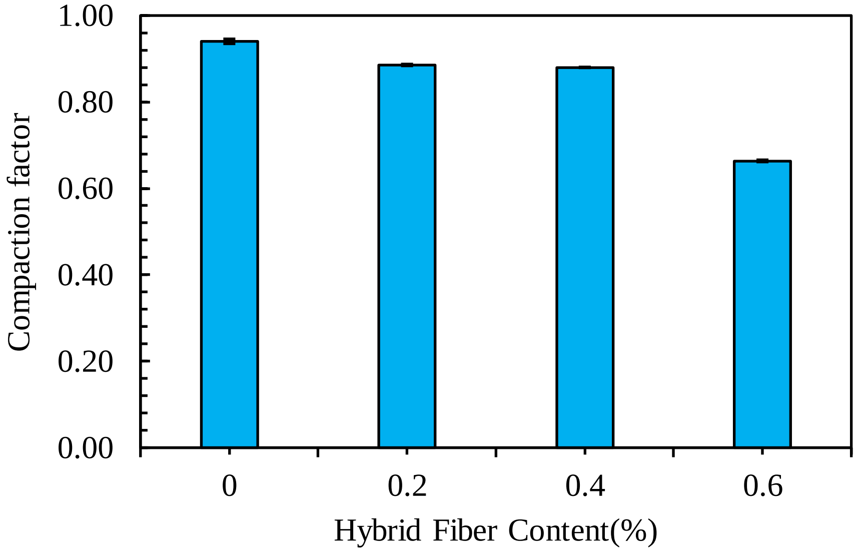

Figure 4.4 Compaction factor values for HFRC and Control Concrete

4.2.3 Density of HFRC

Table 4.13 and Figure 4.5 illustrate the density values of the HFRC and control concrete mixtures. As the amount of fiber in the concrete mix increased, it was observed that the value of hybrid fiber density steadily declined. The density of this hybrid fiber-reinforced fresh concrete was investigated between 2270.81 kg/m^3 and 2032.48 kg/m^3. It's also important to note that the fresh density of the control mix was 2270.81 kg/m^3, whereas the density of the concrete mix including 0.2%, 0.4%, and 0.6% hybrid fibers was 2226.21 kg/m^3, 2180.54 kg/m^3, and 2032.48 kg/m^3, respectively, lower than the control mix.

Table 4.13 Density of fresh concrete for HFRC and control concrete

Mix code	HFRC (%)	Density(kg/m3)
M_0	0	2270.81
M_1	0.2	2226.21
M_2	0.4	2180.54
M_3	0.6	2032.48

Furthermore, the addition of various fiber concentrations may increase the effect of fiber contribution's ability to reduce density. It should be mentioned that the drop in density seen in this experiment for HFRC ranges from 2% to 10% of the conventional concrete. These findings follow similar patterns to earlier research on fiber-reinforced concrete, where it was shown that fresh density decreased by 3% to 16% compared to control concrete (Caggiano et al., 2017; Das et al., 2020; Hwang et al., 2016). Due to the more porous nature of the fiber that is adhered to the aggregates and the formation of a higher percentage of voids, especially at higher fiber concentration levels, the cement grains are unable to fill the spaces between the coarse aggregate and hybrid fiber, which results in a reduction in the density of concrete. The density of HFRC is further impacted by fiber balling and decreased homogeneity in the mix as a result of fiber interlocking with coarse aggregate (Rudraswamy et al., 2018).

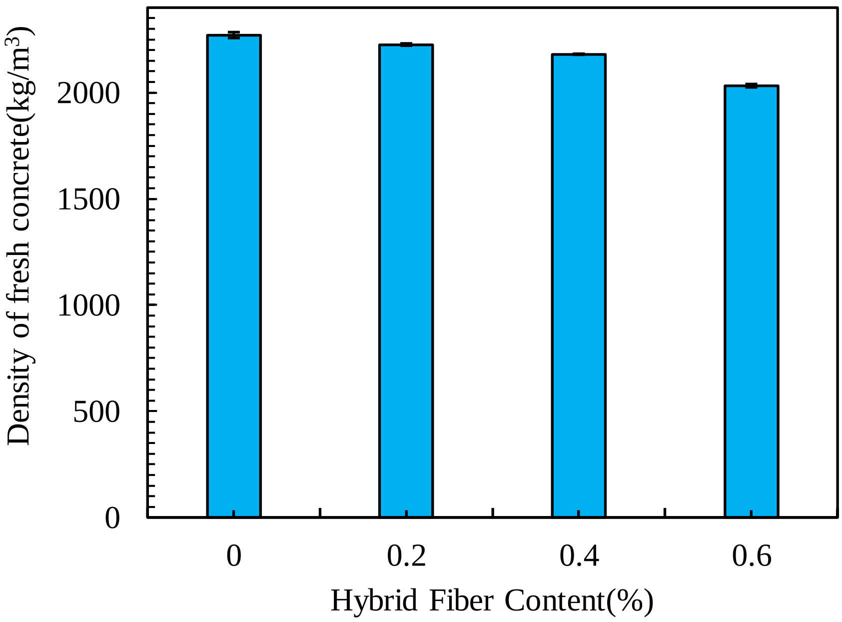

Figure 4.5 Density of fresh concrete for HFRC and control concrete

4.3 Hardened Concrete Test

4.3.1 Effects of hybrid fibers on compressive strength

In terms of mean strength, standard deviation, coefficient of variation (CV), standard error, and the lower and upper 95% confidence intervals of the compressive strength, Table 4.14 summarizes the compressive strength test findings of HFRC and control concrete mixes. It is important to note that three specimens were examined for each fiber concentration in the laboratory, and mean values were computed to get the results of the compressive strength test at 7 and 28 days. From the standpoint of statistical analysis, Table 4.14 shows that the compressive strength ranged from 12.54 MPa to 35.72 MPa. Additionally, it should be mentioned that the standard deviation of the examined specimens is 0.35 to 1.34, with a corresponding CV of 0.98% to 5.14% and a standard error of 0.202 to 0.774. The maximum compressive strength reached at 7 days was 26.05 MPa with a 95% confidence interval of 22.72 MPa to 29.38 MPa, while the lowest compressive strength was determined to be 12.54 MPa with a 95% confidence interval of 10.53 MPa to 14.55 MPa.

Table 4.14 Summary of the compressive strength test results of the HFRC and Control Concrete

Mixes	Days	Mean strength(MPa)	Standard deviation	CV (%)	Standard error	95% confidence interval	
						Lower limit	Upper limit
M_0	7	26.05	1.34	5.14	0.774	22.72	29.38
	28	35.72	0.35	0.98	0.202	34.85	36.59
M_1	7	22.05	0.83	3.76	0.479	19.99	24.11
	28	30.33	1.04	3.43	0.600	27.75	32.91
M_2	7	15.94	0.53	3.32	0.306	14.62	17.26
	28	21.72	0.94	4.33	0.543	19.38	24.06
M_3	7	12.54	0.81	6.46	0.468	10.53	14.55
	28	19.21	1.07	5.58	0.619	16.55	21.87

With a 95% confidence interval bound of 16.55 MPa to 21.88 MPa, the lowest compressive strength of 28 days was measured at 19.21 MPa and the greatest compressive strength was measured at 35.72 MPa with a 95% confidence interval bound of 34.85 MPa to 36.59 MPa. Figure 4.6 (a) shows the variation of compressive strength at 7 and 28- days with varying concentrations of HFRC mixes to produce fiber-reinforced concrete.

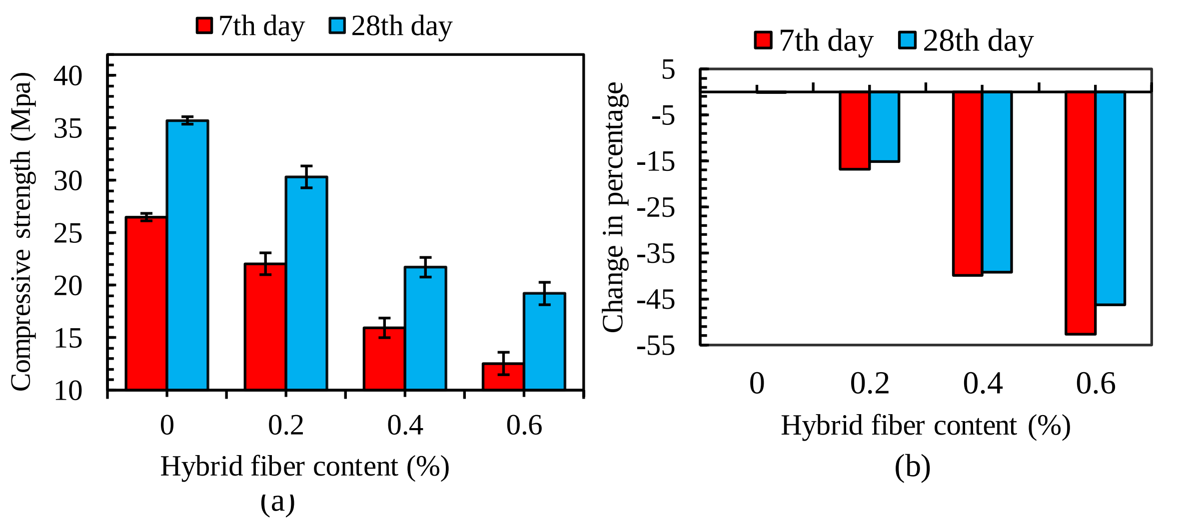

Figure 4.6 (a) Compressive strength values for HFRC and control concrete at 7 and 28-days (b) Percentage change in compressive strength of HFRC mixes compared to the reference mix

Table 4.16 shows that the compressive strength of the HFRC specimens at 7 days is between 65.27 and 74.19 % of the strength at 28 days of the concrete specimens. According to test results, all HFRC mixtures had less strength than the control mix. For the control mix, the compressive strength at 7 days attained 26.05 MPa; whereas at 28- days the strength of the control mix was found around 35.72 MPa. The compressive strength of concrete with fiber concentrations of 0.2%, 0.4%, and 0.6% were found to be 15.08%, 39.19 %, and 46.21%lower than the control mix, respectively, at 30.33 MPa, 21.72 MPa, and 19.21 MPa. This result is consistent with the various experimental studies conducted by researchers who reported compressive strength loss of HFRC at different fiber concentrations, particularly at higher concentration levels of fiber in the concrete mix (Caggiano et al., 2017; Das et al., 2020; Mastali et al., 2018; Raj et al., 2020). It is possible that the increased fiber content in concrete mixes, which resulted in the balling effect of fiber and concrete, made it too difficult to compact, which led to the falling trend in compressive strength. However, it increases the void in the concrete mix thus weakening the bond between the coarse aggregate, hybrid fiber, and the cement paste and therefore reduces the compressive strength. Figure 4.6 (b) represents the percentage change in the strength of each mix compared to the control mix. When comparing the results in Figure 4.6 (b) to the control concrete, all hybrid fiber mixtures consistently showed a decline in the strength of about 15%, 39%, and 46%. This suggests that the higher balling effect of the fiber and inherent heterogeneity of the mix are more pronounced in these hybrid mixtures, which causes a decline in strength (Caggiano et al., 2017).

4.3.1.1 ANOVA results of Compressive strength

To determine if there is a statistically significant difference in compressive strength results between different groups, as well as within individual groups, an analysis of variance (ANOVA) test was conducted. The purpose of this test is to assess whether the observed differences in compressive strength results are due to chance or if there is a significant difference that can be attributed to different group factors. The test takes into account both the variability within each group and the differences between groups to determine the significance of any observed differences in compressive strength. To check whether the compressive strength data set satisfies normality, Shapiro's test was performed by the origin pro 2022 software. The results showed that the compressive strength data set satisfied the normality. In this research, the test dependent variable is compressive strength and two independent variables are the curing period and hybrid fiber percentage. The mean comparisons by Tukey's HSD test were used.

Hypothesis Formulation Testing in Factorial ANOVA

Testing a hypothesis helps in finding the conclusion in an experiment based on the formulated hypothesis of variables. In statistics the hypothesis formulation is based on the Factorial two-way ANOVA, there are two types of hypothesis, the null hypothesis(H_0) is used to disprove or reject a statement, and the alternative hypothesis(H_a) is used to explain the cause of a phenomenon or anticipated relationship of the variables. It can be expressed using the statistical notation:

Null Hypothesis H_0: $\mu_{01} = \mu_{02}$

Alternative Hypothesis H_a: $\mu_{a1} \neq \mu_{a2}$

Where: - μ_{01} and μ_{02} are null hypothesis variables

μ_{a1} and μ_{a2} are alternative hypothesis variables

For this test result, the three hypotheses are drawn, Null Hypothesis (H_o):

μ_{01} = hybrid fiber percentage doesn't affect the compressive strength of concrete

μ_{02} = Curing period doesn't affect the compressive strength of concrete

μ_{03} = hybrid fiber percentage and the curing period doesn't affect the compressive strength of concrete.

In the current study, two-way factorial ANOVA with a confidence interval of 95% and a significant level of $\alpha = 0.05$ is used to analyze the factors affecting the compressive strength of concrete. P-value < 0.05, then the variable is considered as a significant factor that affects the compressive strength of concrete so the null hypothesis is rejected, or for P-value ≥ 0.05, the factor is reflected as a non-significant effect and the null hypothesis will not be rejected.

Table 4.15 Overall ANOVA for compressive strength

	DF	Sum of Squares	Mean Square	F Value	P Value
Curing Period	1	336.38	336.38	396.68	1.02034E-12
Hybrid percentage	3	864.27	288.09	339.73	1.0797E-14
Interaction	3	10.81	3.60	4.25	0.02181
Model	7	1211.46	173.06	204.09	1.9615E-14
Error	16	13.568	0.848		
Corrected Total	23	1225.03			

At the 0.05 level, the population means of Curing day are significantly different.

At the 0.05 level, the population means of Hybrid are significantly different.

At the 0.05 level, the interaction between Curing day and Hybrid is significant.

Based on Table 4.15, the effect of curing period, hybrid percentage and interaction are the significant effect that the P-values of the variables are less than 0.05; which shows that the variables are significant for a 95% confidence interval, and therefore; the null hypothesis is rejected. Based on Table 4.16, a 0.2% hybrid percentage is significantly different because the grouping letter does not share with other groups.

Table 4.16 Interactions' Grouping Letters for compressive strength

Curing Period	Hybrid percentage	Mean	Groups						
28th day	0	35.72	A						
28th day	0.2	30.33		B					
7th day	0	26.49			C				
7th day	0.2	22.05				D			
28th day	0.4	21.72				D	E		
28th day	0.6	19.21					E		
7th day	0.4	15.94						F	
7th day	0.6	12.54							G

Means that do not share a letter are significantly different.

4.3.2.2 Observed crack pattern.

The test specimen failure rate was much lower for the HFRC cubes under compression than conventional concrete. The failed cube of control concrete specimens have a normal cone form, and the walls of its outside come off. The HFRC cubes maintained their structural integrity throughout the compression test because the fibers in them prevented the specimen's failed sections from separating from its core and made it difficult to manually debond the side walls that had failed.

Figure 4.7 Test specimens which failed under compression, (a) control, (b) HFRC

In addition, the cracks in the hybrid fiber-containing specimens are much smaller and thinner than the cracks in the control specimen, demonstrating the function of fibers in inhibiting crack opening and expansion. Figure 4.7 displays an illustrative figure of the test specimens that failed under compression.

4.3.2 Effects of hybrid fibers on splitting tensile strength

For this experiment, the splitting tensile strength of all the HFRC mixtures is shown in Table 4.17. The statistical analysis of the test findings, the mean strength, standard deviation, standard error, coefficient of variation (CV), and 95% confidence interval with lower and upper ranges were determined. It is important to note that, similar to the compressive strength test, the splitting tensile strength test was done on three specimens for each fiber concentration, and the final strength after 7 and 28 days was calculated using the mean results. Table 4.17 shows that the split tensile strength ranged from 1.29 MPa to 2.77 MPa, the tested specimen's standard deviation ranged from 0.086 to 0.34 with the corresponding CV of 6.65% to 12.26%, and the standards error ranged from 0.049 to 0.196. The lowest tensile strength of HFRC mixes for 7 days was found at about 1.29 MPa with a 95% confidence interval of the lower and upper limit of 1.07 MPa and 1.50 MPa; whereas, the highest tensile strength was obtained at around 1.93 MPa with 95% confidence interval of the lower and upper range of 1.59 MPa and 2.26 MPa.

Table 4.17 Summary of the splitting tensile strength test results of the HFRC and control concrete.

Mixes	Days	Mean strength(MPa)	Standard deviation	CV (%)	Standard error	95% confidence interval	
						Lower range	Upper range
M_0	7	1.83	0.058	3.16	0.033	1.69	1.98
	28	2.24	0.079	3.50	0.045	2.05	2.44
M_1	7	1.93	0.135	7.01	0.078	1.59	2.26
	28	2.77	0.340	12.26	0.196	1.93	3.62
M_2	7	1.66	0.089	5.35	0.051	1.44	1.88
	28	1.88	0.135	7.16	0.078	1.55	2.21
M_3	7	1.29	0.086	6.65	0.049	1.07	1.50
	28	1.55	0.102	6.56	0.059	1.29	1.80

The lowest tensile strength of HFRC mixes for 28 days was around 1.55 MPa, with the corresponding 95% confidence interval of the lower and higher limits being 1.29 MPa and 1.80 MPa. In contrast, the highest tensile strength was attained around 2.77 MPa with the lower and upper range of 1.93 MPa and 3.62 MPa for a 95% confidence interval.

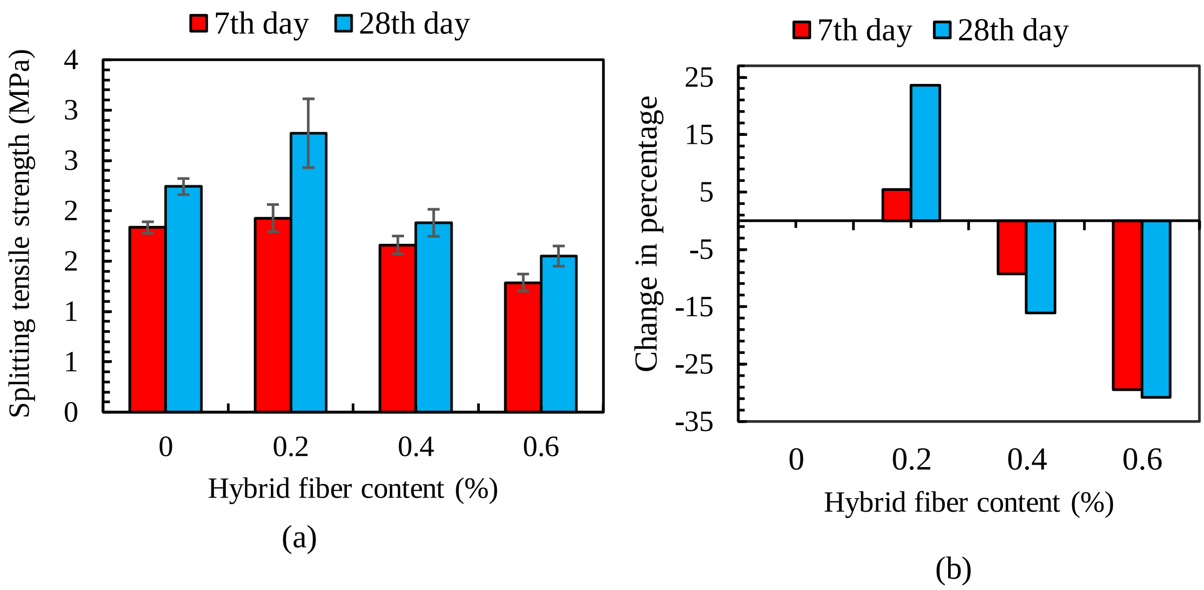

Figure 4. 8 (a) Splitting tensile strength values for HFRC and control concrete at 7 and 28-days (b) Percentage change in tensile strength of HFRC mixes compared to the reference mix.

Figure 4.8 (a) depicts the graphical plot between the splitting tensile strength for the HFRC mixes with various fiber concentrations at 7 and 28 days, comparing these findings to the control mix. Table 4.23 demonstrates that all HFRC specimens, including the control one, reached the splitting tensile strength to the extent of 70–88% of the tested specimens' 28-day strength at 7 days. At both 7 and 28 days of strength, it can be seen that the splitting tensile strength of the M_1 mix was higher than that of the control mix. The control mix's splitting tensile strength was determined to be 1.83 MPa at 7 days and 2.24 MPa at 28 days. Further examining the test results, the highest splitting tensile strength was observed around 2.77 MPa for the M_1 mix at 28 days and it gradually decreased to 1.55 MPa for the mix M_3. The changes in the percentage of splitting tensile strength for the HFRC mixes compared to the control mix are illustrated in Figure 4.8(b). A strength gain of about 23.66% was observed for the lower fiber concentration of M_1 mixtures compared to the control mix at 28 days test in this study. This increase in splitting tensile strength with hybrid fiber suggests that this is because of the non-uniform distribution and random orientation of hybrid fiber in the concrete mix, which results in a fiber-interlocking, homogeneous mix, and strong bond between the concrete aggregate, hybrid fiber, and cement paste and, consequently, an increase in concrete strength. The previous literature also inferred that the initial lower hybrid fiber concentration showed an increased splitting tensile strength than the control concrete; in contrast, the higher concentration of hybrid fiber demonstrated a lower strength (Raj et al., 2020). Other researchers have noted the characteristics of the strength gain that the splitting tensile strength increased in the range of 3% to 27% due to the addition of varying concentrations of hybrid fiber compared to the control concrete; however, they have taken into account the more varying concentrations of hybrid fiber in the mixes (Raj et al., 2020). The result is in also agreement with the experimental investigation conducted by (Das et al., 2020) and they also achieved an improvement in tensile strength using hybrid fibers.

4.3.2.1 ANOVA results of split tensile strength

Hypothesis Formulation Testing in Factorial ANOVA

For this test result, the three hypotheses are drawn, Null Hypothesis (H_o):

μ_{01} = hybrid fiber percentage doesn't affect the split tensile strength of concrete

μ_{02} = Curing period doesn't affect the split tensile strength of concrete

μ_{03} = hybrid fiber percentage and the curing period doesn't affect the split tensile strength of concrete.

Two-way factorial ANOVA with a confidence interval of 95% and a significant level of α = 0.05 is used to analyze the factors affecting the split tensile strength of concrete. P-value < 0.05, then the variable is considered as a significant factor that affects the split tensile strength of concrete so the null hypothesis is rejected, or for P-value ≥ 0.05, the factor is reflected as a non-significant effect and the null hypothesis will not be rejected. Based on Table 4.18, the effect of curing period, hybrid percentage and interaction are the significant effect that the P-values of the variables are less than 0.05; which shows that the variables are significant for a 95% confidence interval, and therefore; the null hypothesis is rejected. Based on Table 4.19, a 0.2% hybrid percentage is significantly different because the grouping letter does not share with other groups.

Table 4.18 Overall ANOVA for split tensile strength

	DF	Sum of Squares	Mean Square	F Value	P Value
Curing period	1	1.12381	1.12381	48.13744	3.34014E-6
Hybrid percentage	3	2.82347	0.94116	40.31363	1.09754E-7
Interaction	3	0.36748	0.12249	5.2469	0.01033
Model	7	4.31476	0.61639	26.40272	1.20021E-7
Error	16	0.37353	0.02335		
Corrected Total	23	4.6883			

At the 0.05 level, the population means of Curing day are significantly different.

At the 0.05 level, the population means of Hybrid are significantly different.

At the 0.05 level, the interaction between Curing day and Hybrid is significant.

Table 4.19 Interactions' Grouping Letters

Curing period	Hybrid percentage	Mean	Groups			
28th day	0.2	2.77	A			
28th day	0	2.24		B		
7th day	0.2	1.93		B	C	
28th day	0.4	1.88		B	C	
7th day	0	1.83		B	C	
7th day	0.4	1.66			C	D
28th day	0.6	1.54			C	D
7th day	0.6	1.28				D

Means that do not share a letter are significantly different.

4.3.2.2 Observed crack pattern.

Figure 4.9 depicts the observed crack pattern for the splitting tensile strength of the HFRC and control concrete specimens in this investigation. It can be shown that when the control specimen, which had no fibers, reached the ultimate load stage, it broke and failed in the brittle condition. However, in the case of specimens containing fibers, the initial crack began at the center of the cylindrical surface and spread quickly throughout the specimens' length and diameter as the applied force increased.

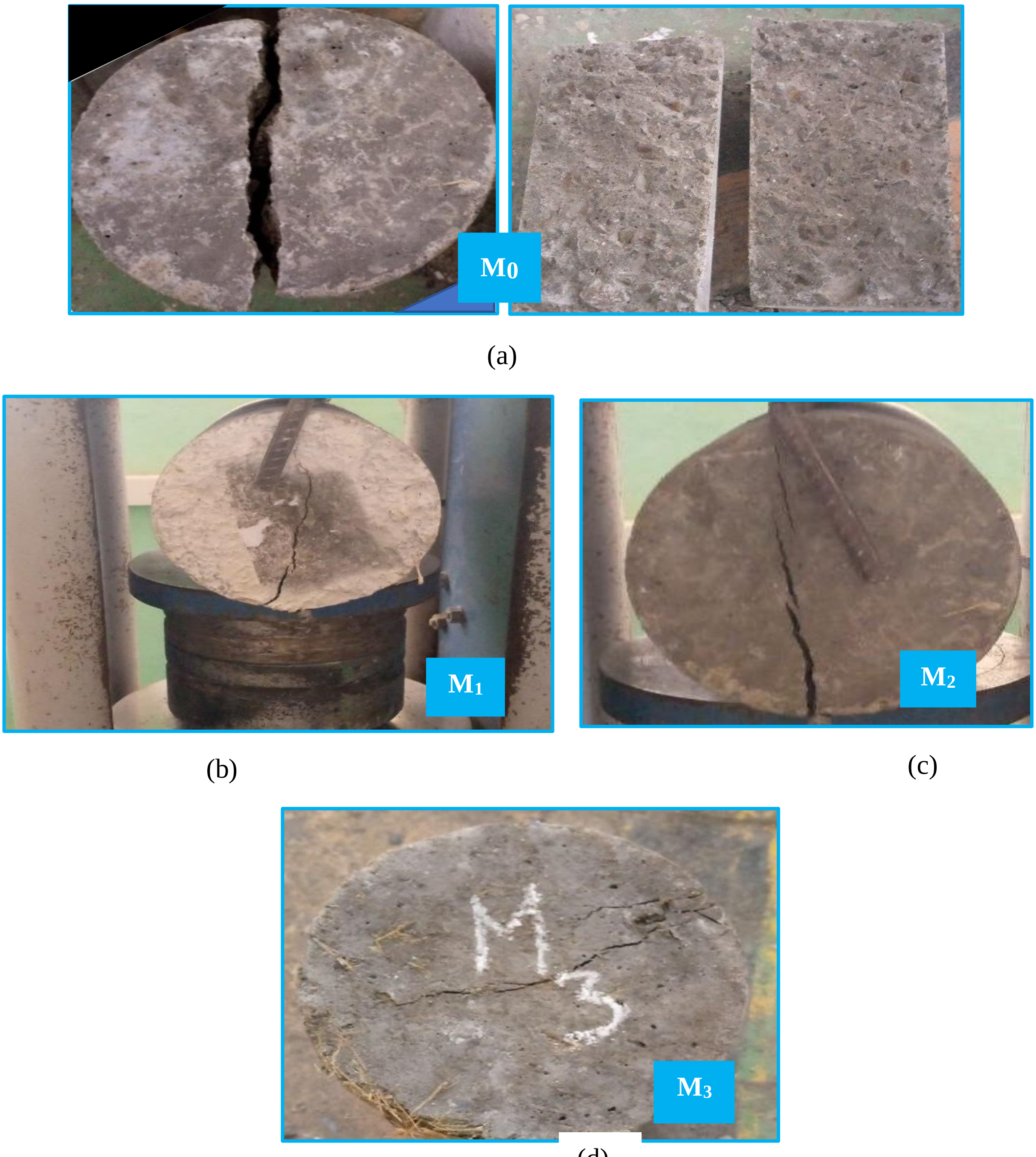

Figure 4.9 Observed crack pattern of HFRC and control mixes for splitting tensile strength test of (a) M_0 (b) M_1 (c) M_2 and (d) M_3.

From the close observations of the fractured HFRC specimens, it can be seen that multiple distributed smaller cracks were initiated in the concrete surface. A strong bond between aggregate, fiber, and cement paste was created by the randomly distributed hybrid fibers, homogeneity of the mixture, and interlocking of the fiber. This strong bond contributed to the ductile failure of the HFRC specimens before they completely failed under loading and split the cylinders into two half portions. This behavior is more pronounced for the HFRC mixes of M_2 and M_3 as shown in Figure 4.9 (c) and (d). As shown in Figure 4.9 (a), the control mix of M_0, on the other hand, showed brittle nature at failure load by entirely breaking the cylinder into two equal pieces. A similar finding in the crack pattern of FRC specimens was reported by (Das et al., 2020). According to their findings, fiber-reinforced concrete exhibits a primary crack in the center of the specimen, followed by minor secondary cracks, before separating into two half-cylinders. Non-fiber-reinforced concrete exhibits a straight, brittle crack pattern.

4.3.3 Effects of hybrid fibers on flexural strength

Table 4.20 shows the flexural strength test results for the control mix and HFRC mixes with various fiber concentrations. For analyzing the flexural strength test data with statistical tools, the mean strength, standard deviation, standard error, CV, and 95% confidence interval with lower and upper limits were determined similar to the compressive and splitting tensile strength. Table 4.20 shows that the flexural strength ranged from 3.11 MPa to 5.09 MPa, the test specimen's standard deviation ranged from 0.08 to 0.38, the corresponding CV ranged from 1.68% to 9.28%, and the standards error ranged from 0.046 to 0.222. In other words, the flexural strength of HFRC among all the mixes for 7 days had a minimum value of 3.11 MPa and a 95% confidence interval between the lower and upper limits of 3.00 MPa and 3.21 MPa. In contrast, the maximum flexural strength was found to be around 4.36 MPa, with a 95% confidence interval ranging from 4.23 MPa and 4.49 MPa for the lower and upper ranges. Additionally, the flexural strength of all HFRC mixes for 28 days showed a minimum value of 3.42 MPa with a 95% confidence interval of 3.30 MPa and 3.54 MPa for the lower and upper bounds, respectively. In contrast, a 95% confidence interval for the flexural strength showed a maximum value of 5.09 MPa with a lower and upper range of 4.87 MPa and 5.30 MPa.

Table 4.20 Summary of the flexural strength test results of the HFRC and control concrete.

Mixes	Days	Mean strength(MPa)	Standard deviation	CV (%)	Standard error	95% confidence interval	
						Lower limit	Upper limit
M_0	7	4.15	0.18	4.33	0.104	4.01	4.29
	28	4.72	0.08	1.68	0.046	4.66	4.78
M_1	7	4.36	0.16	3.73	0.094	4.23	4.49
	28	5.09	0.27	5.22	0.153	4.87	5.30
M_2	7	3.27	0.11	3.39	0.064	3.18	3.35
	28	4.13	0.38	9.28	0.222	3.81	4.46
M_3	7	3.11	0.14	4.38	0.079	3.00	3.21
	28	3.42	0.15	4.51	0.089	3.30	3.54

The observed flexural strength at 7 and 28 days for each hybrid fiber mix with various fiber concentrations is shown in Figure 4.10 (a).

Table 4.20 shows that after testing the specimens in the lab, the flexural strength of HFRC specimens can be easily attained the 7-day strength in the range of 79%-88% of its 28-day strength.

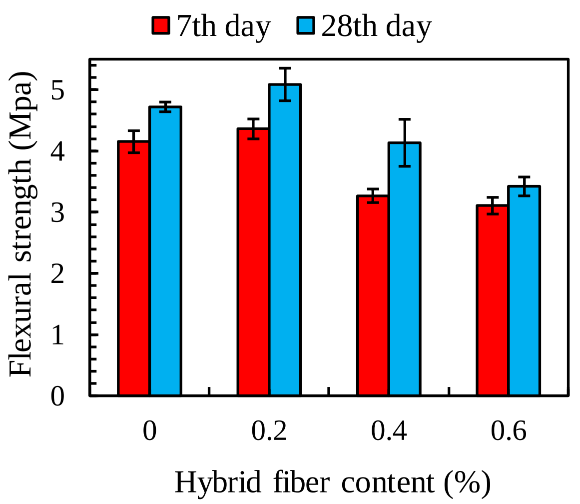

(a)

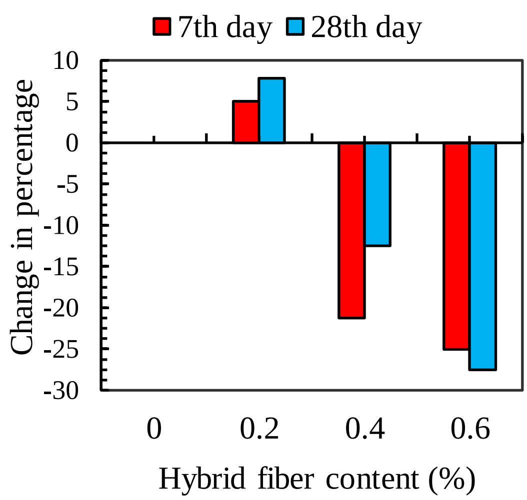

(b)

Figure 4.10 (a) Flexural strength values for HFRC and control concrete at 7 and 28-days (b) Percentage change in flexural strength of HFRC mixes compared to the reference mix.

It should be mentioned that the flexural strength ratio of HFRC specimens at 7 to 28 days has been shown to be, on average, 5.5% greater than the splitting tensile strength for the same mix. Flexural strength for control concrete was 4.15 MPa at 7 days, and it gradually decreased after the M_2 mix to 3.11 MPa. Flexural strength for control concrete was 4.15 MPa at 7 days, and it steadily decreased to 3.11 MPa after the M_2 mix. On the other hand, the control specimen increased in strength by 4.72 MPa after 28 days of curing, while the mix M_3 specimen saw a reduction in strength of up to 3.42 MPa the lowest flexural strength at 28 days in this investigation. Figure 4.10 (b) shows the range in percentage changes in flexural strength for the HFRC mixes when compared to the control mix. In comparison to the control concrete, it can be seen that the addition of 0.2% fibers to the concrete increased flexural strength from 4.72 MPa to 5.09 MPa, a 7.84% increase in strength. The alignment of randomly distributed fibers along the length of the flexural prisms and the strong fiber-bridging effects of HFRC, which began after the first crack was initiated and occurred when the applied load on the prism exceeded the tensile strength of concrete, can be used to explain this strength improvement.

In other words, this bridging effect has contributed to increasing the flexural strength upon the application of load until the final failure of the prism specimens. The test results presented in this study are also comparable with the results obtained from the experimental study carried out by (Das et al., 2020). They reported that the hybridization of fibers in the concrete mix increased the flexural strength value by about 4.92 MPa, which was a 24.87% greater enhancement, compared to the control mix.

4.3.3.1 ANOVA results of flexural strength

Hypothesis Formulation Testing in Factorial ANOVA

For this test result, the three hypotheses are drawn, Null Hypothesis (H_o):

μ_{01} = hybrid fiber percentage doesn't affect the flexural strength of concrete

μ_{02} = Curing period doesn't affect the the flexural strength of concrete

μ_{03} = hybrid fiber percentage and the curing period doesn't affect the flexural strength of concrete.

Two-way factorial ANOVA with a confidence interval of 95% and a significant level of $\alpha = 0.05$ is used to analyze the factors affecting the split tensile strength of concrete. P-value < 0.05, then the variable is considered as a significant factor that affects the split tensile strength of concrete so the null hypothesis is rejected, or for P-value ≥ 0.05, the factor is reflected as a non-significant effect and the null hypothesis will not be rejected.

Table 4.21 Overall ANOVA for flexural strength

	DF	Sum of Squares	Mean Square	F Value	P Value
Curing Period	1	2.29838	2.29838	54.48099	1.55078E-6
Hybrid percentage	3	8.05414	2.68471	63.63861	4.11804E-9
Interaction	3	0.25086	0.08362	1.98214	0.15731
Model	7	10.60338	1.51477	35.90617	1.27502E-8
Error	16	0.67499	0.04219		
Corrected Total	23	11.27837			

At the 0.05 level, the population means of Curing day are significantly different.

At the 0.05 level, the population means of Hybrid are significantly different.

At the 0.05 level, the interaction between Curing day and Hybrid is significant

Table 4.22 Interactions' Grouping Letters

Curing Period	Hybrid percentage	Mean	Groups			
28th day	0.2	5.08	A			
28th day	0	4.72	A	B		
7th day	0.2	4.36		B	C	
7th day	0	4.15		B	C	
28th day	0.4	4.13			C	
28th day	0.6	3.42				D
7th day	0.4	3.26				D
7th day	0.6	3.11				D

Means that do not share a letter are significantly different.

Based on Table 4.21, the effect curing period and hybrid percentage are the significant effects that the P-values of the variables are less than 0.05; which shows that the variables are significant for a 95% confidence interval, and therefore; the null hypothesis is rejected. Whereas interaction effects are not a significant effect as it has α value variables greater than 0.05; so, the decision is not to reject the null hypothesis. Based on Table 4.22, a 0.2% hybrid percentage is significantly different because the grouping letter does not share with other groups.

4.3.3.2 Observed crack pattern.

Control and HFRC prism specimens exhibited different types of failure and the observed crack patterns are shown in Figure 4.11. For control concrete prisms, it can be observed that the specimens were broken suddenly into two pieces when the ultimate flexural strength was reached and there was no advanced warning exhibited it is considered as brittle failure refers in Figure 4.11 (a). Moreover, the specimens containing 0.2%, 0.4%, and 0.6% fiber concentration showed excellent post-crack arresting performance as shown in Figure 4.11 (b), (c), and (d).

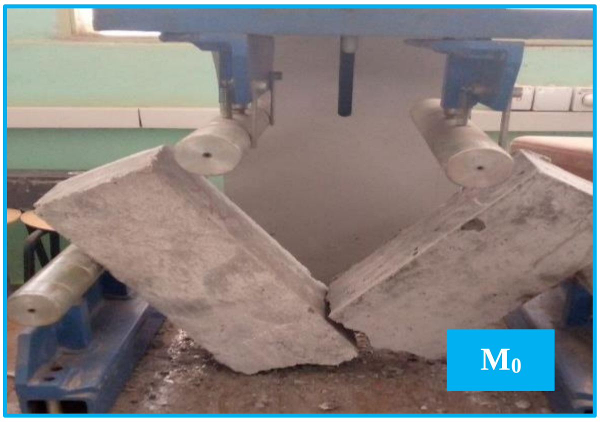

(a)

(b)

(c)

(d)

Figure 4.11 Observed crack pattern of HFRC mixes for flexural strength test of (a) M_0 (b) M_1 (c) M_2 and (d) M_3

The failure of M_1 and M_2 HFRC samples is not brittle like the control concrete prisms and it revealed the flexural crack that is the crack exceeded the neutral axis of the prism and propagated to the straight vertical. Furthermore, for the prisms specimens with 0.6% fiber concentrations designated as M_3 have been investigated the shear crack along the length of the prisms at the high shear zone is illustrated in Figure 4.11 (d). It can also be seen that in the case of all HFRC prisms when the first hairline crack appears on the surface, fibers started to bridge the cracks by interlocking each other, which ultimately sustains more flexural strength and higher ductility than the control samples. The crack pattern observed in the experimental investigation conducted by (Das et al., 2020) showed a similar fashion of crack patterns. They also observed that fiber-bridging effects in the HFRC prisms have a strong influence on the enhancement of the flexural strength and ductility behavior at higher fiber concentrations as compared to conventional concrete.

4.3.4 Effects of hybrid fibers on Density, water absorption, and Voids

The density of concrete is the measure of its unit weight. Density, water absorption and Permeable Voids Space tests were performed for both controls as well as HFRC concrete as per the specifications of ASTM C-642. The average test results are presented in Table 4.23. The density of M_1, M_2, and M_3 was 2.51%, 6.55%, and 8.98% lower than the control concrete.

Table 4.23 Average water absorption, Density, and permeable voids

Mix code	Absorption after Immersion (%)	Absorption after Immersion & Boiling (%)	Bulk Dry Density (kg/m3)	Bulk Density after Immersion (kg/m3)	Bulk Density after Immersion & Boiling(kg/m3)	Apparent Density (kg/m3)	Volume of Permeable Voids Pore Space, Porosity(%)
M_0	6.68	6.71	2201.38	2348.44	2349.04	2582.75	14.77
M_1	7.68	7.83	2146.19	2310.99	2314.24	2579.69	16.80
M_2	9.62	10.26	2057.30	2255.15	2268.28	2607.41	21.10
M_3	10.12	11.06	2003.60	2206.37	2225.29	2574.30	22.17

Further, it is observed that the density was decreased with the addition of different fibers as shown in Figure 4.12. The maximum reduction in density is observed for M_3 and the minimum reduction was for M_1. This may be due to the fact that these fiber materials have a lower density than the concrete mixture. When these fibers are added to the mixture, they displace some of the heavier aggregates, such as sand and gravel, which results in a lower overall density of the concrete. Additionally, the fibers themselves may also be less dense than the other materials used in the mixture, which further contributes to the decrease in density.

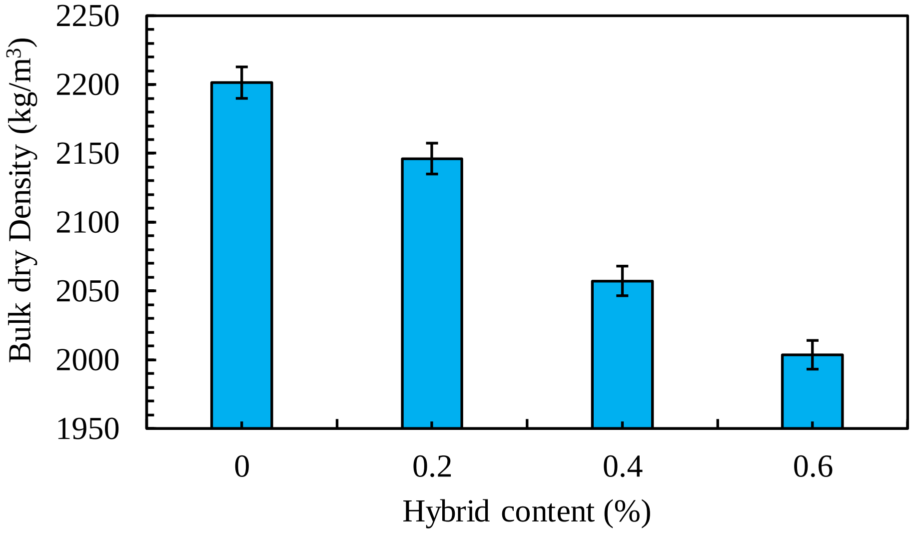

Figure 4.12 Density of HFRC and control concrete

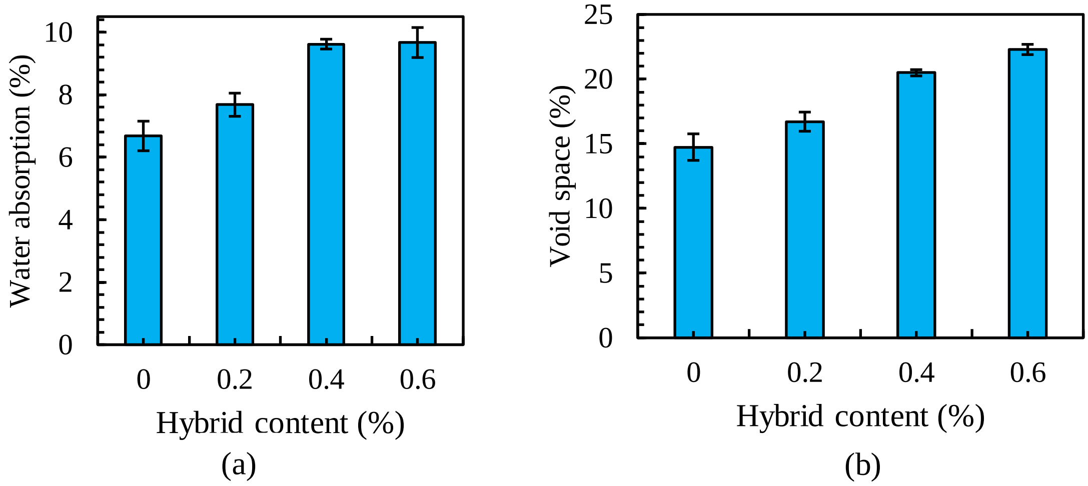

Figure 4.13 (a) Water absorption values for HFRC and control concrete (b) permeable void spaces of HFRC HFRC and control concrete

Thus, the bulk dry density was in the range of 2000 - 2600kg/m^3 for normal concrete stipulated by BS EN 206 (2013). The inverse relationship between the density and percentage of hybrid fibers is a result of the lower bulk density of the fibers which is taking the place of denser constituents, like coarse and fine aggregates (Abayomi, 2018; Hidaya et al., 2017).

The water absorption of HFRC concrete, as well as control concrete, is shown in Figure 4.13 (a). At 28 days, it was discovered that there was an increment in water absorption after immersion (Wi) and water absorption after immersion and boiling (Wib) as the percentage of fibers of HFRC content increased. The highest percentage of water absorptions was 10.12% for Wi and 11.06% for Wib. Generally, the water absorption of HFRC samples had high water absorption as compared with control concrete. This may be due to the fact that the teff straw fibers tend to absorb moisture, which can lead to an increase in the water absorption of the concrete. Additionally, as the percentage of these fibers increases, the amount of voids or empty spaces in the concrete also increases. These voids can act as pathways for water to penetrate and be absorbed by the concrete. This results in an increase in the water absorption of the concrete as the percentage of fibers increases. In summary, the water absorption of concrete cubes was observed to increase with a rising percentage of hybrid fiber addition in the mix. A similar result was reported by (Hidaya et al., 2017).

The permeable (porosity) void spaces of HFRC concrete increased with an increase in fiber content as seen in 4.13 (b). A sharp increment in the void by 50.14% from 14.77% to 22.17% as the fiber content was increased from 0 – 0.6%. This may be due to fact that the bulky nature of fibers, which means they occupy some space in the concrete and create voids. As the percentage of fibers added increases, more voids are created in the concrete and leading to an overall increase in permeable voids.

4.4 Life cycle cost analysis

A period of 40 years was considered for the analysis as shown in the Table 2.24 to include one rehabilitation activity for the rigid pavement.

Table 4.24 Life Cycle Cost analysis periods

Pavement Type	Design period	Analysis period	Segment of road considered	Remark
Rigid pavement without	40 years	40 years	1km length and 7m width	To consider at least one Rehabilitation of rigid pavement
Rigid pavement with fiber	40 years	40 years	1km length and 7m width	To consider at least one Rehabilitation of rigid pavement

Table 4.25 Activity Parameters and cost schedule

Type	Descriptions	Frequency	Cost Base line
Rigid Pavement	Initial Construction Cost	in 2023 G.C	Cost of 2023
	Routine Maintenance Cost	Every 8th years	
	Periodic Maintenance	Every 12th years	
	Rehabilitation Cost	At 40th year(2063 G.C)	
	Salvage value	At 40th year(2063 G.C)	

4.4.1 Initial construction Cost of pavements

The cost was calculated after determining the quantity and cost break down for 1km and 7 meter road width base on the typical road section of pavement. The break down calculation include direct and indirect costs of concrete pavement but other costs like Sub base materials, Texturing and Curing, Joints are ignored since they have the same effect on comparison of the pavement costs.

Table 4.26 Initial cost Summary for rigid pavement (from Appendix H3 table)

S/no	**Description**	**Total ETB**
1	Concrete Pavement	33,562,760.00
2	Reinforcing steel Bars	9,677,552.04
	Cost for 1km per km	**43,240,312.04**

Table 4.27 Initial cost Summary for rigid pavement with hybrid fibers (from Appendix H3 Table)

S/no	DESCRIPTION	TOTAL ETB
1	Concrete Pavement	33,562,760.00
2	Reinforcing steel Bars	9,677,552.04
3	Teff straw fiber	92,344.00
4	Polyethylene terephthalate fiber	461,720.00
	Cost for 1km per KM	**43,794,376.04**

PET bottles that were collected from the surrounding environment had costs of collection, cleaning, and cutting into rectangular fibers. This particular research used a manual method of cutting the bottles into fibers. The labor cost was 50 ETB per kilogram of PET fibers. For 0.2% hybrid (optimum), 3.88kg for 1m^3 and for 1km length, 7m width and 0.34m depth 9234.4kg was required. Therefore, 461,720 ETB were required. Teff straw was collected from farmers around Adama and the total cost of teff straw for collection, cleaning, and chopping was 10 ETB per kg. A 92,344 ETB was required for teff straw fiber.

Table 4.28 Initial Cost comparison of the two pavements

Pavement Type	Length(km)	No of lane	width per lane(m)	Cost per km (Birr)
Rigid pavement	1	2	3.5	43,240,312.04
Rigid pavement with fibers	1	2	3.5	43,794,376.04

4.4.2 Maintenance cost of pavements

4.4.2.1 Maintenance and rehabilitation of rigid pavement

The major routine maintenance activities were scheduled to be conducted at every 8 years and periodic activities at 12 years before wet season. At 40 years after construction, rehabilitation was scheduled for the particular project.

Table 4.29 Schedule of Maintenance and rehabilitation of rigid pavement (Anne Holt, 2011)

Maintenance Type	Activity	Frequency
Routine Maintenance	Joint Sealing Crack Sealing	Every 8 years
Periodic maintenance	Partial Depth repair	every 12 years
Rehabilitation	Full depth repair	at 40 years

4.4.2.2 Discount Rate and Interest Rate

Even if calculation and selection of the discount rate is quite complex and is the subject of ongoing debate in academic circles, the exact mathematical relationship between the discount rate, the interest rate, and the inflation rate presented by (Demos, 2006) was employed in selecting a discount rate for this particular case. The relationship between real discount rate, nominal discount rate, and inflation rate is:

$$dr = [\frac{1+i}{1+f}]-1$$

Given; f = inflation rate in decimal = 0.293 i = interest rate in decimal = 0.070

$$dr = [\frac{1+0.07}{1+0.293}]-1= -0.172$$

A negative discount rate means that present value of a future liability is higher today than at the future date when that liability will have to be paid and this is due to a high inflation rate in Ethiopia. The discount rate is a function of risk and return, there is no such thing as negative risk and it is illogical. Every company has systemic and non-systemic risk inherent in its model. Therefore, it was found good to use the maximum allowable value presented in [36] in such case. Hence, a discount rate of 3.5% was adopted in this particular case. The inflation rate in Ethiopia was recorded at 29.3 % in June 2023.

In Ethiopia, interest rates decisions are taken by Monetary Committee of the National Bank of Ethiopia. The official rate is the bank’s savings rate. The benchmark interest rate in Ethiopia was last recorded at 7 percent by the end of the first quarter 2023, according to Trading Economics global macro models and analysts’ expectations. Therefore, the interest rate adopted in this particular case was 7%.

4.4.3 Salvage Value of rigid pavement

According to (Scheving, 2011), the following equation was adopted in this case to calculate salvage value.

Salvage Value = LC $[\frac{TEL}{ERL}]$ Equation 4.1

Where, LC = Last rehabilitation costs of pavement

ERL = Expected remaining life of the last rehabilitation of pavements

TEL = Total expected life of the last rehabilitation pavements

Salvage Value = 1,628,000.00 [8/12] = 1,085,333.33

Table 4.30 Cost of rigid pavement without fibers

Activity	Cost (ETB)	Remark
Construction Cost	43,240,312.04	
Routine Maintenance Cost	500,000.00	Every 8 years
Periodic Maintenance Cost	170,000.00	Every 12 years
Rehabilitation Cost	1,628,000.00	At 40 years
Salvage Value	1,085,333.33	After 40 Years

Table 4.31 Cost of rigid pavement with fibers

Activity	**Cost (ETB)**	**Remark**
Construction Cost	43,794,376.04	
Routine Maintenance Cost	350,000.00	Every 8 years
Periodic Maintenance Cost	119,000.00	Every 12 years
Rehabilitation Cost	1,628,000.00	At 40 years
Salvage Value	1,085,333.33	After 40 Years

The maintenance cost of fiber reinforced concrete is (20-40) % less compared to conventional concrete (Stempihar et al., 2012). The average value (30%) was taken.

4.4.4 Future Value of Costs

Since all the costs other than initial construction will occur in the future analysis years, future value of money should be determined for maintenance, rehabilitation and salvage values by considering the inflation rate. Inflation Rate, the rate of increase in the general price levels, caused usually by an increase in the volume of money and credit relative to available goods. The inflation rate is also reflective of the rate of decline in the general purchasing power of a currency.

$$Fc = Pv\,[1+if]^n \qquad \text{Equation 4.2}$$

Where Fc =Future cost at time of n years

PV = Present Value of Money in birr

if = inflation adjusted interest rate

n = number of years

4.4.5 Present worth Calculations

The net present worth formula used was the following:-

$$NPW = IC + [\textstyle\sum_n^N MC\,]\left[\frac{1}{1+dr)n}\right] + [\textstyle\sum_n^N RC]\left[\frac{1}{1+dr)n}\right] - Sv\left[\frac{1}{1+dr)n}\right] \qquad \text{Equation 4.3}$$

The initial construction cost for the rigid pavement was 43,240,312.04 Birr/Km and for rigid pavement with fibers was 43,794,376.04 Birr/Km at the end of 2023 and the discount rate used was 3.5%. Here the future value of all costs except the initial construction of pavements was calculated with the corresponding occurrence years to account inflation and then brought to the present value as of 2023.

The waste PET bottles collected from the surrounding environment had costs of collection and transportation to land fill for the municipality. The assumed disposal site was 10km. The collection and transportation cost was assumed 300 ETB per m^3. For 0.2% hybrid (optimum), 3.88kg for $1m^3$ and for 1km length, 7m width and 0.34m depth, $2380m^3$ was required. Therefore, 714,000.00 ETB were required.

Table 4.32 Present worth of pavements with the corresponding cost

Alternatives	Description	PW (Birr/km)
Rigid pavement	Construction	43,240,312.04
	Routine Maintenance	1,165,701.78
	Periodic Maintenance	266,824.37
	Rehabilitation	33,087.41
	Salvage Value	-22,058.28
Net PW		**44,683,867.32**
Rigid pavement with fibers	Construction	43,794,376.04
	Routine Maintenance	815,991.23
	Periodic Maintenance	186,777.05
	Rehabilitation	33,087.41
	Salvage Value	-22,058.28
Net PW		**44,808,173.45**
The amount of cost to be saved using fibers = (44,683,867.32+ 714,000.00) - 44,808,173.45 **= 589,693.87 ETB**		

CHAPTER FIVE

CONCLUSIONS AND RECOMMENDATIONS

5.1 Conclusions

An experimental investigation was carried out to determine the fresh and mechanical properties of control and HTPFRC specimens with different concentrations of fiber in the concrete mixes. The following conclusions were drawn based on current experimental results:

- The slump and compaction factor values were found to decrease as the percentage of HTP fibers increased. In comparison to control concrete, the slump value dropped by 25.25%, 61.81%, and 80.6%, while the compaction factor reduced by 5.74%, 6.38%, and 29.36% at hybrid fiber concentrations of 0.2%, 0.4%, and 0.6%.This is because the interlocking of fibers and the incorporation of fibers absorbed more water from the concrete mix.
- The inclusion of fibers in the concrete mix resulted in a decrease in compressive strength. A concrete mix with 0.2%, 0.4%, and 0.6% fibers concentration showed a compressive strength reduction of 15.08%, 39.19%, and 46.21% lower than the control mix. This is due to fiber balling effects and concrete becoming too hard to compact which in turn leads to more air voids thereby a decline in compressive strength.
- The splitting tensile and flexural strengths have shown that the highest strength was obtained at about 2.77 MPa and 5.09 MPa at 28 days, respectively. Splitting tensile and flexural strengths displayed 23.66% and 7.84% strength enhancement for the addition of 0.2% hybrid fiber concentration over the mixture with hybrid fiber concrete, respectively. This behavior is attributed to the randomly distributed fibers in the mixtures and the strong hybrid fiber-bridging effects increasing the strength.
- The failure mode of HTPF concrete has been changed to a more ductile one with a smaller distribution of cracks than the brittle failure of control concrete. This behavior is more noticeable with higher fiber concentration and it is suggested that due to the ductile nature, which will provide a sufficient warning before the final failure.
- The water absorption and void space were found to be increased with the addition of hybrid fibers. In that, the mix containing 0.6% has more water absorption and void space than other mixes.

- The optimum fiber combination recommended is the 0.2% of hybrid fiber mix in this study, due to the improvement of fresh and mechanical properties as compared to the subsequent HTP concrete mixes.

5.2 Recommendations

5.2.1 Recommendations from the Study

- For experimental purposes and small-scale concrete production, HTPFRC preparation processes do not have problems; nevertheless, for mass production to meet quality, accuracy, and efficiency requirements, it is necessary to use some kind of methodology. It is strongly advised to develop a new technique for obtaining teff straw and polythene terephthalate fibers using mechanical machines that prepare them with the requirements and required quality, accuracy, and efficiency in order to solve these issues.
- Higher slump values, compared to conventional mixes, should be targeted for HFRC mixes in order to compensate for the reduced workability of HFRC mixes. A superplasticizer might be added.
- Up to a 15% reduction in compressive strength should be taken into account when designing HTPFRC mixes.
- Manual compaction should be completely avoided.

5.2.2 Recommendations for future works

The researcher forwarded the following recommendations for future study.

- Additional tests other than water absorption and permeable void space such as permeability, Chloride attack, and Sulfuric acid attack resistance need to be conducted the determine the long-term durability of concrete.
- Microstructural tests such as scanning electron microscope (SEM) need to be conducted to observe the interface between matrix and fibers.
- Further work is required to determine the strength of different concrete grades and varying aspect ratios of fibers.
- Environmental and Cost implications of using hybrid teff straw and polythene terephthalate fibers could be studied.

Research Fund Acknowledgement

This research project is funded by Adama science and Technology University under the grant number ASTU/SM-R/799/23,Adama, Ethiopia

REFERENCES

Abayomi, O. A. (2018). *Behaviour of Sisal Fibre-Reinforced Concrete in Exterior Beam-Column Joints Under Monotonic Loading.* JKUAT-PAUSTI.

ACI Committee 211. (2002). Standard Practice for Selecting Proportions for Normal, Heavyweight, and Mass Concrete. Farmington Hills: American Concrete Institute.

Adnan, H. M., & Dawood, A. O. (2020). Strength behavior of reinforced concrete beam using re-cycle of PET wastes as synthetic fibers. *Case Studies in Construction Materials, 13*, e00367.

Afroughsabet, V., Biolzi, L., & Ozbakkaloglu, T. (2016). High-performance fiber-reinforced concrete: a review. *Journal of materials science, 51*(14), 6517-6551.

Afroughsabet, V., & Ozbakkaloglu, T. (2015). Mechanical and durability properties of high-strength concrete containing steel and polypropylene fibers. *Construction and Building Materials, 94*, 73-82.

Al-Hadithi, A. I., Noaman, A. T., & Mosleh, W. K. (2019). Mechanical properties and impact behavior of PET fiber reinforced self-compacting concrete (SCC). *Composite Structures, 224*, 111021. doi: https://doi.org/10.1016/j.compstruct.2019.111021

Amentae, T. K., Tura, E. G., Gebresenbet, G., & Ljungberg, D. (2016). Exploring value chain and post-harvest losses of Teff in Bacho and Dawo districts of central Ethiopia.

Anne Holt, P. (2011). I. Applied Research Associates, and S. 5401 Eglinton Avenue West, Toronto, ON, Canada, M9C 5K6. *Life Cycle Cost Analysis of Municipal Pavements in Southern and Eastern Ontario*, 10.

ASTM C33/C33M. (2018). Standard Specification for Concrete Aggregates. West Conshohocken, PA: ASTM International.

ASTM C39. (2018). Standard Test Method for Compressive Strength of Cylindrical Concrete Specimens. West Conshohocken, PA: ASTM International.

ASTM C78. (2002). Standard Test Method for Flexural Strength of Concrete (Using Simple Beam with Third-Point Loading)

West Conshohocken, PA: ASTM International.

ASTM C117. (2017). Standard Test Method for Materials Finer than 75-µm (No. 200) Sieve in Mineral Aggregates by Washing. West Conshohocken, PA: ASTM International.

ASTM C127. (2015). Standard Test Method for Relative Density (Specific Gravity) and Absorption of Coarse Aggregate. West Conshohocken, PA: ASTM International.

ASTM C128. (2015). Standard Test Method for Relative Density (Specific Gravity) and Absorption of Fine Aggregate. West Conshohocken, PA: ASTM international.

ASTM C136. (2006). Standard Test Method for Sieve Analysis of Fine and Coarse Aggregates. West Conshohocken, PA: ASTM International.

ASTM C143. (2012). Standard Test Method for Slump of Hydraulic-Cement Concrete. West Conshohocken, PA: ASTM International.

ASTM C150/C150M. (2012). Standard Specification for Portland Cement. West Conshohocken, PA: ASTM International.

ASTM C187. (2016). Standard Test Method for Amount of Water Required for Normal Consistency of Hydraulic Cement Paste. West Conshohocken, PA: ASTM International.

ASTM C192. (2000). Standard Practice for Making and Curing Concrete Test Specimens in the Laboratory. West Conshohocken, PA: ASTM International.

ASTM C496. (2004). Standard Test Method for Splitting Tensile Strength of Cylinderical Concrete. West Conshohocken, PA: ASTM International.

ASTM C566. (2019). Standard Test Method for Total Evaporable moisture content of Aggregate by Drying. West Conshohocken, PA: ASTM International.

ASTM C642. (2006). Standard Test Method for Density, Absorption, and Voids in Hardened Concrete *Materials Today: Proceedings*. West Conshohocken, PA: ASTM International.

Ataei, H., Kalbasi Anaraki, K., & Ma, R. (2017). Mechanical properties of polyethylene terephthalate particle-based concrete: A review. *Airfield and Highway Pavements 2017*, 57-68.

Atiş, C. D., & Karahan, O. (2009). Properties of steel fiber reinforced fly ash concrete. *Construction and Building Materials, 23*(1), 392-399.

Awang, H., Mydin, A. O., & Ahmad, M. H. (2013). Mechanical and durability properties of fibre lightweight foamed concrete. *Aust. J. Basic Appl. Sci, 7*(7), 14-21.

Awoyera, P. O., Olalusi, O. B., & Ekpe, C. O. (2021). Plastic fiber-strengthened interlocking bricks for load bearing applications. *Innovative Infrastructure Solutions, 6*, 1-10.

Aziz, K. I. (2017). Mechanical properties for ordinary concrete containing waste plastic fibers. *Iraqi Journal of Civil Engineering, 11*(2).

Bachewe, F., Regassa, M. D., Minten, B., Taffesse, A. S., Tamru, S., & Hassen, I. W. (2019). The transforming value chain of Ethiopia's "orphan" tef crop. *Planta, 250*, 769-781.

Bankir, M. B., & Sevim, U. K. (2020). Performance optimization of hybrid fiber concrete according to mechanical properties. *Construction and Building Materials, 261*, 119952.

Bayable, M., Tsunekawa, A., Haregeweyn, N., Alemayehu, G., Tsuji, W., Tsubo, M., . . . Masunaga, T. (2021). Yield Potential and Variability of Teff (Eragrostis tef (Zucc.) Trotter) Germplasms under Intensive and Conventional Management Conditions. *Agronomy, 11*(2), 220. doi: 10.3390/agronomy11020220

Beaudoin, J., & Odler, I. (2019). Hydration, setting and hardening of Portland cement. *Lea's chemistry of cement and concrete, 5*, 157-250.

Bederina, M., Belhadj, B., Ammari, M., Gouilleux, A., Makhloufi, Z., Montrelay, N., & Quéneudéc, M. (2016). Improvement of the properties of a sand concrete containing barley straws–treatment of the barley straws. *Construction and Building Materials, 115*, 464-477.

Bei-Xing, L., Ming-xiang, C., Fang, C., & Lu-ping, L. (2004). The mechanical properties of polypropylene fiber reinforced concrete. *Journal of Wuhan University of Technology. Materials Science Edition, 19*(3), 68.

Belhadj, B., Bederina, M., Montrelay, N., Houessou, J., & Quéneudec, M. (2014). Effect of substitution of wood shavings by barley straws on the physico-mechanical properties of lightweight sand concrete. *Construction and Building Materials, 66*, 247-258.

Biratu, M. K., Thanappan, S., Hailu, H., Swamy Nadh, V., & Mahesh Kumar, C. (2022). Nanosilica-Based Teff Straw as an Eco-Friendly Substitute for Special Concrete. *Journal of Nanomaterials, 2022*.

BS 1881. (1983). Method for determination of compacting factor. London, UK: British Standards Institution.

BS EN 206. (2013). Concrete — Specification, performance, production and conformity. London, UK: BSI Standards Publication.

Caggiano, A., Folino, P., Lima, C., Martinelli, E., & Pepe, M. (2017). On the mechanical response of hybrid fiber reinforced concrete with recycled and industrial steel fibers. *Construction and Building Materials, 147*, 286-295.

Cao, M., Zhang, C., & Lv, H. (2014). Mechanical response and shrinkage performance of cementitious composites with a new fiber hybridization. *Construction and Building Materials, 57*, 45-52.

Cao, Z., & Myers, R. J. (2020). The sponge effect and carbon emission mitigation potentials of the global cement cycle. *11*(1), 3777. doi: 10.1038/s41467-020-17583-w

Chabi, E., Lecomte, A., Adjovi, E. C., Dieye, A., & Merlin, A. (2018). Mix design method for plant aggregates concrete: example of the rice husk. *Construction and Building Materials, 174*, 233-243.

Das, S., Sobuz, M. H. R., Tam, V. W., Akid, A. S. M., Sutan, N. M., & Rahman, F. M. (2020). Effects of incorporating hybrid fibres on rheological and mechanical properties of fibre reinforced concrete. *Construction and Building Materials, 262*, 120561.

Dawood, E. T., & Ramli, M. (2012). Mechanical properties of high strength flowing concrete with hybrid fibers. *Construction and Building Materials, 28*(1), 193-200. doi: https://doi.org/10.1016/j.conbuildmat.2011.08.057

de Souza Castoldi, R., de Souza, L. M. S., & de A. Silva, F. (2022, 2022//). *Effect of Alkali Treatment to Improve Fiber-Matrix Bonding and Mechanical Behavior of Sisal Fiber Reinforced Cementitious Composites.* Paper presented at the Fibre Reinforced Concrete: Improvements and Innovations II, Cham.

Demissew, A., Fufa, F., & Assefa, S. (2019). Partial replacement of cement by coffee husk ash for C-25 concrete production. *Journal of Civil Engineering, Science and Technology, 10*(1), 12-21.

Demos, G. P. (2006). Life cycle cost analysis and discount rate on pavements for the Colorado Department of Transportation.

Devnani, G., & Sinha, S. (2020). African teff straw as a potential reinforcement in polymer composites for light-weight applications: mechanical, thermal, physical, and chemical characterization before and after alkali treatment. *Journal of Natural Fibers, 17*(7), 1011-1025.

Dinku, A. (2002). Construction materials laboratory manual. *Addis Ababa University Printing Press, Addis Ababa*.

Dnyanoba, d. p., & madhukar, r. h. (2020). Concrete Curing Method. *Iconic Research and Engineering Journals, 3*(7), 142-144.

Durairaj, S. K., Ong, S. K., Nee, A. Y., & Tan, R. B. (2002). Evaluation of life cycle cost analysis methodologies. *Corporate Environmental Strategy, 9*(1), 30-39.

El-Din, H. K. S., Eisa, A. S., Aziz, B. H. A., & Ibrahim, A. (2017). Mechanical performance of high strength concrete made from high volume of Metakaolin and hybrid fibers. *Construction and Building Materials, 140*, 203-209.

Farooqila, M., & Ali, M. (2016). *Compressive behavior of wheat straw reinforced concrete for pavement applications.* Paper presented at the Proceedings of the Fourth

International Conference on Sustainable Construction Materials and Technologies, Las Vegas, NV, USA.

Figueiredo, A. D. d., & Ceccato, M. R. (2015). Workability analysis of steel fiber reinforced concrete using slump and Ve-Be test. *Materials Research, 18,* 1284-1290.

França, W. T., Barros, M. V., Salvador, R., de Francisco, A. C., Moreira, M. T., & Piekarski, C. M. (2021). Integrating life cycle assessment and life cycle cost: A review of environmental-economic studies. *The International Journal of Life Cycle Assessment, 26,* 244-274.

Fuller, S. (2010). Life-cycle cost analysis (LCCA). *National Institute of Building Sciences, An Authoritative Source of Innovative Solutions for the Built Environment, 1090*.

Gagg, C. R. (2014). Cement and concrete as an engineering material: An historic appraisal and case study analysis. *Engineering Failure Analysis, 40,* 114-140.

Gashaahun, A. (2020). Assessment on Cement Production Practice and Potential Cement Replacing Materials in Ethiopia. *12*, 22-28. doi: 10.7176/CER/12-1-03

Ghalampour, A., & Ozbakkaloglu, T. (2019). In New Trends Eco-Efficient and Recycled concrete: Woodhead Publishing, Sawston, United Kingdom.

Grzymski, F., Musiał, M., & Trapko, T. (2019). Mechanical properties of fibre reinforced concrete with recycled fibres. *Construction and Building Materials, 198,* 323-331.

Hagos, K., Jayanth, C., & Somashekar, R. (2012). Characterization of white and red teff grains using X-ray technique.

He, W., Kong, X., Fu, Y., Zhou, C., & Zheng, Z. (2020). Experimental investigation on the mechanical properties and microstructure of hybrid fiber reinforced recycled aggregate concrete. *Construction and Building Materials, 261,* 120488.

Hedidor, D., & Bondinuba, F. (2017). Exploring concrete materials batching behaviour of artisans in Ghana's informal construction sector. *Journal of Civil Engineering and Construction Technology, 8*(5), 35-52.

Hidaya, N., Mutuku, R. N., & Mwero, J. N. (2017). Physical and mechanical experimental investigation of concrete incorporated with polyethylene terephthalate (PET) fibers. *Eur. Int. J. Sci. Technol, 6*(8), 2304-9693.

Hwang, C.-L., Tran, V.-A., Hong, J.-W., & Hsieh, Y.-C. (2016). Effects of short coconut fiber on the mechanical properties, plastic cracking behavior, and impact resistance of cementitious composites. *Construction and Building Materials, 127,* 984-992.

Jiang, C., Fan, K., Wu, F., & Chen, D. (2014). Experimental study on the mechanical properties and microstructure of chopped basalt fibre reinforced concrete. *Materials & Design, 58*, 187-193.

Joshua, O., Fagbenle, O. I., Olusola, K. O., Shamaki, S. J., Abuka-Joshua, J. A., Ogunde, A. O., . . . Omuh, I. O. (2018). *A comparative analysis of batching by weight and volume towards improved concrete production.* Paper presented at the Construction Research Congress 2018.

jun Li, J., gang Niu, J., jun Wan, C., Jin, B., & liu Yin, Y. (2016). Investigation on mechanical properties and microstructure of high performance polypropylene fiber reinforced lightweight aggregate concrete. *Construction and Building Materials, 118*, 27-35.

Kassa, R. B., Kanali, C., & Ambassah, N. (2019a). Engineering properties of polyethylene terephthalate fibre reinforced concrete with fly ash as a partial cement replacement. *Civil and Environmental Research, 11*(6).

Kassa, R. B., Kanali, C., & Ambassah, N. (2019b). Environmental and Cost Advantages of Using Polyethylene Terephthalate Fibre Reinforced Concrete with Fly Ash as a Partial Cement Replacement. *Open Journal of Civil Engineering, 9*(4), 281-290.

Khan, M., Cao, M., & Ali, M. (2018). Effect of basalt fibers on mechanical properties of calcium carbonate whisker-steel fiber reinforced concrete. *Construction and Building Materials, 192*, 742-753.

Khatib, Z. K., & Bayomy, F. M. (1999). Rubberized Portland cement concrete. *Journal of Materials in Civil Engineering, 11*(3), 206-213.

Kim, S. B., Yi, N. H., Kim, H. Y., Kim, J.-H. J., & Song, Y.-C. (2010). Material and structural performance evaluation of recycled PET fiber reinforced concrete. *Cement and Concrete Composites, 32*(3), 232-240.

Kreem, O. M. A. (2012). Influence of Concrete Mix Proportions and Curing Regimes on Density, Absorption, and Voids in Hardened Concrete. *Al-Rafadain Engineering Journal, 20*(4).

Li, B., Chi, Y., Xu, L., Shi, Y., & Li, C. (2018). Experimental investigation on the flexural behavior of steel-polypropylene hybrid fiber reinforced concrete. *Construction and Building Materials, 191*, 80-94.

Li, F.-Y., Li, L.-Y., Dang, Y., & Wu, P.-F. (2018). Study of the effect of fibre orientation on artificially directed steel fibre-reinforced concrete. *Advances in Materials Science and Engineering, 2018.*

Li, Z.-X., Li, C.-H., Shi, Y.-D., & Zhou, X.-J. (2017). Experimental investigation on mechanical properties of Hybrid Fibre Reinforced Concrete. *Construction and Building Materials, 157*, 930-942.

Li, Z., Wang, X., & Wang, L. (2006). Properties of hemp fibre reinforced concrete composites. *Composites part A: applied science and manufacturing, 37*(3), 497-505.

Manatura, K., & Samaksaman, U. (2021). Characteristics and combustion kinetics of fuel pellets composed of waste of polyethylene terephthalate and biomass. *Global Journal of Environmental Science and Management, 7*(4), 625-642.

Martinelli, E., Caggiano, A., & Xargay, H. (2015). An experimental study on the post-cracking behaviour of Hybrid Industrial/Recycled Steel Fibre-Reinforced Concrete. *Construction and Building Materials, 94*, 290-298.

Mastali, M., Dalvand, A., Sattarifard, A., Abdollahnejad, Z., & Illikainen, M. (2018). Characterization and optimization of hardened properties of self-consolidating concrete incorporating recycled steel, industrial steel, polypropylene and hybrid fibers. *Composites Part B: Engineering, 151*, 186-200.

Matar, P., & Assaad, J. J. (2019). Concurrent effects of recycled aggregates and polypropylene fibers on workability and key strength properties of self-consolidating concrete. *Construction and Building Materials*, *199*, 492-500.

Mohammed, A. A., & Rahim, A. A. F. (2020). Experimental behavior and analysis of high strength concrete beams reinforced with PET waste fiber. *Construction and Building Materials, 244*, 118350.

Monteiro, P. (2006). *Concrete: microstructure, properties, and materials*: McGraw-Hill Publishing.

Mostofinejad, D., Moshiri, N., & Mortazavi, N. (2015). Effect of corner radius and aspect ratio on compressive behavior of rectangular concrete columns confined with CFRP. *Materials and Structures, 48*, 107-122.

Najaf, E., & Abbasi, H. (2022). Impact resistance and mechanical properties of fiber-reinforced concrete using string and fibrillated polypropylene fibers in a hybrid form. *Structural Concrete*.

Neves, R. D., & Fernandes de Almeida, J. (2005). Compressive behaviour of steel fibre reinforced concrete. *Structural Concrete, 6*(1), 1-8.

Neville, A. (2000). Water cinderella ingredient of concrete. *Concrete International, 22*(9), 66-71.

Nibudey, R., Nagarnaik, P., Parbat, D., & Pande, A. (2013). Strength and fracture properties of post consumed waste plastic fiber reinforced concrete. *Int. J. Civ. Struct. Environ. Infrastruct. Eng. Res. Dev, 3*(2), 9-16.

Nilforoush, R., Nilsson, M., & Elfgren, L. (2017). Experimental evaluation of tensile behaviour of single cast-in-place anchor bolts in plain and steel fibre-reinforced normal-and high-strength concrete. *Engineering Structures, 147*, 195-206.

Nkomo, N., Masu, L., & Nziu, P. (2022). Effects of Polyethylene Terephthalate Fibre Reinforcement on Mechanical Properties of Concrete. *Advances in Materials Science and Engineering, 2022*.

Passuello, A., Moriconi, G., & Shah, S. P. (2009). Cracking behavior of concrete with shrinkage reducing admixtures and PVA fibers. *Cement and Concrete Composites, 31*(10), 699-704.

Patil, B. S. T. a. A. S. (2015). A Study on Durability of Steel Fiber Reinforced Concrete.pdf. *International Journal for Scientific Research & Development, 3*.

Pereira, E. L., de Oliveira Junior, A. L., & Fineza, A. G. (2017). Optimization of mechanical properties in concrete reinforced with fibers from solid urban wastes (PET bottles) for the production of ecological concrete. *Construction and Building Materials, 149,* 837-848. doi: https://doi.org/10.1016/j.conbuildmat.2017.05.148

Rahman, S., & Azad, A. (2020). Effects on Properties of Coarse Aggregate with Respect to Different Sources: Chittagong: University Bangladesh.

Rahmani, E., Dehestani, M., Beygi, M., Allahyari, H., & Nikbin, I. (2013). On the mechanical properties of concrete containing waste PET particles. *Construction and Building Materials, 47*, 1302-1308.

Raj, B., Sathyan, D., Madhavan, M. K., & Raj, A. (2020). Mechanical and durability properties of hybrid fiber reinforced foam concrete. *Construction and Building Materials, 245,* 118373.

Rudraswamy, M., PATAGUNDI, B., & PRAKASH, K. (2018). THE WORKABILITY STUDIES OF HYBRID FIBER REINFORCED CONCRETE FORMED BY USING FIB S OF DIFFERENT ASPECT RATIO ER.

Sabarish, K., Dhanasekar, K., Manikandan, R., Ancil, R., Venkat Raman, R., & Selva Surender, P. (2017). Strength and durability evaluation of sisal fibre reinforced concrete. *International Journal of Civil Engineering and Technology, 8*(9), 741-748.

Scheving, A. G. (2011). *Life cycle cost analysis of asphalt and concrete pavements.*

Stempihar, J. J., Souliman, M. I., & Kaloush, K. E. (2012). Fiber-reinforced asphalt concrete as sustainable paving material for airfields. *Transportation research record, 2266*(1), 60-68.

Sudhikumar, G., Prakash, K., & Rao, M. S. (2014). Effect of aspect ratio of fibers on the strength characteristics of slurry infiltrated fibrous ferrocement. *J. Civ. Struct. Eng, 3*, 29-37.

Swaroop, A., Venkateswararao, K., & Kodandaramarao, P. (2013). Durability studies on concrete with fly ash & Ggbs. *International Journal of Engineering Research and Applications, 3*(4), 285-289.

Tadesse, A. (2019). Experimental study on mechanical properties of nanofiber-based teff straw as a fiber in reinforced concrete. *Global Scientific Journals, 7*(10), 123-139.

Tadesse, A. K. (2019). Experimental study on mechanical properties of teff straw as a fiber in reinforced concrete.

Tarekegn, M., Getachew, K., & Kenea, G. (2022). Experimental Investigation of Concrete Characteristics Strength with Partial Replacement of Cement by Hybrid Coffee Husk and Sugarcane Bagasse Ash. *Advances in Materials Science and Engineering, 2022*.

Teng, S., Afroughsabet, V., & Ostertag, C. P. (2018). Flexural behavior and durability properties of high performance hybrid-fiber-reinforced concrete. *Construction and Building Materials, 182*, 504-515.

Teo, D. C. L., Mannan, M. A., & Kurian, V. J. (2010). Durability of lightweight OPS concrete under different curing conditions. *Materials and Structures, 43*(1), 1-13. doi: 10.1617/s11527-008-9466-7

Tesfaye, H. G. (2021). Experimental study on effect of sodium hydroxide treated teff straw as fiber and cow dung ash on properties of concrete.

Teshome, S. (2022). Experimental Investigation on the Effect of Teff Straw Fiber and Lime on Strength and Compressibility of Black Cotton Soil. *Ethiopian Journal of Science and Sustainable Development, 9*(2), 1-8.

Ukala, C. (2019). Effects of combined aggregate gradation on the compression strength and workability of concrete using fineness modulus. *Journal of Applied Sciences and Environmental Management, 23*, 851. doi: 10.4314/jasem.v23i5.13

Vajje, S., & murthy, D. N. R. K. (2013). Study On Addition Of The Natural Fibers Into Concrete. *International Journal of Scientific & Technology Research, 2*, 213-218.

Vyom, M. R. S. K. M., & Shah, B. P. M. R. A. (2013). Utilization of Fibers in Construction Industries for Properties Improvement of Concrete. *Cellulose, 45*, 55.

Wang, G., & Han, Y. (2018). *Research on the performance of straw fiber concrete.* Paper presented at the IOP Conference Series: Materials Science and Engineering.

Warati, G. K., Darwish, M. M., Feyessa, F. F., & Ghebrab, T. (2019). Suitability of scoria as fine aggregate and its effect on the properties of concrete. *Sustainability, 11*(17), 4647.

Wassie, A. B., & Srivastava, V. C. (2017). *Synthesis and characterization of nano-silica from teff straw.* Paper presented at the Journal of Nano Research.

Yao, W., Li, J., & Wu, K. (2003). Mechanical properties of hybrid fiber-reinforced concrete at low fiber volume fraction. *Cement and concrete research, 33*(1), 27-30.

Yazıcı, Ş., İnan, G., & Tabak, V. (2007). Effect of aspect ratio and volume fraction of steel fiber on the mechanical properties of SFRC. *Construction and Building Materials, 21*(6), 1250-1253.

Yehia, S., Douba, A., Abdullahi, O., & Farrag, S. (2016). Mechanical and durability evaluation of fiber-reinforced self-compacting concrete. *Construction and Building Materials, 121*, 120-133.

Yuan, Z., & Jia, Y. (2021). Mechanical properties and microstructure of glass fiber and polypropylene fiber reinforced concrete: An experimental study. *Construction and Building Materials, 266*, 121048.

Zhang, J., Weissinger, E. A., Peethamparan, S., & Scherer, G. W. (2010). Early hydration and setting of oil well cement. *Cement and concrete research, 40*(7), 1023-1033.

Zhao, Y., Bi, J., Wang, Z., Huo, L., Guan, J., Zhao, Y., & Sun, Y. (2021). Numerical simulation of the casting process of steel fiber reinforced self-compacting concrete: Influence of material and casting parameters on fiber orientation and distribution. *Construction and Building Materials, 312*, 125337.

Zhou, Y., Xi, B., Yu, K., Sui, L., & Xing, F. (2018). Mechanical properties of hybrid ultra-high performance engineered cementitous composites incorporating steel and polyethylene fibers. *Materials, 11*(8), 1448.

APPENDIX

Appendix A: Consistency test procedure of cement

1. 650 grams of cement were measured.
2. Water amounting to a percentage of cement (22-30%) was added to cement and mixed.
3. Within 3-5 minutes, properly combine the paste. Gauging time is the time it takes to get cement paste after adding water.
4. Fill the paste in the Vicat mold appropriately, and removed any surplus paste with a trowel.
5. Then, set the Vicat mold on the glass plate, making sure the plunger lightly touches the surface of the Vicat mold.
6. Allow the plunger to sink into the test mold after it has been released.
7. Take note of the plunger's penetration from the bottom of the mold as indicated on the scale.
8. Repeat the experiment with varied percentages of water until the Vicat apparatus scale reading is between 5-7 mm.
9. The water added is right and the penetration is between 5 mm and 7mm.

Appendix B: Test Procedure for Fine aggregate

Appendix B1: Test Procedure for Silt Content

1. A graduated cylinder having a capacity of 1000 ml was taken.
2. 300 ml of sand was poured into the cylinder.
3. Approximately 3/4 of the jar was filled with water.
4. The jar was shaken vigorously for about a minute.
5. The jar was left for an hour to allow the silt to settle on the layer of sand.
6. The amount of fine forming a separate layer on the top was measured.

Appendix B2: Procedure for grading fine aggregate

1. The researcher weighted a sample of 2 kg of fine aggregates (FA) and the sample was quartered.
2. From the quartered sample, weighing 500 g,
3. The empty sieves were weighted, and the data was recorded properly.
4. The pan was placed on the bottom and the other sieves were put on the pan with increasing opening sizes of the sieves.
5. Placed the 500 g of sample on the top of the sieves (having a larger opening size).

6. Smashed the sample for about 10 minutes in a sieve shaker.
7. Each sieve, together with the aggregate retained on it, was measured and the weight retained on each sieve was calculated.

Appendix B3: Procedure for specific gravity and water absorption of fine aggregate

1. The S.S.D sample was weighted at 500 g.
2. Partially fill the Pycnometer with water and put 500 g of saturated surface dry aggregates into the Pycnometer.
3. Then they filled the pycnometer with additional water to fill it to 90% of its capacity.
4. The pycnometer was rolled and inverted to eliminate all air bubbles.
5. Place the Pycnometer in a water bath at 23 °C for an hour.
6. Brought the water level in the pycnometer to its calibrated capacity.
7. Then, the total weight of the pycnometer, specimen, and water was measured.
8. The researcher removed the fine aggregate from the pycnometer, dried it to a constant weight at 105 °C, cooled it in room temperature air for one hour, and measured it.The weight of the pycnometer filled with water was determined at 23°c.

Appendix B4: Test Procedure of Unit Weight of Fine Aggregate

1. The measure was filled one-third full and leveled with fingers. Then, the layer of aggregate was rodded with 25 strokes evenly distributed over the surface. The measure was then filled to two-thirds capacity, leveled, and rodded again. Finally, the measuring cup was filled to overflowing and rodded.
2. The surface of the aggregate was leveled with fingers in such a way that any slight projections of the large pieces of the coarse aggregate approximately balance the larger voids in the surface below the top of the measure.
3. While rodding the first layer, the researcher did not allow the rod to strike the bottom of the measure forcibly. In rodding the second and third layers, only enough force was used to cause the taping rod to penetrate the previous layers of aggregate.

Appendix C: Test Procedure for Fine aggregate

Appendix C1: Sieve Analysis for Coarse Aggregate

1. 20 kg of coarse aggregates were weighed and a representative sample was selected by quartering.
2. From the quartered sample, 2 kg was taken.
3. The empty sieves were weighted and the data was recorded properly.
4. Placed the 2 kg of sample on the top sieves (which have a large opening size).
5. Smashed the sample for about 10 minutes in a sieve shaker.

6. Each sieve, together with the aggregate retained on it, was measured and the weight retained on each sieve was calculated.

Appendix C2: Test Procedures Specific Gravity and Water Absorption of Coarse Aggregate

1. The sample of coarse aggregate was taken by using the sample splitter.
2. The sample was sieved with a 4.75 mm sieve, and the sample passing through the 4.75 mm sieve was ignored.
3. The sample was washed to remove dust and put the sample in the oven at 105°C for 24 hours.
4. The sample was taken out of the oven, left to cool, and then the weight was measured.
5. The sample was submerged in water for 24 hours, removed from the water, and rolled in a large absorbent cloth until all visible films of water were removed.The required weight of the sample in its (S.S.D) condition was taken. Then, the S.S.D sample was placed in the sample container, determined the weight in water at 23 °C.

Appendix C3: Test procedure of moisture content of aggregates

1. The empty weight of the cleaned container was recorded (A).
2. The weight of the container and the aggregate were recorded (B).
3. The sample was taken to the oven at 105 °C for 24 hours and the sample was left for half an hour and then weight was recorded (C).

Appendix D: The test Procedures of density, water absorption, and voids

1. Start by determining the mass of the specimens and dry them in an oven for 24 hours at a temperature ranging from 100 to 110°C.
2. Once the specimen is removed from the oven, allow it to cool in dry air (preferably in a desiccator) until it reaches a temperature of 20 to 25°C, then determine its mass.
3. If the specimen was dry during the first mass determination and its second mass closely agrees with the first, consider it dry. However, if it was wet during the first mass determination, place it in the oven for an additional 24 hours and determine its mass once again.
4. Repeat the process of drying the specimen for 24-hour periods until check values of mass are obtained, if there is any doubt.
5. In case the difference between the values obtained from two successive values of mass exceeds 0.5% of the lesser value, return the specimen to the oven for an additional 24-hour drying period, and repeat the process until the difference between any two

successive values is less than 0.5% of the lowest value obtained. Designate this last value as A.

6. After the final drying, cooling, and determination of mass, immerse the specimen in water at approximately 21°C for a minimum of 48 hours. Determine the mass at intervals of 24 hours until two successive values of the mass of the surface-dried sample show an increase in mass of less than 0.5% of the larger value.
7. Remove surface moisture with a towel and determine the mass. Designate the final surface-dry mass after immersion as B.
8. Process the specimen as described in step 6 and place it in a suitable receptacle, covered with tap water, and boil for 5 hours. Allow it to cool for a minimum of 14 hours before removing surface moisture with a towel and determining its mass. Designate the soaked, boiled, surface-dried mass as C.
9. Suspend the specimen by a wire and determine the apparent mass in the water. Designate this apparent mass as D.

Appendix E: Mix design procedures

Step 1: Calculate the required mean compressive strength from the given characteristic strength of 30 MPa. Concrete that has values between 21 MPa - 35MPa concrete grade factor is 8.5 from Appendix F1.

$$fck' = fck + 8.5$$

Where, fck - Characteristic compressive strength at 28 days in N/mm².

f 'ck - Target mean compressive strength at 28 days in N/mm².

X- Factor based on the grade of concrete.

Therefore, the target mean compressive strength for C-30 gives; $fck' = 30 + 8.5 = 38.5$MPa

Step 2: Determining the minimum cement content

From a durability point of view, the minimum cement content was taken as 300 kg/m3.

Step 3: Choose a Slump Value

A concrete slump of 20–80 mm is recommended for pavement and slabs from Appendix F2.

Step 4: Choose the maximum aggregate size.

For higher compressive strength, a reduced maximum size aggregate was selected. In this case, the maximum size aggregate was 25, and the nominal size aggregate was 19 mm with non-air entrained concrete.

Step 5: Mixing water and air content determination

The amount of water per unit volume of concrete required for a required slump value is dependent on aggregate grading, amount of entrained air, and maximum size aggregate. From Appendix F3, with a slump of 20–80 mm and a maximum size aggregate of 25 mm, the water content becomes 180 kg/m3 and 1.5%, or 15 liters of entrapped air.

Step 6: Determine the water-cement ratio

In a concrete mix, the water-cement ratio is the ratio of the weight of water to the weight of cement. The ACI table from Appendix F4 cannot provide the exact value of the water-cement ratio for a 38.5 MPa mean strength. This can be calculated by interpolating the above and below values as follows: 38.5 MPa is found between 35 and 40 MPa.

40 0.42

38.5 x by interpolation, $\frac{40\text{-}38.5}{0.42\text{-}x} = \frac{38.5\text{-}35}{x\text{-}0.47}$

35 0.47

By solving the above equation, x = 0.435

Hence, the minimum water-cement ratio is 0.435

Step 7: Determination of mix cement content

$$\text{Cement content} = \frac{\text{water content}}{\text{water cement ratio}}$$

$$\frac{180}{0.435} = 413.79\text{kg/m3}$$

The computed cement content was greater than the specified minimum cement content, which is 300 kg/m3. Therefore, 413.79 kg/m3 was used for the mix design for this study.

Step 8: Estimate the bulk volume per unit volume of concrete

The bulk volume of dry-rodded aggregate was not found in the appendix F5 table directly. It can be calculated by interpolation since the fineness modulus of 2.82 is found between 2.8 and 3.0 for a 25 mm maximum size aggregate.

2.8 0.62

2.82 x

3.0 0.60 By interpolation,

$$\frac{2.8\text{-}2.82}{0.62\text{-}x} = \frac{2.82\text{-}3.0}{x\text{-}0.60}$$

By solving the equation above, x = 0.618

Hence, the dry volume of aggregate per volume of concrete is 0.618.

Step 9: Calculate the weight of coarse aggregate (WCA) per m^3 of concrete.

WCA= bulk volume x bulk density of coarse aggregate

WCA = 0.618 x 1627.6 kg/m^3

= 1,005.85 kg/m^3

Step 10: Determine the solid volume of coarse aggregate.

$$\text{The solid volume of coarse aggregate} = \frac{\text{WCA}}{\text{Specific gravity}}$$

$$= \frac{1005.85 kg/m^3}{2.65}$$

$$= 379.57 kg/m^3$$

Step 11: Calculate the solid volume of cement, water, and air

$$\text{The volume of cement} = \frac{\text{weight of cement}}{\text{The specific gravity of cement}}$$

$$= \frac{413.79 kg/m3}{3.15}$$

$$= 131.36 kg/m3$$

Volume of water (VW) = 180 kg/m 3

Volume of air (VA) = 1.5% or 15 kg/m3

Step 12: Calculating the solid volume of sand

Solid volume of sand = 1000 - (VCA + VC + VW + VA)

= 1000 - (379.57 + 131.36 + 180 + 15)

= 1000 - 705.93

= 294.07 kg/m^3

The solid weight of sand = dry volume of sand x specific gravity

= 294.07 kg/m3 x 2.63

= 773.40 kg/m^3

Step 13: Adjustments for moisture in the aggregate

If the absorption capacity of aggregate is greater than the moisture content, we need to add mixed water to get better workability of the concrete.

Coarse Aggregate water =Absorption capacity (%)-Moisture content (%) = 3.09-0.79 = 2.3%

Fine Aggregate water = Absorption capacity (%)-Moisture content (%) = 1.70-3.24 = -1.54%

Fine aggregate adsorption = 1.54% and coarse aggregate absorption = 2.3%

Water absorbed by coarse aggregate = 1,005.85 kg/m^3 x 0.023

= 23.13 kg/m3

Water supplied by fine aggregate = 773.40 kg/m^3x 0.0154

= 11.91 kg/m^3

Amount of water needed = 180 kg/m^3 + 23.13 kg/m^3 – 11.91 kg/m^3

= 191.22 kg/m^3

Cement = 413.79 kg/m^3

Fine aggregate = 773.40 kg/m^3 + 11.91 kg/m^3

= 785.31 kg/m^3

Coarse aggregate = 1,005.85 kg/m^3 – 11.91 kg/m^3

= 993.94 kg/m^3

Step 14. Hybrid fiber reinforced concrete mix design

The fiber-reinforced concrete mix design was done for the unit cubic meter of concrete. The amount of fiber added for both hybrid fibers was 0.2%, 0.4%, and 0.6% of the total weight of the concrete. The possibility of the amount of fiber added for the mix design was taken by the researchers (Biratu et al., 2022; A. K. Tadesse, 2019). For a one-meter cube of concrete the percentage of hybrid polyethylene terephthalate and teff straw fiber added varies as 0.1%PETF + 0.1% TSF,0.1%PETF + 0.3%TSF and 0.1% PETF + 0.5%TSF.The total mix design for fiber-reinforced concrete used is shown as follows:

For 1m^3 of concrete weight of (cement + FA +CA + water) is 2,384.26kg

For 0.1% polyethylene terephthalate fiber,

$$= \frac{0.1}{100} \text{ x } 2384.26 = 2.38\text{kg}$$

For 0.1% teff straw fiber

$$= \frac{0.1}{100} \text{ x } 2384.26 = 2.38\text{kg}$$

For 0.3% teff straw fiber

$$= \frac{0.3}{100} \text{ x } 2384.26 = 7.15\text{kg}$$

For 0.5% teff straw fiber

$$= \frac{0.5}{100} \text{ x } 2384.26 = 11.92\text{kg}$$

Weight of hybrid fibers for M_0 = 0kg

Weight of hybrid fibers for M_1 = 2.38kg + 2.38kg = 4.76kg

Weight of hybrid fibers for M_2 = 2.39kg + 7.15kg = 9.53kg

Weight of hybrid fibers for M_3 = 2.39kg + 11.92kg = 14.3kg

Appendix F: Tables for ACI concrete mix design

Appendix F1: Average Compressive Strength Conversion

Specified characteristic compressive strength (f'ck, MPa)	Required average compressive strength in (fck, MPa)
<21	f'ck + 7
21-35	f'ck + 8.5
>35	1.1*f'ck + 5

Appendix F2: Recommended slumps for various types of constructions

Types of constructions	Slump (cm)	
	Minimum	Maximum
Reinforced foundations, walls, and footings	2	8
Plain footings, caissons , and substructure walls	2	8
Beams and reinforced walls	2	10
Building columns	2	10
Pavements and slabs	2	8
Heavy mass concrete	2	8

Appendix F3: Mixing Water for Different Slump and Maximum Size Aggregate

Slump (cm)	Water kg/m3 of concrete for indicated max. sizes of aggregate in mm							
	10	12.5	20	25	40	50	70	150
Non-air entrained concrete								
3-10	205	200	185	180	160	155	145	125
8-10	225	215	200	195	175	170	160	140
15-18	240	230	210	205	185	180	170	-
Amount of Entrapped air (%)	3	2.5	2	1.5	1	0.5	0.3	0.2

Appendix F4: Average Compressive Strength with water cement ratio

Compressive strength at 28 days (MPa)	Water cement ratio by mass	
	Non-air entrained	Air entrained
45	0.38	-
40	0.42	-
35	0.47	0.39
30	0.54	0.45
25	0.61	0.52
20	0.69	0.60
15	0.79	0.71

Appendix F5: Volume of coarse aggregate per unit volume of concrete

Maximum size of aggregate	The volume of dry rodded coarse aggregate per unit volume of concrete for different fineness modulus		
	2.6	2.8	3.0
10	0.50	0.46	0.44
12.5	0.59	0.55	0.53
20	0.66	0.62	0.60
25	0.71	0.67	0.65
40	0.76	0.72	0.70
50	0.78	0.74	0.72
70	0.81	0.77	0.75

Appendix G: Different Test Results

Appendix G1: Detail Slump value of HFRC and Control Concrete

Mix code	HFRC (%)	Sample	Slump value (mm)
M_0	0	1	53
		2	57
		3	55
		Avg.	55
M_1	0.2	1	39
		2	41

		3	43
		Avg.	41
M_2	0.4	1	21
		2	19
		3	23
		Avg.	21
M_3	0.6	1	12
		2	9
		3	11
		Avg.	10.67

Appendix G2: Detail Compaction factor value of HFRC and Control Concrete

Mix code	HFRC (%)	Sample	Compaction factor value
M_0	0	1	0.945
		2	0.942
		3	0.934
		Avg.	0.940
M_1	0.2	1	0.888
		2	0.885
		3	0.884
		Avg.	0.886
M_2	0.4	1	0.881
		2	0.879
		3	0.880
		Avg.	0.880
M_3	0.6	1	0.666
		2	0.664
		3	0.661
		Avg.	0.664

Appendix G3: Density of fresh concrete for HFRC and control concrete

Mix code	HFRC (%)	Sample	Density(kg/m3)
M_0	0	1	2282.08
		2	2274.83
		3	2255.51
		Avg.	2270.81
M_1	0.2	1	2232.08
		2	2224.53
		3	2222.02
		Avg.	2226.21
M_2	0.4	1	2183.02
		2	2178.06
		3	2180.54
		Avg.	2180.54
M_3	0.6	1	2039.62
		2	2033.50
		3	2024.31
		Avg.	2032.48

Appendix G4: Detail result of compressive strength for different mixes.

Mix code	HFRC (%)	Sample	Peak Load(kN)		Compressive stress (MPa)	
			7th day	28th day	7th day	28th day
M_0	0	1	629	802	27.98	35.65
		2	592	797	26.30	35.40
		3	567	812	25.22	36.10
		avg			26.50	35.72
M_1	0.2%	1	484	680	21.52	30.21
		2	518	661	23.01	29.36
		3	487	707	21.63	31.43
		avg			22.05	30.33
M_2	0.4%	1	357	510	15.85	22.67
		2	348	488	15.46	21.69

		3	371	468	16.51	20.80
		avg			15.94	21.72
M_3	0.6%	1	291	435	12.92	19.33
		2	261	407	11.62	18.09
		3	295	455	13.09	20.22
		avg			12.54	19.21

Appendix G5: Detail result of flexural stress for different mixes.

Mix code	HFRC (%)	Sample	Peak Load(kN)		flexural stress (MPa)	
			7th day	28th day	7th day	28th day
M_0	0	1	14.48	16.03	4.34	4.81
		2	13.73	15.53	4.12	4.66
		3	13.30	15.63	3.99	4.69
		avg			4.15	4.72
M_1	0.2%	1	14.55	17.03	4.36	5.11
		2	15.07	17.80	4.52	5.34
		3	13.99	16.03	4.20	4.81
		avg			4.36	5.09
M_2	0.4%	1	11.22	14.77	3.36	4.43
		2	10.49	12.33	3.15	3.70
		3	10.97	14.23	3.29	4.27
		avg			3.27	4.13
M_3	0.6%	1	10.83	11.67	3.25	3.50
		2	9.93	10.81	2.98	3.24
		3	10.30	11.73	3.09	3.52
		avg			3.11	3.42

Appendix G6: Detail result of tensile stress for different mixes.

Mix code	HFRC (%)	Sample	Peak Load(kN)		Tensile stress (MPa)	
			7th day	28th day	7th day	28th day
M0	0	1	131	164	1.85	2.32

		2	125	153	1.77	2.16
		3	133	158	1.88	2.24
		avg			1.83	2.24
M1	0.2%	1	136	218	1.93	3.09
		2	126	171	1.79	2.41
		3	146	199	2.06	2.81
		avg			1.93	2.77
M2	0.4%	1	119	141	1.69	1.99
		2	122	122	1.73	1.73
		3	110	136	1.56	1.92
		avg			1.66	1.88
M3	0.6%	1	95.47	109.15	1.35	1.55
		2	84.07	102.22	1.19	1.45
		3	93.26	116.57	1.32	1.65
		avg			1.29	1.55

APPENDIX H

H1: Quantity Take off for rigid pavement for 1km and 2 lanes

T	D	S	Description
			1. Concrete (rigid) pavement
			Concrete pavement 340mm thick (C-30) concrete
1	1,000.00		
	7		
	0.34	2380	m^3

H2: Reinforcing steel bar quantity Take off for rigid pavement for 1km and 2 lanes (as per the typical road section)

Description	Position of Bar	ø	Length	No of Member	NO of Bar(No)	Diam. ø12	ø14	ø24
Dowel Bars	Transversal joint	25	0.4	40	23			373.33

Tie Bars	Longitudinal Joint	12	1	1	1,667	1,666.67		
End caps at anchor key	every 39 meters	12	0.35	26	24	218.38		
		12	6.6	26	125	21,369.25		
Longitudinal bar	top main bar	14	24.89	40	29		28,872.40	
Transversal bar	top bar	12	6.6	40	29	7,656.00		
			Total Length			30,910.29	28,872.40	373.33
			Wt/Lm (Kg/m)			0.888	1.21	3.854
			Total Weight (Kg)			**27,448.34**	**34,935.60**	**1,438.83**

H3: BOQ for Rigid pavement for 1km and 2 lanes at end of 2023

Item No	**Description**	**unit**	**Quantity**	**Rate**	**Amount**
1	**Rigid Pavement**				
1.1	**Concrete pavement**				
1.1.1	Concrete pavement 340mm thick (C-30) concrete for the concrete slabs	m^3	2380.00	14,102.00	33,562,760.00
	Carried to Summary				**33,562,760.00**
2	**Reinforcement Bar**				
2.1	Dowels Bars(Mild steel plain bars, epoxy coated) Ø24mm and 400mm long @300mm spacing	Kg	1,326.08	151.90	201,431.55
2.2	Tie Bars(Ø12mm high strength deformed bars) and 1000mm long @600mm spacing, with 15cm long protective coating as per the drawing)	Kg	1,480.00	151.90	224,812.00

2.3	End Caps(**Anchor Key**) (Ø12mm high strength deformed bars) and 300mm long @300mm spacing vertical and 3Ø12 ,6900mm long transversal bars @ 170mm spacing as per the drawing)	Kg	19,169.81	151.90	2,911,894.14
2.4	High Tensile strength steel bars (Ø14mm) diameter longitudinal bar for main concrete pavement top reinforcement	Kg	34,935.60	151.90	5,306,717.64
2.5	Ditto but (Ø12mm) diameter transversal bar for main concrete pavement top reinforcement	Kg	6,798.53	151.90	1,032,696.71
	Carried to Summary				**9,677,552.04**

H4: Maintenance and rehabilitation cost for of rigid pavement at end of 2023

Maintenance Type	Activity Description	Unit	Quantity (per km)	Quantity(m2) for 2 lane	Unit Rate	Amount (ETB birr)
Routine	Joint Sealing	ml	50%	500	500	250,000.00
	Crack Sealing	ml	50%	500	500	250,000.00
Periodic	Partial depth PCC repair	m3	20%	34	5000	170,000.00
Rehabilitation	Full depth PCC repair	m3	70%	238	6000	1,428,000.00
	Texturizing	m2	80%	800	250	200,000.00

	Year	(1+if)	$(1+if)^n$	Rehabilitation	Salvage Value	Rehabilitation	Salvage Value
40	2063	1.0058	1.260	1,628,000.00	1,085,333.33	2,051,280.00	1,367,520
		Grand Total (Birr/Km)				2,051,280.00	1,367,520

H5: Rigid pavement Present value calculation

	Year	(1+dr)	$(1+dr)^n$	Maintenance cost		Maintenance cost (PV)=FV/$(1+dr)^n$	
				Routine(FV)	Periodic(FV)	Routine	Periodic
0	2023						
8	2031	1.035	1.317	523,676.46		397,628.29	-
12	2035	1.035	1.511	-	182,216.83	-	120,593.53
16	2039	1.035	1.734	548,474.08	-	316,305.69	-
24	2047	1.035	2.283	574,445.93	195,311.62	251,618.89	85,550.42
32	2055	1.035	3.006	601,647.62	-	200,148.91	-
36	2059	1.035	3.450		209,347.44	-	60,680.42
				Grand Total (Birr/Km)		**1,165,701.78**	**266,824.37**

H6: Rigid pavement with fibers Present value calculation

	Year	(1+dr)	$(1+dr)^n$	Maintenance cost		Maintenance cost (PV)=FV/$(1+dr)^n$	
				Routine(FV)	Periodic(FV)	Routine	Periodic
0	2023						
8	2031	1.035	1.317	366,573.52		278,339.80	-
12	2035	1.035	1.511	-	127,551.78	-	84,415.47

16	2039	1.035	1.734	383,931.85	-	221,413.98	-
24	2047	1.035	2.283	402,112.15	136,718.13	176,133.22	59,885.29
32	2055	1.035	3.006	421,153.34	-	140,104.23	-
36	2059	1.035	3.450		146,543.21	-	42,476.29
				Grand Total (Birr/Km)		**815,991.23**	**186,777.05**

Year	(1+dr)	$(1+dr)^n$	Rehabilitation (FV)	Salvage Value (FV)	Rehabilitation	Salvage Value
40 2063	1.1023	49.203	1,628,000.00	1,085,333.33	33,087.41	22,058.28
Grand Total (Birr/Km)					33,087.41	22,058.28

H7: Rigid pavement section (taken example for life cycle cost)

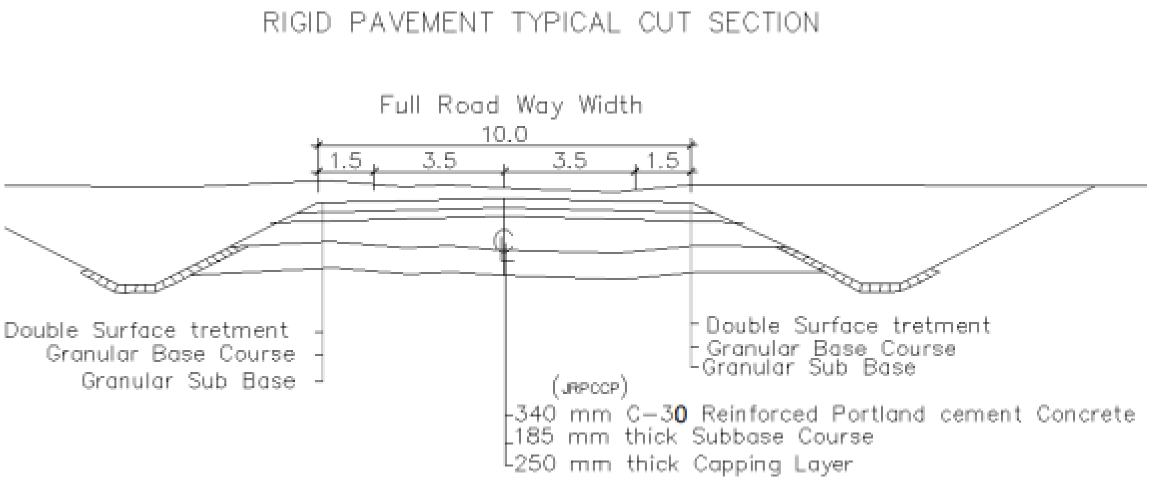

H8: Rigid pavement lay out (taken example for life cycle cost)

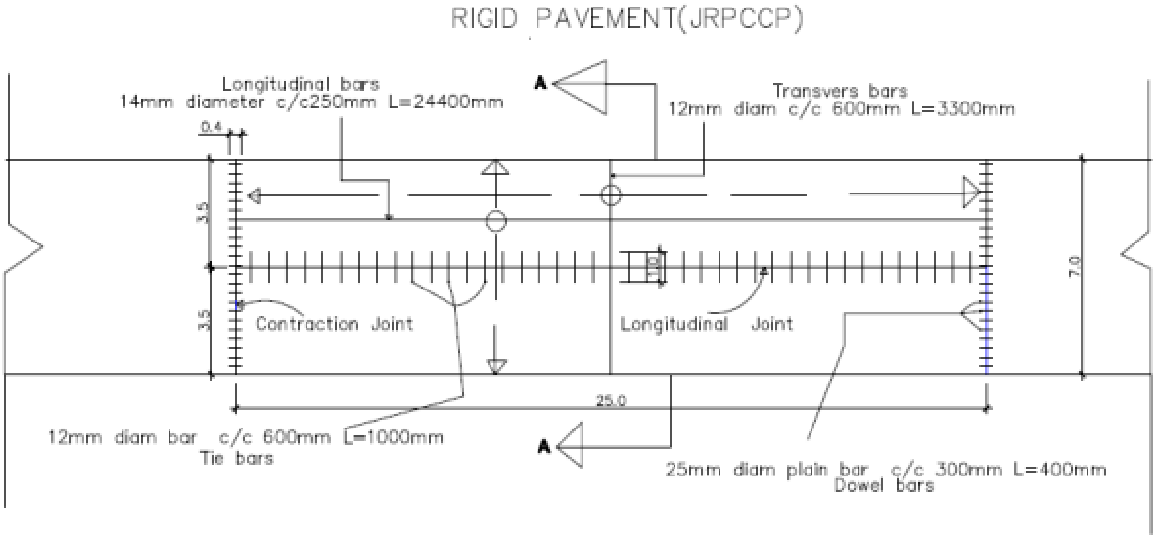

H9: Rigid pavement detail (taken example for life cycle cost)